FUNCTIONAL IMPLICATIONS OF ELECTROPHILIC PROTEIN ADDUCTS

By

Jeannie Marie Camarillo

Dissertation
Submitted to the Faculty of the
Graduate School of Vanderbilt University
in partial fulfillment of the requirements
for the degree of

DOCTOR OF PHILOSOPHY
In

Biochemistry
December, 2016
Nashville, Tennessee

Approved:

Lawrence J. Marnett, Ph.D.

Daniel C. Liebler, Ph.D.

Jennifer A. Pietenpol, Ph.D.

David Cortez, Ph.D.

William P. Tansey, Ph.D.

To my loving partner, Will, my amazing family, and my incredible friends. I would never have survived without your unwavering support and never-ending entertainment.

ACKNOWLEDGEMENTS

First, I would like to thank Dr. Larry Marnett for accepting me into his laboratory and supporting my all my scientific endeavors and creativity. He has always found a way to motivate me even when all the experimental failures have gotten me down. His constant encouragement and helped me push through during the hard times and I would never have survived graduate school without his guidance. I would also like to thank all the members of the Marnett lab, both past and present, for their friendship and support. All the lemmings have made science a lot more entertaining. Dr. Carol Rouzer has been absolutely invaluable to me. She makes my science and writing better and I am so thankful that I have had the unique opportunity to work with her. I have been funded by a number of grants over the years, including the IMSD Training Grant (R25 GM062459), the Molecular Toxicology Training Grant (T32 ES007028), my own predoctoral fellowship (F31 CA192861), and multiple grants from Larry (R01 087819, R37 087819, and P01 ES013125). I am incredibly grateful that I have been so generously supported over the years.

I would like to thank Dr. Kristie Rose and Dr. Mitch Reyzer for all their help with mass spectrometry techniques. My research would not have been possible without you ladies. I must also thank my committee, Dr. Dan Liebler, Dr. Bill Tansey, Dr. Jennifer Pietenpol, and Dr. Dave Cortez. Dan, you let me, a first year graduate student straight out of Arizona, into your lab during my first summer in Nashville. It was an email to your lab during that time, encouraging us to attend Larry's seminar, which sparked my interest in his group. I am immensely grateful for that opportunity you unknowingly gave me.

I have so many friends and loved ones that have been there for me over these last five years. First, my parents, who always valued my education above all else and tell me constantly how proud

they are of my accomplishments. To my brother, Chris, and my sister, Bridget, for always being there when I needed to talk to someone. To my former roommate and best friend, Ashley, who decided it was a great idea to move to Nashville after we finished undergrad. You have been with me through all my struggles over these past few years and I am ever grateful to have you in my life. I am so glad you are stuck with me. To all my friends, Rebecca Levinson, Bill Martin, Daniel LePage, Tim Shaver, Sam Mayden, Connie Allison, Angela Evans, Erica Simpson, Elizabeth Michels, Katie Fredericks, Dave Rohman, Terri Rohman, Jessica Vincent, Artem Serganov, Brittney Blaise, Sarah Stow, Jeff Allen, and Lane Williams, you guys are the best. You have known me for various amounts of time, but you have all encouraged me and made me laugh over the years of struggle. I would never had made it without you all. Finally, I need to thank my loving partner, Will Turnage. You make me feel as if I am the best scientist in the world on a daily basis. Thank you for loving burnt broccoli as much as I do and allowing me to torture my coworkers with its smell every day. I love you.

TABLE OF CONTENTS

LIST OF TABLES

LIST OF FIGURES

LIST OF ABBREVIATIONS

AA	acetic anhydride
AcLys	acetylated Lys
aHNE	alkynyl-4-hydroxy-2-nonenal
aONE	alkynyl-4-oxo-2-nonenal
ARE	antioxidant response element
ADMA	asymmetric dimethyl arginine
AD	Alzheimer's disease
PD	Parkinson's disease
TBTA	*tris*-(benzyltriazolylmethyl)amine
BAG3	BCL2 Associated Athanogene 3
Cam	carbamidomethylation
Click-Seq	chromatin click precipitation and sequencing
ChIP	chromatin immunoprecipitation
CHCA	α-cyano-hydroxycinnamic acid
CDK2	cyclin-dependent kinase 2
DMSO	dimethyl sulfoxide
DNPH	dinitrophenylhydrazine
DTT	dithiothreitol
DMEM	Dulbecco's modified eagle medium with glutamax
DPBS	Dulbecco's phosphate buffered saline
EpRE	electrophile response element

ENCODE	encyclopedia of DNA elements
FBS	fetal bovine serum
GSH	glutathione
HSP	heat shock protein
HSF1	heat shock factor 1
HFBA	heptafluorobutyric acid
HPNE	4-hydroperoxy-2-nonenal
HPODE	hydroperoxy octadecadienoic acid
HNE	4-hydroxy-2-nonenal
iNOS	inducible nitric oxide synthase
IKK	inhibitor of nuclear factor kappa-light-chain-enhancer of activated B cells kinase
In·	initiator radical
INFγ	interferon-γ
IA	iodoacetamide
Keap1	kelch-like ECH-associated protein 1
LH	lipid
LOOH	lipid hydroperoxide
LOO·	lipid peroxyl radical
L·	lipid radical
LC-MS/MS	liquid chromatography-coupled tandem mass spectrometry
m/z	mass to charge ratio
MNase	micrococcal nuclease
NOX2	NADPH oxidase 2

NADPH	nicotinamide adenine dinucleotide phosphate, reduced
Nrf2	nuclear factor (erythroid dervied-2)-like 2
NF-κB	nuclear factor kappa-light-chain-enhancer of activated B cells
ONE	4-oxo-2-nonenal
PUFA	polyunsaturated fatty acids
PTM	post-translational modifications
PIN1	peptidyl-prolyl *cis/trans* isomerase
PDB	protein data bank
PPAR	peroxisome-proliferator-activated receptor
QuARK-Mod	quantitative analysis of arginine and lysine modifications
RNS	reactive nitrogen species
ROS	reactive oxygen species
RT	room temperature
SOD	superoxide dismutase
me_3Lys	trimethyl Lys
TRX	thioredoxin
TXNIP	thioredoxin interacting protein
TBST	*tris* buffered saline with tween-20
TNF	tumor necrosis factor

CHAPTER I

INTRODUCTION

Inflammation and Disease

Inflammation and Oxidative Stress

The hallmarks of inflammation have been recognized for millennia, as documented by writings from the ancient civilizations of Mesopotamia, Egypt, and Greece.[7] The Greek physician, Celsus, defined the clinical manifestations associated with inflammation: rubor (redness), tumor (swelling), calor (heat), dolor (pain),[8] with a fifth sign, functio laesa (loss of function), added in the 19th century by Rudolf Virchow.[9] Our understanding of inflammation has changed drastically over the years. Acute inflammation was predominantly regarded as a disease prior to the late 18th century when surgeon and anatomist John Hunter proposed a beneficial role.[9] Today, acute inflammation is known to be a beneficial process that wards off infection and leads to the repair of damaged tissues.

The inflammatory response is initiated in response to stimuli emanating from sites of tissue injury that may be caused by pathogens, environmental toxins, trauma, etc. A cascade of events contributes to the inflammatory response as a whole, but one important component is production of reactive oxygen (ROS) and nitrogen species (RNS) by various immune cells at the primary site of inflammation (Figure 1).[10,11] The persistence of a bodily injury or the lack of resolution of the inflammatory response result in the development of chronic inflammation. Under these conditions, nearby host cells are continuously exposed to ROS and RNS, and the imbalance of oxidant

production relative to antioxidant defense systems in the cell contributes to oxidative stress and disease generation.

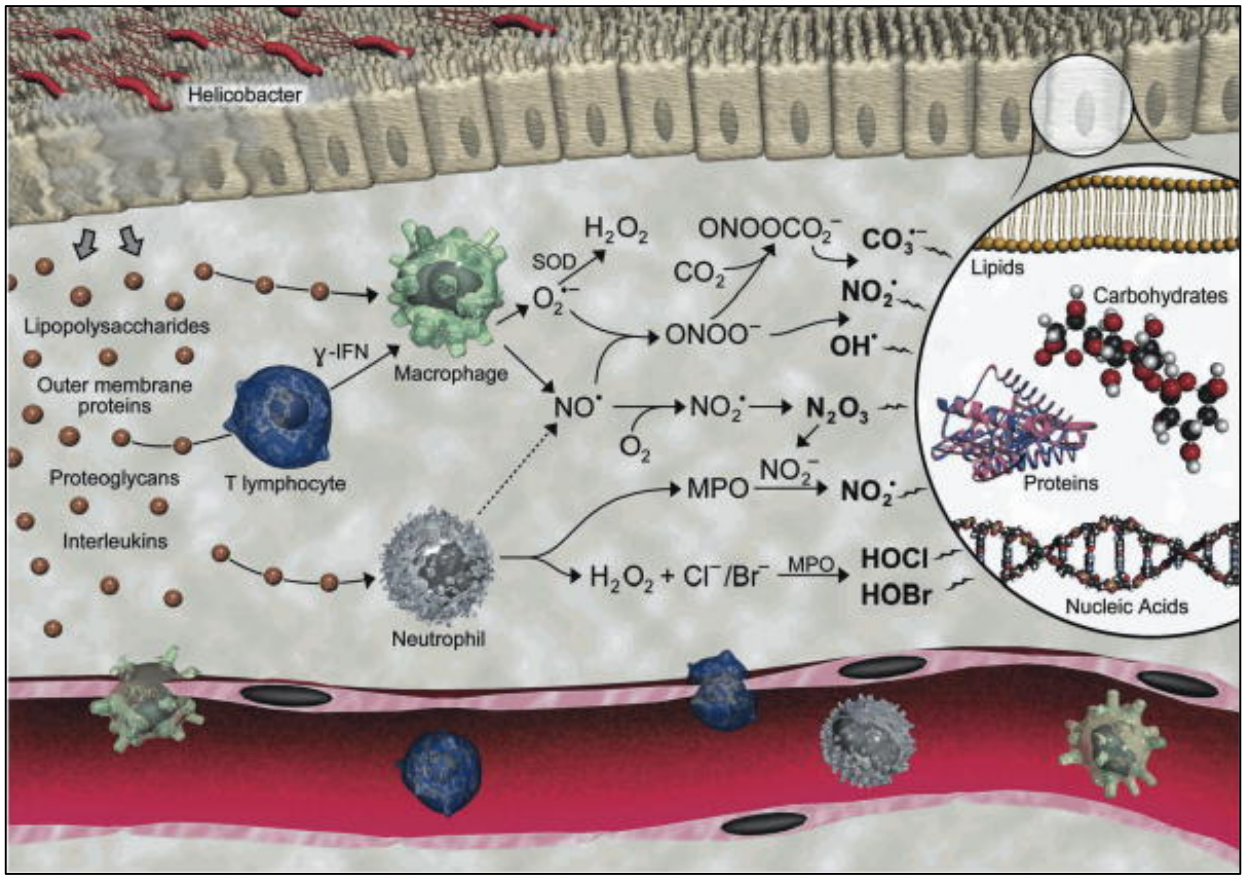

Figure 1. Generation of reactive species in the immune response. During an inflammatory response, macrophages and neutrophils are recruited to the site of infection or injury and generate a multitude of reactive species to combat the pathogen. These reactive metabolites can damage pathogen and host cellular molecules, including proteins, nucleic acids, carbohydrates, and lipids. Reprinted by permission from Macmillan Publishers Ltd: *Nature Protocols* Taghizadeh et al. (2008) *Nat. Protoc.* 3(8):1287-98. Copyright 2008.[3]

Inflammation and Diseases

The link between inflammation and disease has long been hypothesized. In 1863, Rudolf Virchow noted the presence of leukocytes in neoplastic tissue and proposed that the "lymophoreticular infiltrate" suggested the origin of cancer at sites of chronic inflammation.[12] Much more is now known about Virchow's initial observations. There is a growing body of

evidence suggesting that many malignancies are the result of or exacerbated by chronic inflammation and oxidative stress. ROS and RNS can damage lipids, proteins, and DNA in proliferating host cells, and persistent DNA damage can result in mutations, deletions, and rearrangements.[13] Loss-of-function mutations in tumor suppressor proteins, such as p53[14] and PTEN,[15] or dysregulation of oncogenes, such as Ras[16] and Myc[17], can contribute to aberrant cell growth, thereby promoting tumorigenesis.

Virchow's initial hypothesis has been supported by a multitude of studies over the past 150 years and has expanded to include diseases other than cancer. A large body of work has supported the role of inflammation and oxidative stress in the pathogenesis of neurodegenerative disease. From an epidemiological perspective, long-term use of nonsteroidal anti-inflammatory drugs has a beneficial effect on Alzheimer's disease (AD) and Parkinson's disease (PD), suggesting that a suppression of inflammation inhibits disease progression.[18-20] Genetic polymorphisms in inflammatory cytokines, most notably interleukin-1, increase the risk of developing AD and PD.[21,22] Additionally, a number of *in vitro* and *in vivo* models have shown that reduction in inflammatory processes alleviates neurologic symptoms.[23-26] Thus, neurodegenerative disease initiation and progression appear to be strongly correlated with inflammation.

Inflammation also plays a large role in the development of atherosclerosis. Atherosclerotic plaques are composed of a large number of immune cells, particularly macrophages and T-cells.[27] In fact, the majority of the cells present during plaque formation are lipid-laden macrophages known as foam cells. Activation of these immune cells results in the production of pro-inflammatory cytokines, such as tumor necrosis factor (TNF) and interferon-γ (INFγ).[28] Studies have shown beneficial outcomes with the use of peroxisome-proliferator-activated receptor (PPAR) activators that decrease TNF and INFγ secretion by inhibiting T-cell activation. Inhibition

of immune cell activation and reduction in pro-inflammatory mediators is a promising therapeutic approach to reducing the progression of atherosclerosis.[29]

Lipid Peroxidation

Chemistry of Oxidant Formation During Inflammation

While Celsus was able to describe the physical manifestations of inflammation two millennia ago, the cellular damage that occurs during chronic inflammation has only been appreciated for the past half-century. In response to an inflammatory stimulus, such as recognition of a pathogen by cell surface receptors, the cells produce a multitude of bioactive peptides, cytokines, and chemokines, to initiate the inflammatory response. Synthesis of these molecules helps to recruit leukocytes, most notably neutrophils and macrophages, to the site of the stimulus. These cells will then contribute to a respiratory burst, consisting of a rapid release of ROS and RNS.

Under normal cellular conditions, the balance between pro-oxidant generation and anti-oxidant defenses is well maintained. The respiratory burst generates large amounts of oxidants in an attempt to combat the inflammatory stimulus. NADPH oxidases catalyze the reaction that produces superoxide ($O_2^{\cdot -}$), the one election reduction of molecular oxygen. In leukocytes, NADPH oxidase 2 (NOX2) is the main enzyme responsible for this reaction (Figure 2). Upon leukocyte activation, NOX2 and the constitutively associated $p22^{phox}$ are translocated to the plasma membrane from intracellular vesicles.[30,31] Exchange of GDP for GTP contributes to activation of Rac kinase, which phosphorylates $p47^{phox}$, causing a large conformational change allowing for its direct association with $p22^{phox}$.[32,33] The conformational change in $p47^{phox}$ also enables the recruitment of $p67^{phox}$ and $p40^{phox}$ to produce the fully active NOX2 complex.[34,35]

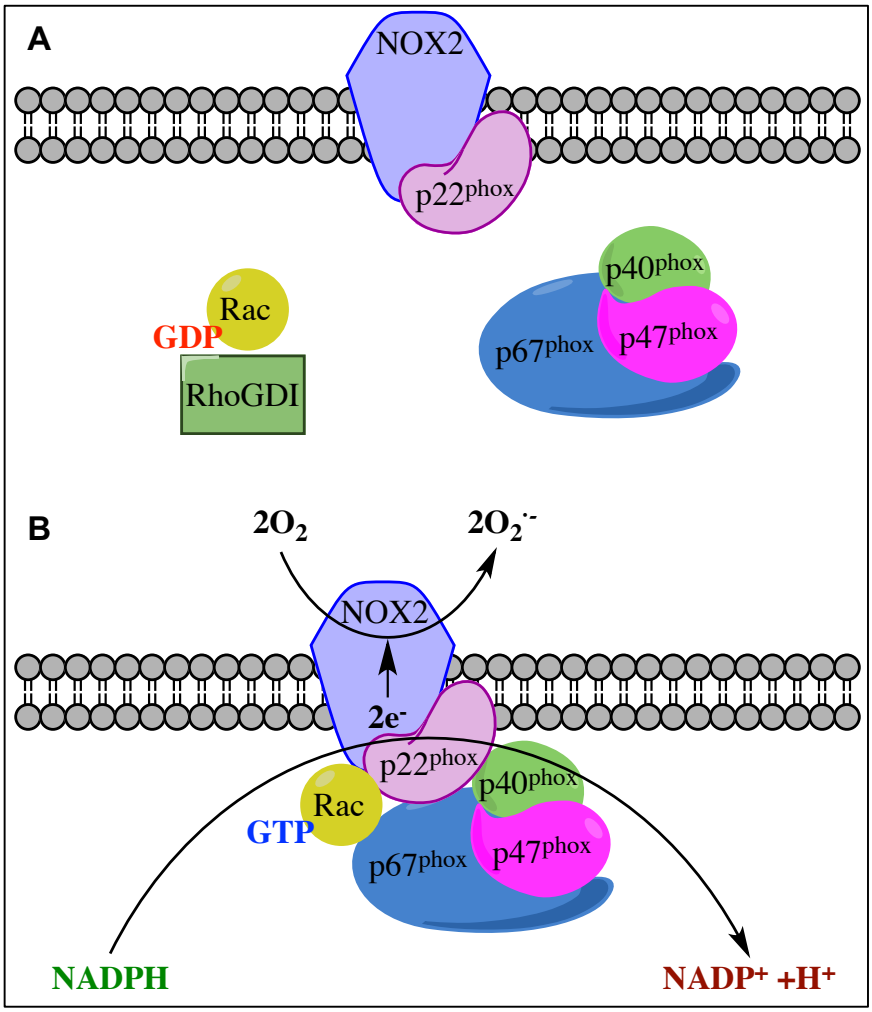

Figure 2. NADPH oxidase activation. A) Inactive NADPH oxidase (NOX2) is in the membrane associated with $p22^{phox}$. Proteins required for activation remain in the cytosol, and GDP is bound to Rac. B) Upon inflammatory stimulation, GTP binds to Rac, and NOX2 binding partners translocate to NOX2. NADPH is hydrolyzed to $NADP^+$ and H^+ with a $2e^-$ transfer. Molecular oxygen is reduced by NOX2 to $O_2^{\cdot-}$. Figure adapted with permission from McCann and Roulston *Brain Sci.* (2013) 3(2):561-598. Copyright 2013.[4]

The NOX2 complex comprises a transmembrane redox chain, with an electron donor (NADPH) on the cytosolic side and bound oxygen on the luminal side of the plasma membrane. Electrons are transferred from NADPH to FAD by $p67^{phox}$. A single electron is then transferred from fully reduced $FADH_2$ to the inner heme within NOX2. The inner heme then donates the electron to the outer heme prior to accepting the second electron from partially reduced FADH. Oxygen that is bound to the outer heme accepts the electron bound to the outer heme, resulting in the generation of $O_2^{\cdot-}$ on the luminal side.[36]

While its production contributes to the respiratory burst, $O_2^{\cdot -}$ is not a strong oxidant and has a short half-life in aqueous solution. Dismutation of $O_2^{\cdot -}$ occurs non-enzymatically and enzymatically, by the activity of superoxide dismutase (SOD), to form hydrogen peroxide (H_2O_2) and O_2.[37] H_2O_2 can undergo the Fenton reaction to form hydroxyl radical ($OH\cdot$).[38,39] Nitric oxide ($NO\cdot$), which is produced as a signaling molecule in high quantities during the respiratory burst by inducible nitric oxide synthase (iNOS)[40] can react with $O_2^{\cdot -}$ at near-diffusion-controlled limits to produce the strong oxidant peroxynitrite ($ONOO^-$).[41]

ROS can also be generated as a result of normal physiological processes. Aerobic tissues require oxidative respiration to synthesize ATP. The electron transport chain within mitochondria is a carefully controlled system that couples the movement of electrons to the creation of a proton gradient necessary to produce ATP. Leakage of electrons from the electron transport chain results in the formation of $O_2^{\cdot -}$ in the intermembrane space and the mitochondrial matrix.[42] Concentrations of $O_2^{\cdot -}$ within the matrix are estimated to range from 10-200 pM.[43,44] SODs act in both the mitochondria and the cytosol to remove the endogenously generated $O_2^{\cdot -}$ to limit its negative effects.[45]

The collection of radical and non-radical reactive species is generated during inflammation to combat the sources of the inflammatory stimuli, but host cells can also be caught in the cross-fire. ROS and RNS can react with DNA to form DNA adducts or produce strand breaks, both of which can contribute to mutations. Oxidants can also directly react with the side chains of amino acids on proteins. An example is the reaction of peroxynitrite with tyrosine to form nitrotyrosine, a modification that can disrupt protein function.[46] Of particular interest is the reaction of strong oxidants, $OH\cdot$ and $ONOO^-$, with polyunsaturated fatty acids (PUFAs) in cell membranes,

contributing to lipid peroxidation and the production of electrophiles. These electrophiles can react with proteins to form adducts that contribute to dysregulation of protein function.

Formation of Lipid Electrophiles

As noted above, ROS can react directly with DNA and proteins to form site-specific oxidative modifications. In addition, ROS can abstract hydrogen atoms from the *bis*-allylic position of PUFAs within cell membranes. Oxidation of PUFAs occurs via the common free radical initiation, propagation, and termination mechanism (Figure 3).[47] First, a radical initiator abstracts a hydrogen atom from a methylene group located between two double bonds of the PUFA (Figure 4). The carbon-to-hydrogen bonds at this position are relatively weak, allowing them to be readily broken.[47,48] The product is a delocalized radical across the carbon centers that make up the adjacent *cis* double bonds. This resonance-stabilized pentadienyl radical intermediate can proceed to the propagation steps of the radical mechanism, which includes oxygen addition, and hydrogen atom transfer. The addition of molecular oxygen to the carbon-centered radical leads to the formation of the lipid peroxyl radical. Transfer of a hydrogen atom from a nearby PUFA to the peroxyl radical results in formation of a hydroperoxide (LOOH) with termination of the reaction on the original oxidized lipid and propagation of the reaction via the radical formed on the second lipid. This step is slow in the overall radical mechanism as evidenced by the low rate constant for H-atom transfer,[49,50] suggesting that the peroxyl radical is relatively unreactive. Termination of the chain involves reduction of the peroxyl radical by a non-PUFA species.

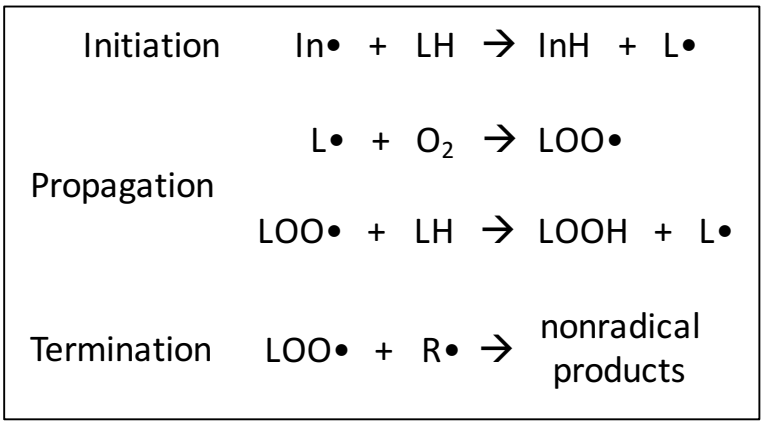

Figure 3. Radical mechanism of lipid peroxidation. Representative scheme for lipid (LH) peroxidation. An initiator radical (In·) abstracts an H-atom from a lipid to form a lipid radical (L·). This can react with molecular oxygen to form a lipid peroxyl radical (LOO·). This can act as an initiator to propagate the reaction. In the termination step, the lipid peroxyl radical can produce non-radical products.

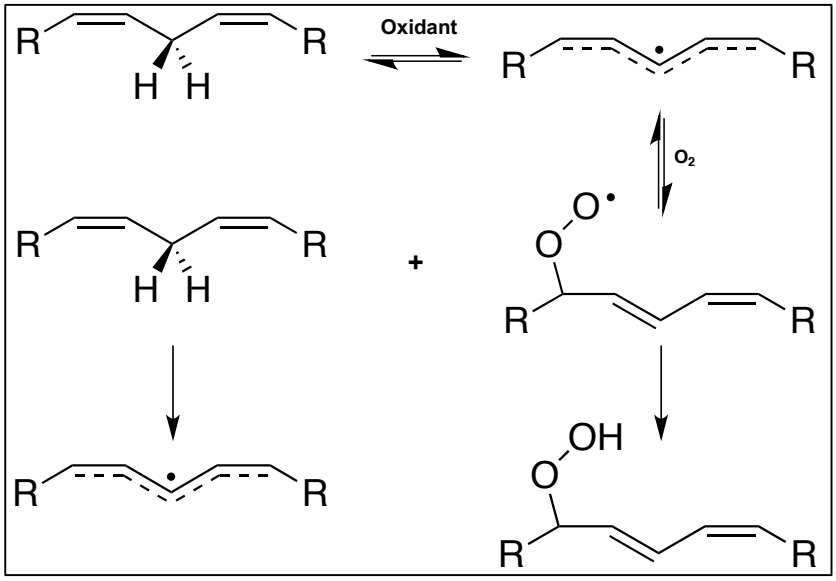

Figure 4. General mechanism of autoxidation of polyunsaturated fatty acids. In the first step, an oxidant abstracts an H-atom from the *bis*-allylic position of a PUFA to form a delocalized radical. This can react with molecular oxygen, forming a lipid peroxyl radical that can abstract an H-atom from a nearby PUFA to propagate the reaction while terminating itself by the formation of the lipid hydroperoxide.

An array of LOOH products can be formed as a result of the autoxidation process. In the simple example of linoleic acid, an 18 carbon fatty acid containing two *cis* double bonds, there are three possible positional isomeric products. Initial hydrogen abstraction occurs at C-11, resulting in a delocalized pentadienyl radical across five carbons. Formation of the peroxyl radical can occur

at C-9, -11, or -13, with preference being at C-9 and C-13 in the absence of a good hydrogen donor.[47,51] Quenching of the peroxyl radical forms 9-, 11-, or 13-hydroperoxy octadecadienoic acid (HPODE).[52]

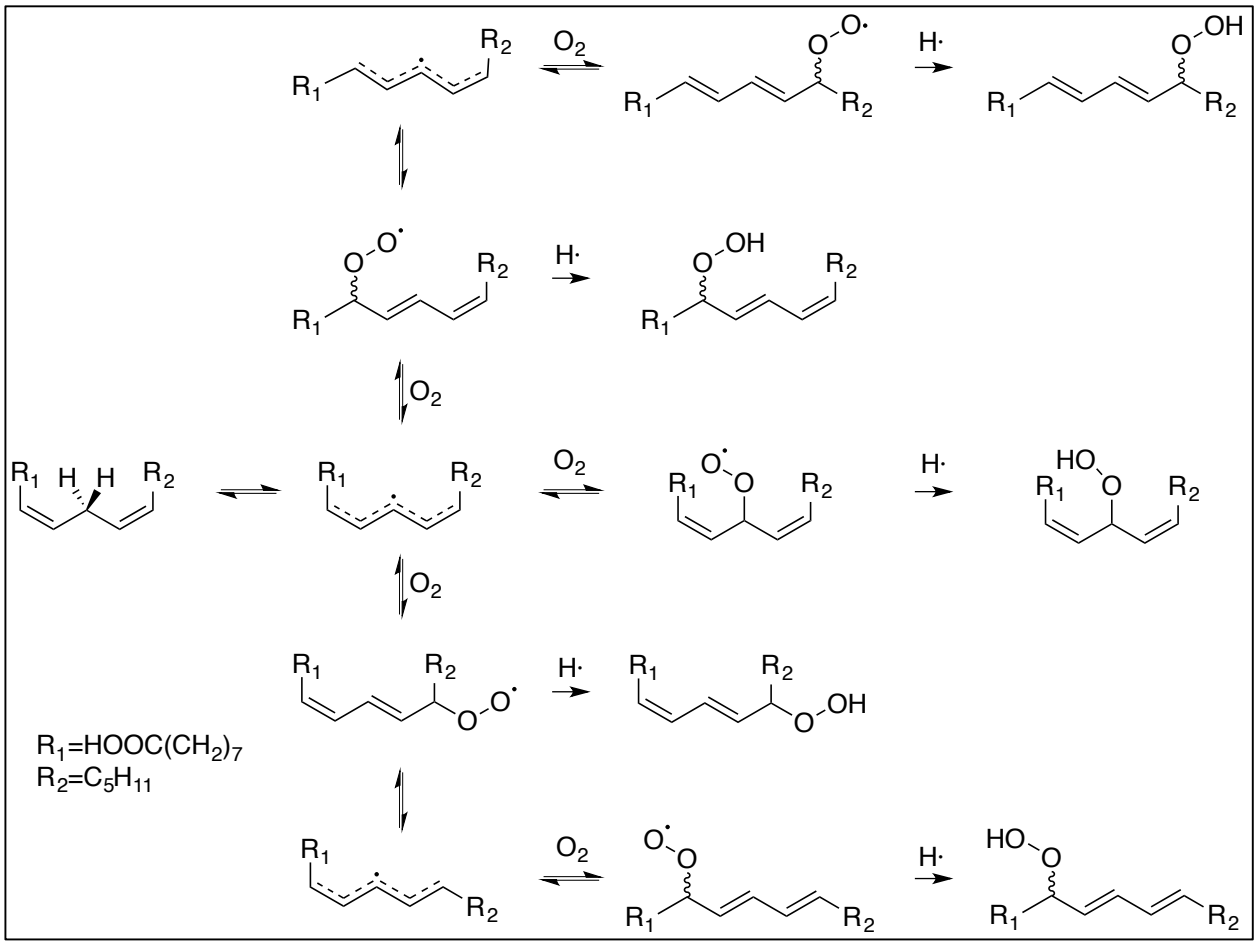

Figure 5. Autoxidation of linoleic acid. Abstraction of an H-atom at the *bis*-allylic position results in a delocalized radical, which can react with molecular oxygen at three different positions to generate peroxyl radicals. These peroxyl radicals can be quenched to form the HPODE, or reversed to reform the pentadienyl radical. Reversal results in isomerization of the *cis* double bond and represents a lower energy state.

It is the breakdown of the lipid hydroperoxide that mainly contributes to the formation of α,β-unsaturated aldehydes.[53] 4-Hydroxy-2-nonenal (HNE) was originally discovered by Hermann Esterbauer as the most cytotoxic product of lipid peroxidation. He identified HNE as a

peroxidation product of linoleic acid and arachidonic acid in the presence of ascorbate and $FeSO_4$ in aqueous solution, as well as from lipid in liver microsomes.[54,55] Today, HNE is one of the most intensely studied lipid electrophiles, and the mechanism of lipid hydroperoxide fragmentation that leads to its formation is widely debated. HNE can be generated from HPODEs or from other oxidized ω-6 fatty acids by Hock cleavage or β-scission (Figure 6).[54,56-60] Both of these fragmentation mechanisms can yield additional α,β-unsaturated aldehydes, such as 4-oxo-2-nonenal (ONE), malondialdehyde, and acrolein.[61,62] These electrophilic aldehydes show differing levels of reactivity to nucleophilic substrates within DNA and on proteins.

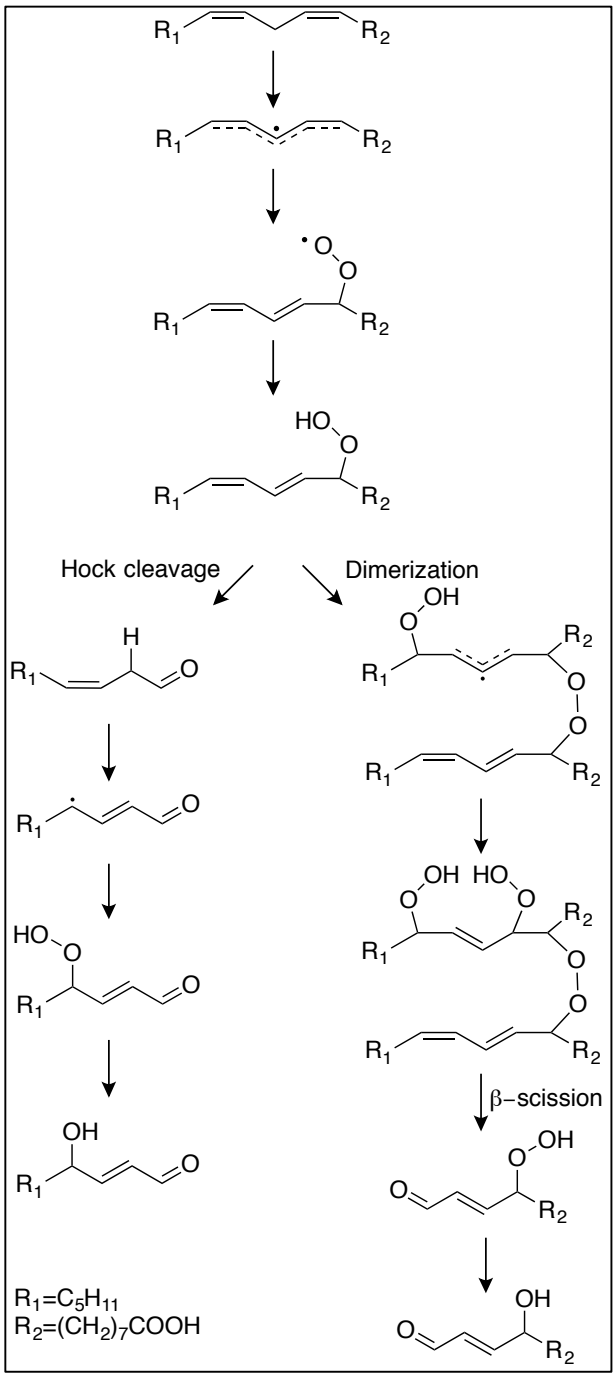

Figure 6. Mechanism of formation for HNE from linoleic acid. Two possible routes of HNE formation have been proposed from 9-HPODE. Hock cleavage of 9-HPODE followed by an H-atom abstraction produces 4-hydroperoxy-2-nonenal (HPNE), which is reduced to HNE. In a second possible mechanism, dimerization between 9-HPODE and 13-HPODE with an additional H-atom abstraction is followed by β-scission of the dimer to produce HPNE then HNE.

Mechanisms of Adduction by Reactive Aldehydes

HNE and ONE are of particular interest due to the physiologic and pathophysiologic levels that have previously been reported. Levels of HNE have been reported to range from 10 μM to as high as 5 mM, locally, in response to an oxidative insult.[63] The high levels of electrophile can contribute to extensive adduction of DNA bases and amino acid side chains. Protein adduction can disrupt cell signaling, alter gene expression, inhibit enzymatic activity, and initiate cell death by necrosis or apoptosis.

Since HNE is the most thoroughly studied lipid electrophile, numerous investigations of the relative reactivity of HNE with the nucleophilic protein side chains have been reported. Michael addition is the most common reaction observed between HNE and the thiol, imidazole, and amine of cysteine, histidine, and lysine residues, respectively, and *in vitro* studies have shown that HNE reacts with these residues in the rank order Cys >> His > Lys (Figure 7).[64] The hydroxyl at C-4 of HNE elicits an electron-withdrawing effect, contributing to increased electrophilicity of C-3.[63] The Michael adducts are stabilized by the formation of cyclic hemiacetals, and modifications on Cys and His are stable while those on the ε-amine of Lys are readily reversible.[64,65] Reduction of the more labile Michael adducts with $NaBH_4$ converts free aldehydes and ketones to the corresponding alcohol, making the adduct insensitive to a retro-Michael reaction.

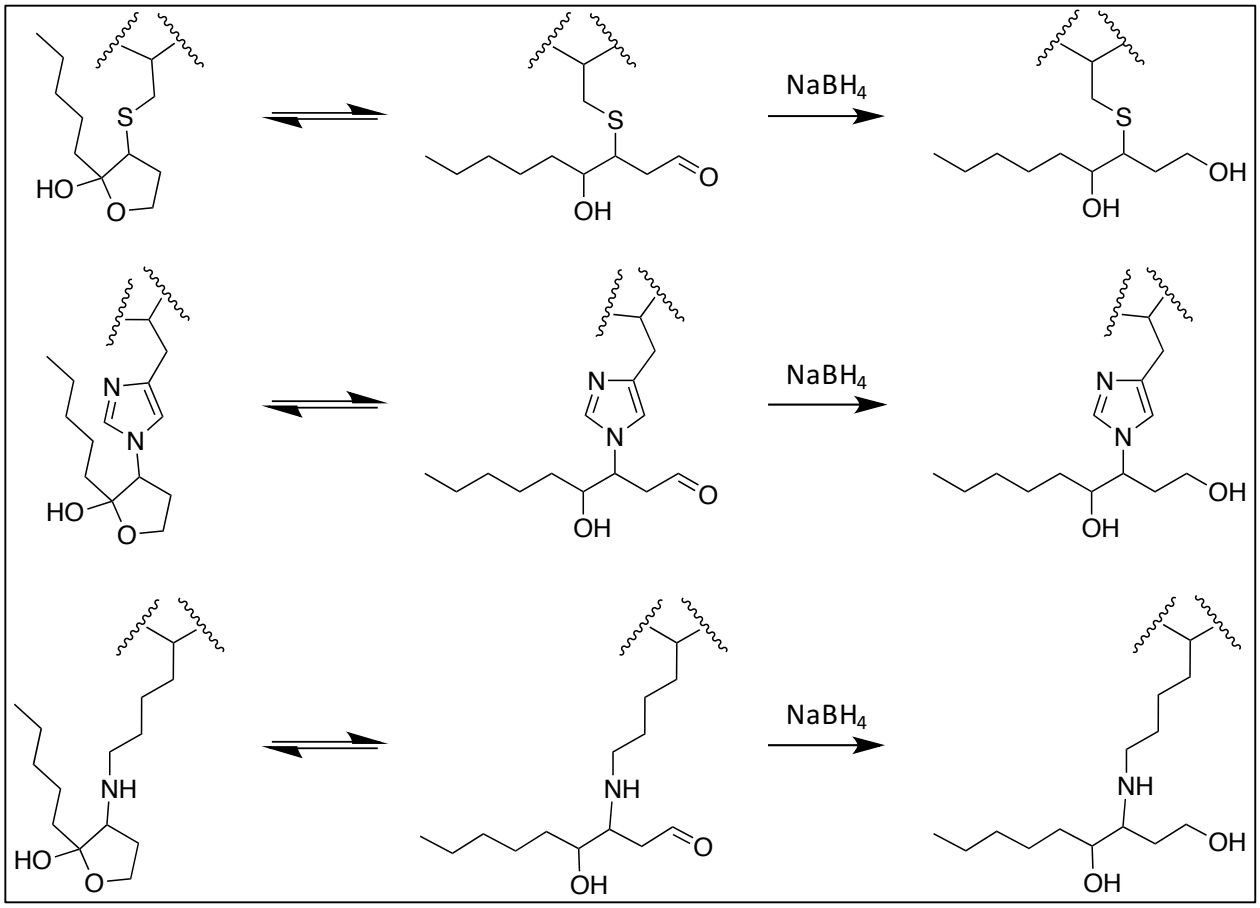

Figure 7. HNE Michael adducts. HNE reacts with Cys (top) His (middle) and Lys (bottom) to form the Michael adduct (center). These adducts and cyclize to form the hemiacetal (left) or be reduced with $NaBH_4$ to stabilize the adducts through reduction of the aldehyde (right).

Schiff base formation can occur by reaction of either HNE or ONE with Lys residues (Figure 8A). The products are labile, with adduct reversal occurring upon exposure to weak acid or heating;[66] however both HNE- and ONE-derived Schiff base adducts have been shown to undergo a cyclization to form a stable pyrrole (Figure 8B).[67,68] While this reaction occurs at levels significantly lower than those of Michael addition, the presence of the pyrrole adducts in diseased tissues from patients with Alzheimer's disease and in plasma of patients with atherosclerosis,[69,70] suggests that they are physiologically relevant and potential biomarkers.

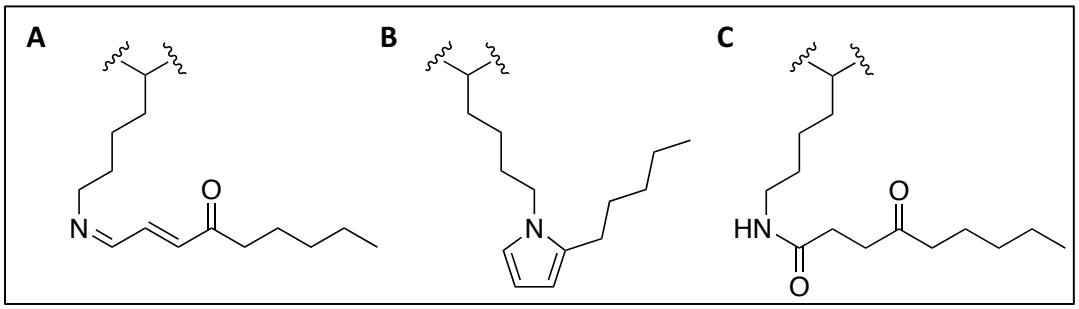

Figure 8. Lysine-specific adducts. A) ONE-derived Schiff base modification on Lys, which can also be formed with HNE. B) Cyclic pyrrole adduct derived from ONE or HNE. C) 4-Ketoamide adduct of ONE on Lys.

ONE displays unique reactivity toward Lys residues that was unappreciated until recent years. There have been numerous studies over past decades that wrongly identified the ONE-Lys modification as a Michael adduct due to the corresponding mass shift observed by mass spectrometry. In the mid 2000s, work from the Sayre laboratory confirmed that the reaction of ONE with Lys resulted in a mass shift of +154 *m/z* from native Lys, consistent with a Michael adduct. However, upon treatment with $NaBH_4$, the +154 *m/z* peak was replaced with one at +156 *m/z*. This mass shift was inconsistent with a reduced Michael adduct, which would result in a +158 *m/z* mass shift. The data led to the realization that the 4-ketoamide modification, rather than the Michael adduct, was the prevalent ONE adduct on Lys (Figure 8C).[71] The group went on to show that the 4-ketoamide adduct was chemically stable and long-lived, making it a significant marker for protein modifications by ONE.[72]

The ability to form cross-links between two nucleophilic amino acid side chains has previously been shown to occur with many α,β-unsaturated aldehydes. *In vitro* cross-links of HNE and ONE have been extensively investigated and characterized.[73-77] Consistent with its higher reactivity to single modifications,[78] ONE also displays a greater ability to form cross-links than HNE.[73] These cross-links can occur between two Lys residues, a Cys and a Lys residue, or a His and a Lys residue. Oe et al.[79] were the first to identify the site-specificity of an ONE cross-link

within a protein. Using bovine histone H4, the authors were able to identify an intrapeptide cross-link between His75 and Lys77 and proposed that an –HAK– motif was necessary for cross-link formation. This cyclic modification, containing the imidazole of the His and a Lys-derived pyrrole was hypothesized to have biological implications for transcription and gene expression.

Detection of Protein Adducts

Endogenous and Exogenous Electrophiles

There are two main approaches for investigating the effects of lipid electrophiles, each of which brings its own advantages and disadvantages. The first explores the generation of endogenous electrophiles in intact cells or animals subjected to a stimulus that contributes to an acute or chronic inflammatory response. An example is chronic ethanol consumption, which generates a panoply of reactive lipid aldehydes.[80] This is clearly the more biologically relevant scenario, as electrophiles are generated at physiological/pathophysiological levels at distinct locations and can affect relevant cells/tissues. However, the wide diversity of electrophiles that may be produced creates a great challenge in the identification of the precise chemical nature of the damage. In the absence of exhaustive mass spectrometric methods for the unbiased identification of protein adducts, determination of the targets and the adducting species is difficult, if not impossible.

In the exogenous addition approach, the electrophile of interest, such as HNE or ONE, is added in a bolus dose to cells or purified proteins. The added HNE can then enter the cells to adduct proteins and elicit a cellular response or react directly with the protein in solution. Following addition of electrophile to the buffer, lysate, or cell culture medium, samples are incubated for a desired amount of time to allow for protein adduction prior to detection, isolation,

and/or quantitation. While this approach may not be the most physiologically relevant due to the addition of high concentrations of exogenous electrophile, it remains the best approach for differentiating the targets of structurally defined electrophiles.

Regardless of whether endogenous or exogenous electrophile-mediated damage is the focus of study, methods are required to capture and identify the targets of that damage. Over the years, a variety of techniques have been developed that vary in their specificity and sensitivity. The most widely used of these will be discussed below, with a focus on identifying damage caused by HNE and/or ONE.

Labeling of Protein Carbonyls

HNE and ONE contribute to a constellation of protein modifications, and since their original discovery, many methods have been employed to label, detect, isolate, and/or quantitate these adducts. While the small difference in structure between the two electrophiles, consisting of only two H-atoms, renders ONE much more reactive than HNE, their adducts are nearly indistinguishable by many labeling techniques. The majority of labeling methods employs a chemical derivatization to tag modified proteins, taking advantage of the free aldehyde that remains following Michael addition. These approaches, however, have a number of drawbacks. First, they will only detect adducts with a carbonyl, and would therefore not detect Schiff base adducts or cross-links. Second, the approach will detect any free aldehyde or ketone, thereby lacking the specificity for HNE or ONE adducts. An advantage to some of these approaches is that they can be used for labeling endogenously generated protein adducts from structurally similar electrophiles, making them ideal for *in vivo* studies.

Hydrazide chemistry is commonly used for the chemical derivatization of carbonylated proteins. Hydrazides react with aldehydes and ketones to form a reducible hydrazone, and a number of reagents have been developed to utilize this chemistry (Figure 9). Of particular interest is biotin hydrazide, which is used to biotinylate carbonylated proteins, making it amenable to avidin detection/capture (Figure 9A). An alternative approach is the use of dinitrophenylhydrazine (DNPH) followed by the immunologic detection of carbonylated proteins using antibodies directed against DNP (Figure 9B). Although this approach suffers from the lack of specificity noted above, an advantage is that it can be used to capture proteins modified by endogenous electrophiles, requiring only the presence of a retained carbonyl in the adduct.

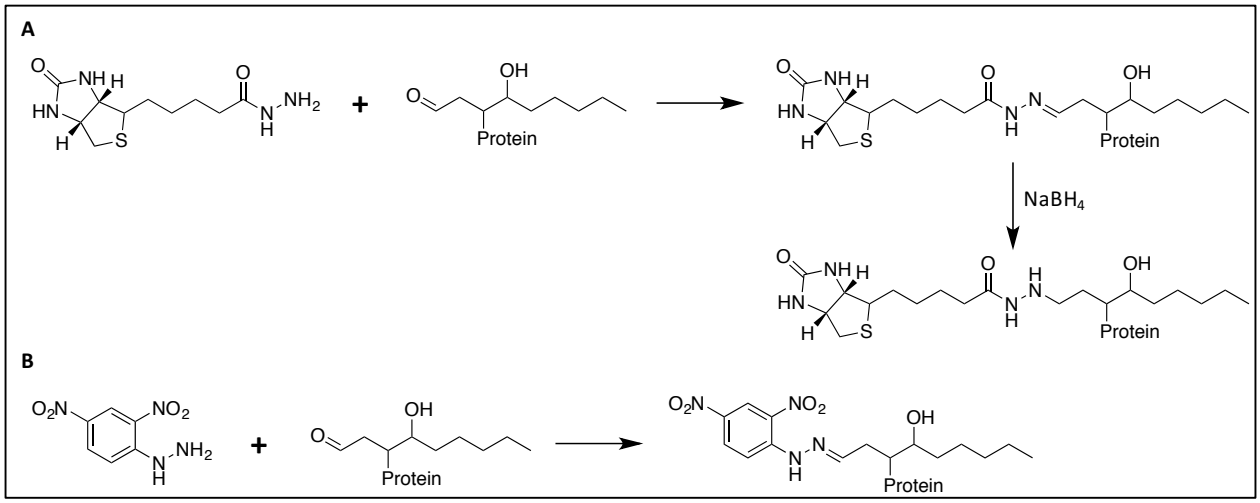

Figure 9. Protein adduct detection with hydrazide chemistry. A) Reaction of biotin hydrazide with an HNE adduct on a protein to yield a Schiff base. Reduction of the Schiff base with $NaBH_4$ stabilizes the product. B) DNPH reaction with an HNE adduct on a protein, resulting in a Schiff base. Antibodies can detect the dinitrophenyl group for visualization of modified proteins.

Click Chemistry of Alkyne-Tagged Electrophiles

A more recently developed method for protein adduct labeling utilizes click chemistry. Originally discovered by Rolf Huisgen in the 1960s,[81] click chemistry approaches were refined by Barry Sharpless in the early 2000s for application to biological systems.[82] The reaction requires an

azide and an alkyne, which in the presence of a Cu(I) catalyst, undergo a 1,3-dipolar cycloaddition to form a 1,2,3-triazole (Figure 10A). *Tris*-(benzyltriazolylmethyl)amine (TBTA) can also be employed as a triazole ligand to stabilize the Cu(I) during the reaction.[83] The application of click chemistry to the study of HNE and ONE adducts was pioneered by the Marnett, Porter, and Liebler laboratories.[5,84,85] Alkyne analogues of HNE (Figure 10B) and ONE (Figure 10C) were synthesized to contain a terminal alkyne. These molecules retained the electrophilic reactivity of the native analogues, but could be conjugated to azido-biotin compounds to enable isolation and detection by avidin affinity methodology (Figure 10D). This approach has provided large advantages over the traditional carbonyl detection methods, mainly due to the increased specificity and decreased background; however, it is limited to the detection of damage caused by exogenous electrophiles.

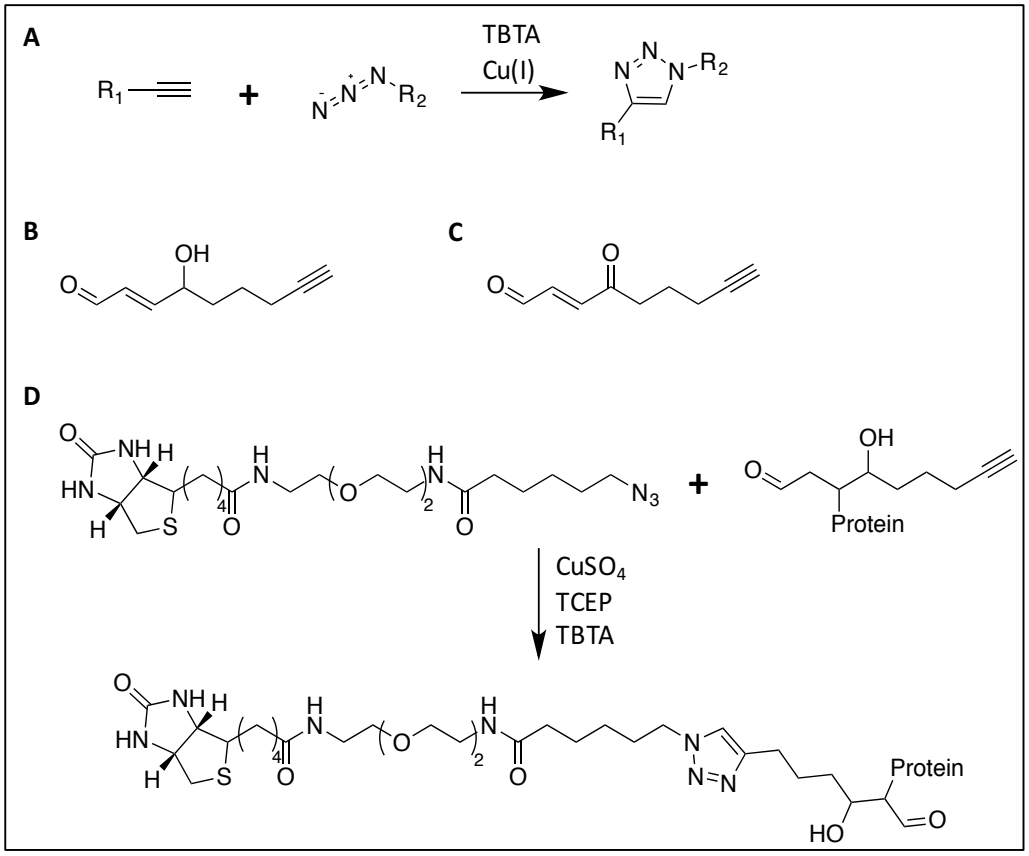

Figure 10. Click chemistry. A) Representative click chemistry reaction. In the presence of a Cu(I) catalyst and TBTA, an alkyne and an azide cyclize to form a 1,2,3-triazole. B) Alkyne analogue of HNE (aHNE). B) Alkyne analogue of ONE (aONE). D) Click chemistry scheme developed by Vila et al.[5] Adducted proteins are conjugated to an azido-biotin for selective isolation or detection.

Detection of Chemically Labeled Proteins

These various labeling techniques provide different avenues for the detection and isolation of adducted protein. Proteome-wide visualization of carbonylated proteins can be achieved by western blot. For example, following derivatization with DNPH, carbonylated proteins can be detected with anti-DNPH antibodies in what is commonly referred to as an "Oxyblot." Both biotin hydrazide and click chemistry using alkyne analogues allow for detection by western blot using streptavidin probes in place of antibodies.

In proteomic-based approaches, biotin-tagged proteins can be isolated using streptavidin beads, washed, and eluted. Proteins are separated by SDS-PAGE and stained with Coomassie blue,

allowing for excision of bands for in-gel digestion coupled with LC-MS/MS. Although peptides identified by this approach do not contain the adduct, they enable identification of the protein targets of adduction.

Whole Proteome Analysis of Adducted Proteins

In 2009, Codreanu et al.[86] developed the first whole proteome inventory of proteins modified by HNE. The authors treated cells exogenously with HNE and used biotin hydrazide to biotinylate carbonylated proteins. Following streptavidin capture, isolated proteins were subjected to mass spectrometry-based proteomics analysis. This approach identified 1500+ captured proteins, but only 417 of these showed a statistically significant increase in adduction with increasing HNE. The lack of dose-dependency between adduct amount and HNE concentration suggested that a high number of identifications were nonspecific, due either to the reactivity of biotin hydrazide with protein carbonyls that did not result from adduction or to non-specific binding of proteins to the capture beads.

The emergence of the click chemistry approach to study HNE and ONE allowed for more in-depth studies into the specific targets of the electrophiles along with a better understanding of their differential reactivity. In 2014, Codreanu et al.[84] refined their proteomic approach to take advantage of the increased specificity of click chemistry. In these studies, cells were treated with alkynyl-HNE (aHNE) or alkynyl-ONE (aONE), and adducted proteins were selectively conjugated to an azido-biotin tag containing a UV-cleavable linker (Figure 11). Tagged proteins were then captured on streptavidin beads, and the UV-cleavable linker in the biotin tag enabled elution of the adducted proteins following exposure to UV light. This eliminated the need for boiling samples to

dissociate them from the streptavidin beads, and led to a substantial decrease in background. The approach identified 1119 proteins in RKO cells that were targets of aHNE and/or aONE.

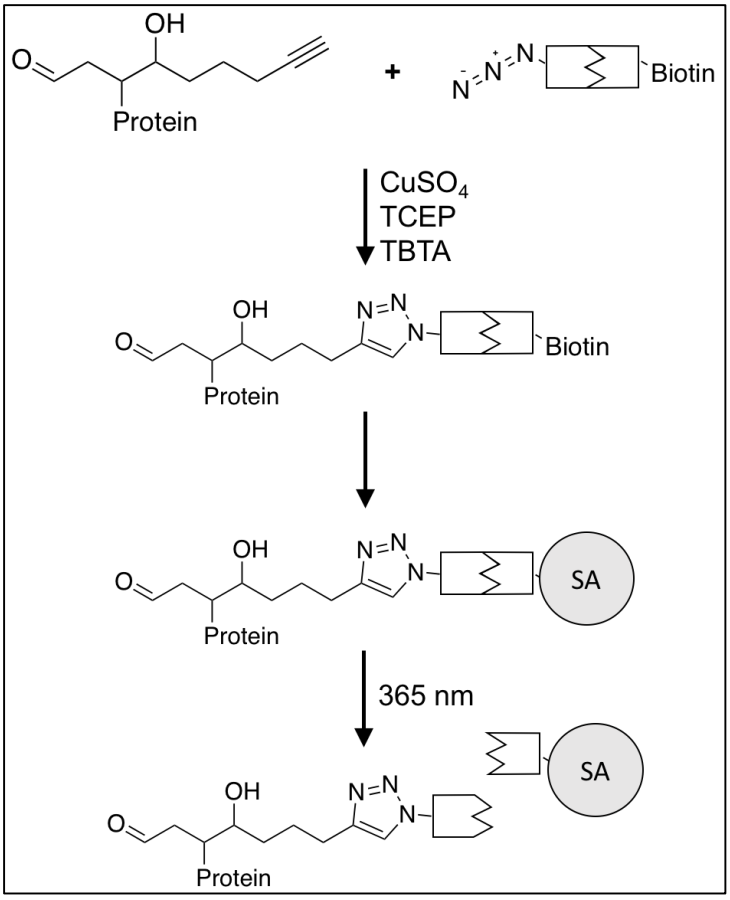

Figure 11. Click chemistry with a photo-cleavable biotin. Adducted proteins are conjugated to a UV-cleavable N_3-biotin under standard click chemistry conditions. After binding to streptavidin bead and washing to remove nonspecific binding, adducted protein can be selectively eluted with exposure to 365 nm UV light.

One striking feature of the adduct inventory generated by Codreanu et al.[84] was the differential target specificity between aHNE and aONE. Of 1119 adducted proteins, only 595 were targeted by both electrophiles. There were 252 proteins that were only targets of aONE, and 272 proteins that were only adducted by aHNE. These large differences in protein susceptibility may be attributed to the relative reactivity of HNE and ONE to different amino acids. When the protein

inventories were further investigated, a distinct difference in the nuclear targets of adduction was noted. Specifically, histone proteins, which are rich in Lys residues, were major targets of aONE adduction, whereas other chromatin-associated proteins, such as histone acetyl transferases that lack Lys and have multiple Cys and His residues, were targets of aHNE. These stark differences in protein targets highlight the importance of electrophile reactivity to specific nucleophilic targets and provide new avenues for the investigation of the functional implications of these adducts.

Site-Specific Detection of Protein Adducts

The proteomic inventories described above have provided a wealth of knowledge on the protein targets of HNE and ONE in the cell, but the approaches employed did not allow for determination of the specific residue adducted within each protein. Site-specific detection of adducts remains a challenge at the proteome-wide scale. A newer method, developed in Benjamin Cravatt's laboratory to investigate Cys targets of HNE in cells, employs a TEV-cleavable, isotopically labelled iodoacetamide-alkyne probe to modify free reactive Cys (Figure 12).[2] Cys residues adducted with HNE are not tagged with the probe. Click chemistry is then performed to biotinylate tagged proteins, which are then isolated with avidin capture. Captured proteins are digested with trypsin, followed by TEV protease to release the tagged peptides for proteomic analysis. The loss of a peptide with increasing concentrations of HNE suggests that the Cys in the peptide is a site of HNE modification.

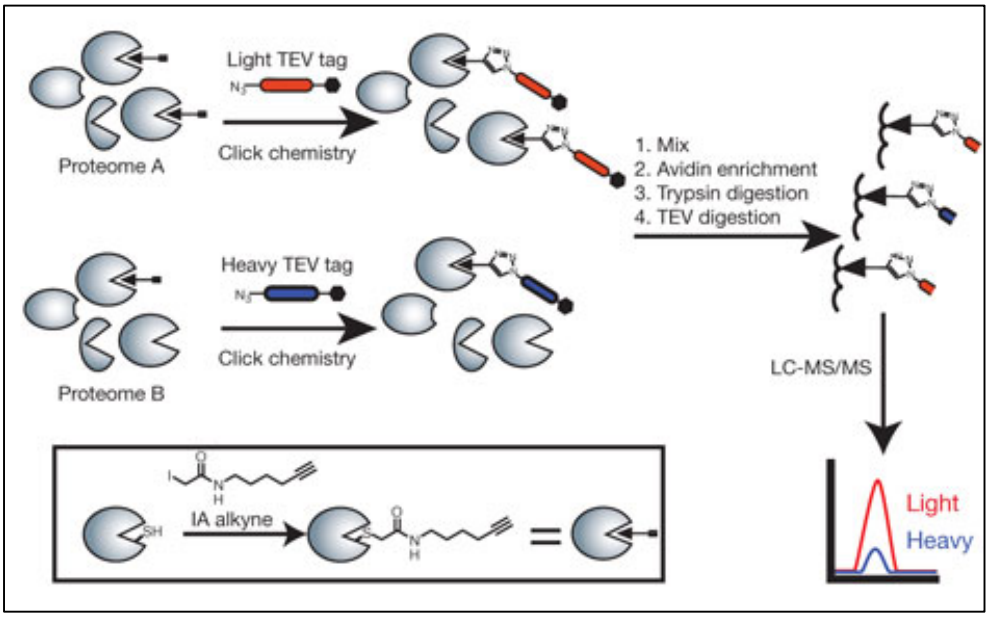

Figure 12. Activity-based protein profiling for determination of HNE-adducted Cys. Reprinted by permission from Macmillan Publishers Ltd: *Nature Protocols* Weerapana et al. (2010) *Nature* 468:790-5. Copyright 2010.[2]

While this approach allows for a larger scale analysis of adduction sites, it is far from comprehensive. First, since the method only targets Cys residues, adducts of His and Lys are not detected. Second, this approach does not directly interrogate the HNE adduct, but rather implies an adduct with the loss of a reactive Cys residue. Finally, the method lacks specificity for any particular electrophile. Despite the fact that it is based on a concentration-dependence relationship with bolus addition of exogenous electrophile, a large number of additional electrophiles may be generated during the oxidative stress response to the toxicity of the exogenous electrophile exposure. Therefore, while adduction of specific Cys residues can be identified with this technique, the exact identity of the adducting species remains uncertain.

A direct, global approach was developed by Yang et al.{Yang, 2015 #526} In this method, cells are treated with aHNE and click chemistry is performed with isotopically labelled, photocleavable azido-biotin. Adducted proteins can be isolated and tandem mass spectrometry used to determine the sites of adduction and the amount of each modified residue. This approach

has large advantage in that it directly maps the precise site of adduction, as opposed to the indirect mapping in the Cravatt approach. The drawbacks of this method is that it does not detect all sites of adduction. While the proteomic inventory shows >1000 proteins as targets of aHNE adduction, only ~400 residues were identified as specific sites of adduction.

Currently, the most comprehensive means to identifying specific sites of modification is by mass spectrometric analysis of recombinant, immunoprecipitated, or otherwise purified protein. For example, recombinant protein may be adducted *in vitro* with electrophile, reduced with $NaBH_4$, digested with trypsin, and analyzed by mass spectrometry. The identified peptides can then be searched with the possible mass shifts for each residue of interest. Variations of this method can be applied to proteins immunoprecipitated from cells treated with HNE. In this case, utilizing overexpressed tagged cDNA constructs facilitates isolation of the protein of interest and provides larger amounts of material for analysis.[87] Recently, Galligan et al.[88] utilized a proteomic approach to identify specific sites of adduction on histones. Chromatin from cells treated with ONE was extracted with a high salt buffer, providing an extract that was highly enriched with histones. The proteins were separated by SDS-PAGE and in-gel digested for proteomic analysis, leading to the discovery of the 4-ketoamide adduct on histones.

The identification of adducts at specific residues remains a challenge in the field. The best method to determine sites of adduction requires pure proteins, or low complexity protein isolates, coupled with exhaustive computational searches for possible adducts and manual validation of adducted peptides. While very labor-intensive and low-throughput, this is the most comprehensive approach to adduct discovery and insight into the possible impact that adducts may have on protein function.

Cellular Implications of Protein Adduction by Lipid Peroxidation Products

Antioxidant Responses to Oxidative Stress and Lipid Electrophiles

Oxidative stress and lipid peroxidation can be particularly damaging to the cell, but a number of pathways and antioxidant mechanisms have evolved to combat toxic insults that can arise. The primary function of these various antioxidant pathways is to convert the reactive molecules to less reactive metabolites. Enzymatic antioxidants that work directly to remove oxidants from the cell have various levels of specificity toward their substrates. As described above, SOD acts specifically on $O_2^{\cdot -}$ to form H_2O_2 and O_2, and expression of protein isoforms in different subcellular locations contributes to cellular defense.[89] Similarly, catalase converts H_2O_2 produced by SOD to H_2O and O_2, thereby preventing the formation of the more harmful $HO\cdot$ via the Fenton reaction.[90] There are many less specific antioxidant enzymes that act on a range of exogenous and endogenous oxidants. An example is the glutathione peroxidase family that reduces organic hydroperoxides to their corresponding alcohols.[91]

Many antioxidant enzymes, such as glutathione peroxidases, utilize glutathione as a cofactor for detoxification. Glutathione (GSH) is an endogenously generated small molecule that has the primary function of protecting cellular components. The action of GSH as both a nucleophile and a reductant contributes to the detoxification of reactive electrophiles and ROS.[92] While most of these defense mechanisms are present under basal conditions, regulation at the gene expression level can increase their availability in response to exposure to toxicants such as HNE and ONE in an attempt to maintain homeostasis.

Gene Expression Alterations

West and Marnett[93] were the first to exhaustively explore global gene expression alterations in response to exogenous HNE exposure. At sub-cytotoxic concentrations of HNE, significant changes in gene expression were only observed in antioxidant response element-(ARE)-regulated genes. These genes are upregulated in response to oxidative stress conditions, including electrophile exposure. The encoded proteins assist in detoxifying oxidant-dependent reactive species in the cell by multiple mechanisms, including synthesis of GSH and maintenance of protein structure. Cytotoxic levels of HNE induced significant alterations in the heat shock, ER stress, and nutrient deprivation responses in addition to ARE upregulation.

Further investigations utilizing RNA-Seq demonstrated an even larger number of gene expression changes in response to HNE exposure.[94] Genes associated with glutathione metabolism, cell cycle regulation, pyrimidine metabolism, and MAPK signaling were overrepresented in the dataset, due to large expression changes in those pathways. These data also revealed changes in transcript isoforms. In one example, the protein NEDD4 has two highly expressed transcripts, one protein-coding and the other noncoding. HNE treatment resulted in a significant decrease in the protein-coding transcript, while the noncoding transcript remained unchanged. Thus, the data revealed HNE-dependent gene expression regulation on multiple levels, and suggested the interesting possibility that alterations in chromatin or transcription factors and transcriptional machinery may contribute to the observed isoform switches.

Disruption of Cell Signaling Pathways by Electrophile Adduction

Electrophiles have the ability to modulate gene expression by direct adduction of transcription factors or their regulatory proteins, thereby altering transcription factor binding to the

target *cis*-regulatory regions. For example, electrophiles can activate the ARE and electrophile response element (EpRE) to increase transcription of genes encoding phase II detoxifying enzymes,[95,96] regulate expression of heat shock proteins to maintain protein structure during oxidative stress, or inhibit additional pro-inflammatory responses.

Electrophile stress is mainly sensed through the Kelch-like ECH-Associated Protein 1 (Keap1) and the associated Nuclear Factor (Erythroid Dervied-2)-like 2 (Nrf2) pathway. Under normal conditions, cytosolic Keap1 binds to Nrf2 and promotes its degradation via cullin-3-dependent ubiquitination and proteasomal degradation.[97,98] Under conditions of oxidative stress, oxidants and lipid electrophiles modify Cys residues on Keap1, resulting in dissociation of Nrf2. The reduction in Nrf2 degradation results in increased levels and its accumulation in the nucleus.[99,100] There, Nrf2 forms heterodimers with Maf proteins and other transcription factors to activate ARE-dependent gene expression.[101] Target genes include heme oxygenase,[102] glutathione S-transferases,[103] glutamate-cysteine ligase,[104] and others.[105]

Heat shock proteins (HSPs) inhibit protein aggregation and oxidation as well as assist in protein translocation by acting as molecular chaperones.[106] Expression of HSPs is predominantly regulated by the transcription factor, heat shock factor 1 (HSF1). Under normal conditions, HSF1 is localized in the cytosol where it interacts with HSP90 and HSP72, a member of the Hsp70 family.[107,108] Electrophile adduction or oxidation of HSP90 and HSP72 results in dissociation of the complex, HSF1 translocation to the nucleus, trimerization, phosphorylation, and binding to heat shock response elements.[109] HNE has been shown to adduct Cys572 of HSP90 and Cys267 of HSP72. Both of these modifications inhibit chaperone activity.[110,111] HSF1 binding to heat shock response elements induces transcription of HSPs to maintain protein homeostasis and promotes BAG3 expression to inhibit apoptosis.[112,113]

Regulation of NF-κB, a transcription factor that modulates inflammatory gene transcription, by electrophiles has been extensively investigated due to the association of oxidatives stress with inflammation. Under normal conditions, NF-κB remains in the cytosol, bound to its inhibitor, IκB. IκB kinase (IKK) is activated in response to pro-inflammatory stimuli and phosphorylates IκB, resulting in its ubiquitination and proteasomal degradation. In the absence of IκB, NF-κB accumulates and translocates to the nucleus where it induces transcription of pro-inflammatory cytokines, chemokines, and enzymes. HNE adduction has been shown to be inhibitory to NF-κB activation, both indirectly and directly. Indirectly, HNE adducts the conserved Cys179 on the activation loop of IKKβ, contributing to IKK inhibition, stabilization of IκB, and retention of NF-κB in the cytosol.[114] A similar, indirect inhibitory mechanism has been proposed for 15-deoxy-$\Delta^{12\text{-}14}$-prostaglandin J_2 ($15dPGJ_2$), an electrophilic metabolite of prostaglandin D_2.[115] $15dPGJ_2$ was also shown to inhibit NF-κB directly by adduction of Cys38 on the DNA-binding domain of the transcription factors p65 subunit, thereby contributing to loss of transcriptional activity.[116]

Dissertation Aims

The main objective of this dissertation is to better understand the direct effects of protein adduction by HNE and ONE. Years of work have been dedicated to developing chemical tools to identify the targets of these electrophiles. However, this work has provided to us a massive proteomics library and gene expression data that require a more in-depth investigation into specific pathways of interest.

Chapter II describes investigations of a key cell cycle protein that is adducted by HNE. I was able to show that adduction of this protein occurs at multiple sites *in vitro* and in cells and

results in kinase inactivation and cell cycle inhibition. Chapter III explores the inactivation of the isomerase Pin1 by an ONE cross-link and proposes a mechanism of cross-link formation. A computational analysis based on this mechanism identifies additional proteins that may be cross-linked by ONE. Chapter IV presents a novel method, Click-Seq, for the isolation of DNA associated with adducted histones. We developed this method to investigate the site-specificity of these chromatin modifications in the genome, which can provide information as to potential gene expression alterations that may occur in response to histone modification. Histone adducts are shown to be long-lived, suggesting they may impact gene expression and chromatin condensation. Levels of the 4-ketoamide adduct on Lys residues were comparable to low-abundance canonical histone modifications, suggesting that these adducts may have biological significance.

CHAPTER II

COVALENT MODIFICATION OF CDK2 BY 4-HYDROXYNONENAL AS A MECHANISM OF INHIBITION OF CELL CYCLE PROGRESSION

Introduction

Oxidative stress results from an imbalance between reactive oxygen species (ROS) generation and the antioxidant defenses of the cell and is a contributing factor in a number of diseases, including cancer, atherosclerosis, neurodegenerative disease, and asthma.[70,117-119] ROS elicit their deleterious effects via reactions with cellular biomolecules, including proteins, DNA, and polyunsaturated fatty acids (PUFAs).[120] The oxidation and subsequent decomposition of PUFAs result in the formation of reactive lipid aldehydes, such as 4-hydroxy-2-nonenal (HNE).[47] These lipid electrophiles are capable of forming covalent adducts with nucleophilic residues on proteins (i.e. Cys, His, and Lys), often proving detrimental to protein function.[66,121]

Cell cycle progression is a tightly controlled process involving a network of signaling events required to maintain genomic fidelity and prevent aberrant cell growth. CDK2 regulates the transition from G1 to S-phase and progression through S-phase via interactions with temporally expressed cyclin partners at different phases in the cell cycle.[122,123] The interaction between CDK2 and Cyclin E in late G1-phase results in hyperphosphorylation of Rb, a main tumor suppressor responsible for inhibiting DNA replication. This hyperphosphorylation causes the complete dissociation of the Rb/E2F1 complex, allowing for E2F1-mediated expression of S-phase genes

and entry into S-phase.[124] During this time, Cyclin A is expressed, further modulating CDK2 activity, so Rb remains hyperphosphorylated throughout S-phase. Under DNA damage conditions, Rb remains hypophosphorylated and bound to E2F1, thereby inhibiting cell cycle progression.[125,126,127] The result is G1 arrest until the damage is repaired and the inhibitory signals are removed or the cell undergoes apoptosis.

Previous studies have investigated the role of lipid peroxidation products, specifically HNE, in the regulation of the cell cycle.[128] Early studies in *S. cerevisiae* revealed that treatment with HNE inhibits cells from entering S-phase, suggesting a defect at the G1/S restriction point, and further studies in mammalian cells have yielded similar results.[129] Treatment of human leukemia and neuroblastoma cell lines with HNE led to a halt in the cell cycle at G0/G1, by both p53-dependent and independent mechanisms.[130,131] In the p53 wild-type neuroblastoma cell line, SK-N-BE, HNE increased levels of p53 and p21 after a 24 h treatment, resulting in G1 arrest. In the p53-deficient leukemic cell line, HL-60, a rapid decrease in Rb phosphorylation coupled with an increase in Rb/E2F1 complexes following HNE treatment is indicative of G1 arrest. In those cells, p21 was not induced until 12 h following HNE treatment, suggesting that a more immediate inhibition of G1-phase CDKs allowed for the maintenance of intact Rb/E2F1 complexes through suppression of Rb hyperphosphorylation.

While these previous studies demonstrate a role for HNE in cell cycle inhibition, the precise mechanism leading to this inhibition remains unclear. Recently, we have utilized alkynyl HNE (aHNE), the ω-alkyne analog of HNE, to identify adducted cellular proteins. aHNE maintains the reactivity of HNE in cells, and it allows for *post-hoc* biotinylation using click chemistry to selectively isolate modified proteins.[86,5] Proteomic analysis identified CDK2 as a target of aHNE, and adduction increased with increased electrophile concentration linearly over the concentrations

studied.[84] Gene expression data from HNE-treated RKO cells provided further insight into pathways significantly altered by HNE treatment. A systems analysis approach that integrates proteomic and gene expression data revealed that treatment of cells with HNE not only results in modification of CDK2, but leads to significant decreases in the genes controlled by CDK2 activation.[132] These data suggest that HNE modification of CDK2 could result in cell cycle arrest at the G1/S-phase transition. Here, we show that modification of recombinant CDK2 by HNE disrupts its kinase activity. We identify the major sites of HNE-mediated CDK2 modification and use aHNE to define the time course of CDK2 adduction in cells. We further show that HNE inhibits CDK2 activity in intact cells, suggesting that HNE-mediated CDK2 kinase inactivation is a direct contributor to cell cycle disruption. Finally, we show that HNE delays entry into S-phase by a mechanism that does not depend on induction of p53 or p21, supporting a role for CDK2 inactivation in that process.

Materials and Methods

Materials and Reagents. All reagents were purchased from Sigma Aldrich (St. Louis, MO) unless otherwise stated. HNE, 8,9-alkynyl-HNE (aHNE), and UV-cleavable azido-biotin were synthesized in the laboratory of Dr. Ned Porter at Vanderbilt University as previously described.[5] Cell culture medium and 1X Dulbecco's Phosphate Buffered Saline (DPBS, pH 7.2) was purchased from Invitrogen (Grand Island, NY). Fetal bovine serum (FBS) was obtained from Atlas Biologicals (Ft. Collins, CO). Recombinant CDK2 protein was purchased from Abcam (Cambridge, MA), and CDK2-Cyclin E and CDK2-Cyclin A recombinant complexes were purchased from EMD Millipore (Billerica, MA). Anti-CDK2 (M2), anti-actin, and Protein A/G Plus Agarose Beads were from Santa Cruz Biotechnology (Santa Cruz, CA). Anti-pT160 CDK2

and anti-PARP antibodies were from Cell Signaling Technologies (Danvers, MA). Anti-cyclin E1 [HE12], anti-p27 KIP1, anti-Rb (phospho T821), anti-cyclin A2 [E23.1], and anti-p21 antibodies were purchased from Abcam. All SDS-PAGE and western blot supplies were obtained from Bio-Rad (Hercules, CA) unless otherwise noted. Streptavidin Sepharose High Performance beads, γ-^{32}P-ATP, calf histone H1 protein, and dithiothreitol (DTT) were purchased from GE Life Sciences (Pittsburg, PA), PerkinElmer (Santa Clara, CA), EMD Millipore, and Research Products International (Mt. Proscpect, IL), respectively.

Cell Culture and Treatments. The human colorectal cancer cell line, RKO, was obtained from American Type Culture Collection (ATCC, Manassas, VA). Cells were cultured in Dulbecco's Modified Eagle Medium (DMEM) with 10% FBS at 37°C with 5% CO_2. Electrophiles were dissolved in DMSO and added to cell culture medium with a final concentration of less than 0.1% DMSO. Concentrations of HNE used in the studies were not cytotoxic as a result of the limited length of exposure and the high concentrations of glutathione in RKO cells.[133,84]

Flow Cytometry for Cell Cycle Analysis. Cells were serum-starved for 24 h to synchronize in G1/G0. Cells were then pretreated with 30 μM HNE or DMSO for 1 h in serum-free medium followed by release into medium containing 10% FBS and harvest at the indicated times. During collection, cells were washed with 1X DPBS (pH 7.2), trypsinized, and washed a second time with 1X DPBS. Cells were fixed with ice-cold absolute ethanol overnight at -20°C, then collected by centrifugation at 1000 *x g* for 5 min and washed twice with 1X DPBS. Following resuspension in 1 ml 1X DPBS, samples were incubated at 37 °C for 15 min with 50 μl of 1mg/ml RNase A, cooled to room temperature (RT) and stained with propidium iodide at a final concentration of 20 μg/ml.

Samples were stored at 4°C in the dark and analyzed on a 3-laser BD LSRII flow cytometer (BD Biosciences, Franklin Lakes, NJ).

Protein Extraction. Cells were scraped into medium, collected by centrifugation at 500 *x* g for 5 min, and washed twice with 1X DPBS. Cells were lysed for 10 min on ice in RIPA buffer [50 mM Tris (pH 7.4), 150mM NaCl, 1% NP-40, 0.1% SDS, 0.5% sodium deoxycholate, 1mM EDTA] containing protease and phosphatase inhibitors (Sigma-Aldrich, St. Louis, MO) and centrifuged at 16,000 *x g* for 20 min. The supernatant was collected, and the pellet was discarded. The BCA assay was used to determine protein concentrations according to manufacturer's protocol (Thermo Fischer Scientific, Waltham, MA).

Click Chemistry. Cell lysates (1 mg protein) were reduced with 20 mM $NaBH_4$ and subjected to click chemistry according to a previously described method.[84] Briefly, the lysates were incubated with 1 mM $CuSO_4$, 1 mM tris(2-carboxyethyl)phosphine, 0.1 mM tris(benzyltriazolylmethyl)amine, and 0.2 mM UV-cleavable azido biotin for 2 h at RT with end-over-end mixing. Protein was precipitated with 2 volumes of ice-cold methanol and resolubilized in 0.5% SDS with sonication and mixing. Streptavidin beads were added overnight at 4 °C in the dark with end-over-end mixing, washed twice each with 1% SDS, 4 M urea, 1 M NaCl in 1X DPBS, and 1X DPBS, and adducted proteins eluted in water under 365 nm UV light for 90 min. Eluates were dried under nitrogen and resuspended in water.

SDS-PAGE and Western Blots. Samples were denatured in 2X Laemmli sample buffer with 5% β-mercaptoethanol and heated at 95°C for 5 min. Proteins were resolved by SDS-PAGE and

transferred onto nitrocellulose membranes. Membranes were blocked in Odyssey Blocking Buffer (Li-Cor Biosciences, Superior, NE) for 1 h at RT, and primary antibodies were applied overnight at 4 °C in Odyssey Blocking Buffer. Membranes were washed three times in tris-buffered saline with Tween-20 (TBST), and infrared secondary antibodies (Li-Cor) were added at a 1:5000 dilution for 1 h at RT. Following three additional washes, blots were developed using the Odyssey Infrared Imaging System (Li-Cor).

In-Solution Modification of Recombinant CDK2. Recombinant CDK2 protein was diluted to 2.5 mg/ml in 1X DPBS. HNE (30 μM) or DMSO (vehicle control) was added to the pure protein at the indicated concentrations and incubated for 1 h with gentle agitation at 37 °C. The reaction mixture was quenched with the addition of $NaBH_4$ to a final concentration of 20 mM, reduced with 150 μM DTT for 30 min at 37 °C, and alkylated with 750 μM iodoacetamide for 15 min at RT in the dark. Samples were digested with 10 ng/μl trypsin overnight and dried by vacuum centrifugation.

Generation of CDK2-His. Cdk2-HA was a gift from Sander van den Heuvel (Addgene plasmid #1884).[134] Cdk2 was PCR-amplified with the following primers to replace the C-terminal HA-tag with a C-terminal 6XHis-tag: forward 5′- CATCATGGATCCATGGAGAACTT-3′, reverse 5′-TTATGAATTCTATCAATGGTGATGGTGATGGTGGAGTCGAAGATGGGGTA-3′. The PCR product was digested with BamHI and EcoRI and ligated into pcDNA3.1 (Invitrogen) for expression in mammalian cells (pcDNA3.1-CDK2-6XHis).

Transfection and Purification of CDK2-His. RKO cells were transfected with pcDNA3.1-CDK2-6XHis (10 μg) with 10 μl Lipofectamine 2000 (Invitrogen) in Opti-MEM medium for 24 h, then medium replaced with serum-free DMEM containing 250 μM HNE for 1 h. Cells were scraped in cold 1X DPBS and lysed on ice in His Lysis Buffer [50 mM sodium phosphate (pH 8.0), 300 mM NaCl, 20 mM imidazole, and 0.05% Tween-20] for 10 min. Lysates were cleared by centrifugation at 16,000 *x g* for 10 min. Lysates were reduced with 20 mM $NaBH_4$ for 15 min to stabilize adducts. Ni-NTA beads (Qiagen) were added to lysates and incubated with end-over-end mixing for 2 h at 4 °C. Beads were washed six times with His Lysis Buffer then eluted with His Elution Buffer [50 mM sodium phosphate (pH 8.0), 300 mM NaCl, 250 mM imidazole, and 0.05% Tween-20] for 5 min at RT. Eluates were denatured in 2X Laemmli sample buffer with 5% β-mercaptoethanol, heated at 95°C for 5 min, and proteins were resolved by SDS-PAGE. Following staining with Simply Stain (Invitrogen), bands corresponding to CDK2-His were excised and cut into 1 mm^3 pieces. Gel pieces were treated with 45 mM DTT for 45 min and carbamidomethylated with 100 mM iodoacetamide for 45 min. Following destaining with 50% acetonitrile in 25 mM ammonium bicarbonate, 10 ng/μL trypsin was added overnight at 37 °C. Peptides were extracted by gel dehydration (60% acetonitrile, 0.1% TFA) and dried by vacuum centrifugation.

Analysis of CDK2 Peptides by LC-MS/MS. Following reconstitution in 0.1% formic acid, peptides were loaded onto a capillary reverse phase analytical column (360 μm O.D. x 100 μm I.D.) using an Eksigent NanoLC Ultra HPLC and autosampler. The analytical column was packed with 20 cm of C18 reverse phase material (Jupiter, 3 μm beads, 300 Å, Phenomenox), directly into a laser-pulled emitter tip. Peptides were gradient-eluted at a flow rate of 500 nL/min, and the mobile phase solvents consisted of 0.1% formic acid, 99.9% water (solvent A) and 0.1% formic acid, 99.9%

acetonitrile (solvent B). A 90 min gradient was performed, consisting of the following: 0-10 min, 2% B; 10-50 min, 2-40% B; 50-60 min, 35-95% B; 60-65 min, 95% B, 65-70 min 95-2% B, 70-90 min, 2% B. Upon gradient elution, peptides were mass analyzed on a Thermo Scientific LTQ Orbitrap Velos mass spectrometer, equipped with a nanoelectrospray ionization source. The mass spectrometer was operated using a data-dependent method with dynamic exclusion enabled. Full scan (*m/z* 300-2000) spectra were acquired with the Orbitrap as the mass analyzer (resolution 60,000), and the ten most abundant ions in each MS scan were selected for fragmentation in the LTQ. An isolation width of 2 *m/z*, activation time of 10 ms, and 35% normalized collision energy were used to generate MS^2 spectra. For identification of modified peptides, tandem mass spectra were searched with Sequest against a human database created from the UniprotKB protein database (www.uniprot.org). Variable modifications of +57.0214 on Cys (carbamidomethylation), +15.9949 on Met (oxidation), +158.1306 on Cys, His, and Lys residues (corresponding to the reduced Michael adduct of HNE), +141.1279 on Lys and Arg (corresponding to the reduced Schiff base adduct of HNE), and +156.1150 on Lys (corresponding to the 4-ketoamide adduct) were included for database searching. Search results were assembled using Scaffold 3.0 (Proteome Software), and sites of modification were validated by manual interrogation of tandem mass spectra.

In vitro Modification of CDK2 for Activity Assays. Recombinant CDK2 complexed with Cyclin E or Cyclin A (15 ng) was incubated with 30 μM HNE in Kinase Assay Buffer [20 mM HEPES (pH 7.4), 10 mM $MgCl_2$] at 37 °C for 1 h with gentle agitation. Samples were immediately subjected to in vitro kinase assays as described below.

CDK2 Immunoprecipitation. Immunoprecipitations were performed according to a previously established protocol.[135] Briefly, 800 μg total cell lysate protein was immunoprecipitated using anti-CDK2 antibodies on ice for 3 h then for 90 min with protein A/G agarose beads with end-over-end mixing. CDK2-bound beads were collected and washed three times with RIPA buffer followed by three washes with Kinase Assay Buffer containing 1 mM DTT. Beads were resuspended in Kinase Assay Buffer containing 1 mM DTT and subjected to western blotting or kinase assays.

In vitro Kinase Assays. Kinase assays were adapted from previous methods.[135] Histone H1 protein (2 μg), 50 μM unlabeled ATP, 10 μCi γ-^{32}P-ATP, and Kinase Assay Buffer containing 1 mM DTT were added to a final volume of 50 μl for in vitro modified samples and 25 μl for CDK2 immunoprecipitates. The reactions were incubated at RT for 20 min with shaking and stopped with the addition of 2X Laemmli sample buffer with 5% β-mercaptoethanol. Samples were heated at 95 °C for 10 min, cooled, and loaded onto a 4-20% polyacrylamide gel. Following electrophoresis, radioactive histone H1 protein was detected with the Molecular Imager PharosFX System (BioRad, Hercules, CA). Images were quantitated with ImageJ (NIMH, Bethesda, MD). The gel was then stained with Simply Stain (Invitrogen) according to the manufacturer's protocol.

Results

HNE modifies a number of sites on recombinant CDK2

To elucidate possible structural and functional implications of CDK2 adduction, the sites of modification were determined by tandem mass spectrometry. Recombinant CDK2 was modified in vitro with HNE, digested, and analyzed by LC-MS/MS. There were a number of peptides that showed a mass shift of 158.1306 *m/z*, corresponding to a reduced Michael adduct, following HNE

treatment (Table 1). When sites of modification were mapped on a previously established crystal structure of CDK2 (1HCL), adducted sites were mainly localized to surface-exposed His residues (Figure 13). Of note, His71 and His161 were modified by HNE. His71 lies on the cyclin-binding interface and hydrogen bonds with residues on both Cyclin E and Cyclin A. His161 immediately follows Thr160, the key CDK2 phosphorylation site required for kinase activity.

Table 1. Sites of HNE modification on recombinant CDK2 identified by LC-MS/MS. Recombinant CDK2 was modified in vitro with 30 μM HNE and analyzed for sites of HNE adduction by tandem mass spectrometry in three independent experiments. Modified residues are indicated by an asterisk. Data shown in the table represent the adducted peptides with the lowest mass error. Reproduced with permission from Camarillo et al. (2016) Chem. Res. Toxicol. 29(3):323-32. Copyright 2016 American Chemical Society.[6]

Peptide	Residue Modified	XCorr	Observed m/z	Charge	Mass Error (ppm)	Peptide Start-Stop	Observed Spectra
ELNH*PPNIVK	His60	3.15	611.3672	2	0.33	57-65	3
LLDVIH*TENK	His71	3.12	670.3999	2	0.15	66-75	4
DLK*PQNLLINTEGAIK	Lys129	3.55	642.3870	3	0.00	127-142	2
TYTH*EVVTLWYR	His161	3.18	863.4668	2	0.17	158-169	8
SLLSQMLH*YDPNKR	His268	3.45	620.6743	3	0.32	261-273	2
AALAH*PFFQDVTK	His283	2.13	534.9724	3	0.37	279-291	7
PVPH*LR	His295	1.89	438.7900	1	1.82	292-298	4

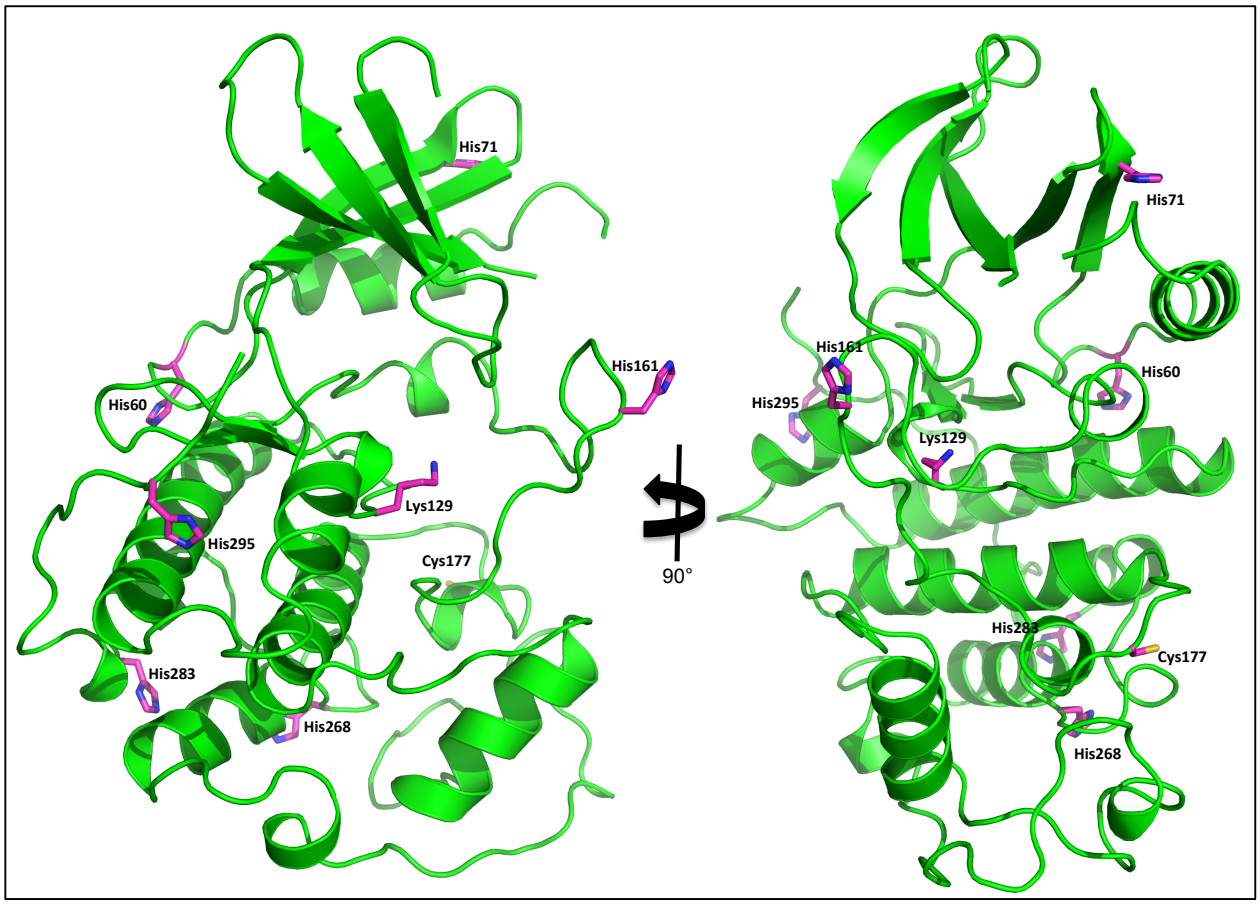

Figure 13. Recombinant CDK2 is modified by HNE at a number of sites. Crystal structure of unphosphorylated CDK2 (PDB 1HCL) with residues modified by HNE in magenta. Reproduced with permission from *Camarillo et al.* (2016) Chem. Res. Toxicol. 29(3):323-32. Copyright 2016 American Chemical Society.[6]

HNE modified CDK2 in RKO cells

As noted above, prior work had demonstrated HNE-dependent CDK2 modification in the RKO colorectal cancer cell line.[84] To verify the sites of CDK2 modification in cells, we transfected RKO cells with a His-tagged CDK2 construct, then treated the cells with HNE. Following isolation of His-tagged protein, we performed in-gel digestion and analyzed the peptides by LC-MS/MS (Table 2). As in the case of recombinant CDK2, His71 was identified as a site of modification (Figure 14A). Interestingly, Cys177 was also modified by HNE in cells (Figure 14B). This modification

has previously been observed in the literature,[2] though we did not observe it in recombinant protein, possibly due to oxidation of that Cys residue during storage.

Table 2. Sites of HNE modification on endogenous CDK2 identified by LC-MS/MS. RKO cells were transfected with CDK2-His and treated with HNE. Following isolation of His-tagged proteins and separation by SDS-PAGE, bands corresponding to CDK2-His were excised, subjected to in-gel digestion, and analyzed by tandem mass spectrometry. Modified residues are indicated by an asterisk. Data shown in the table represent the adducted peptides with the lowest mass error. Reproduced with permission from Camarillo et al. (2016) Chem. Res. Toxicol. 29(3):323-32.

Peptide	Residue Modified	XCorr	Observed m/z	Charge	Mass Error (ppm)	Peptide Start-Stop	Observed Spectra
LLDVIH*TENK	His71	3.58	670.3919	2	4.92	66-75	3
APEILLGC*K	Cys177	2.87	1101.6543	1	3.99	170-178	5

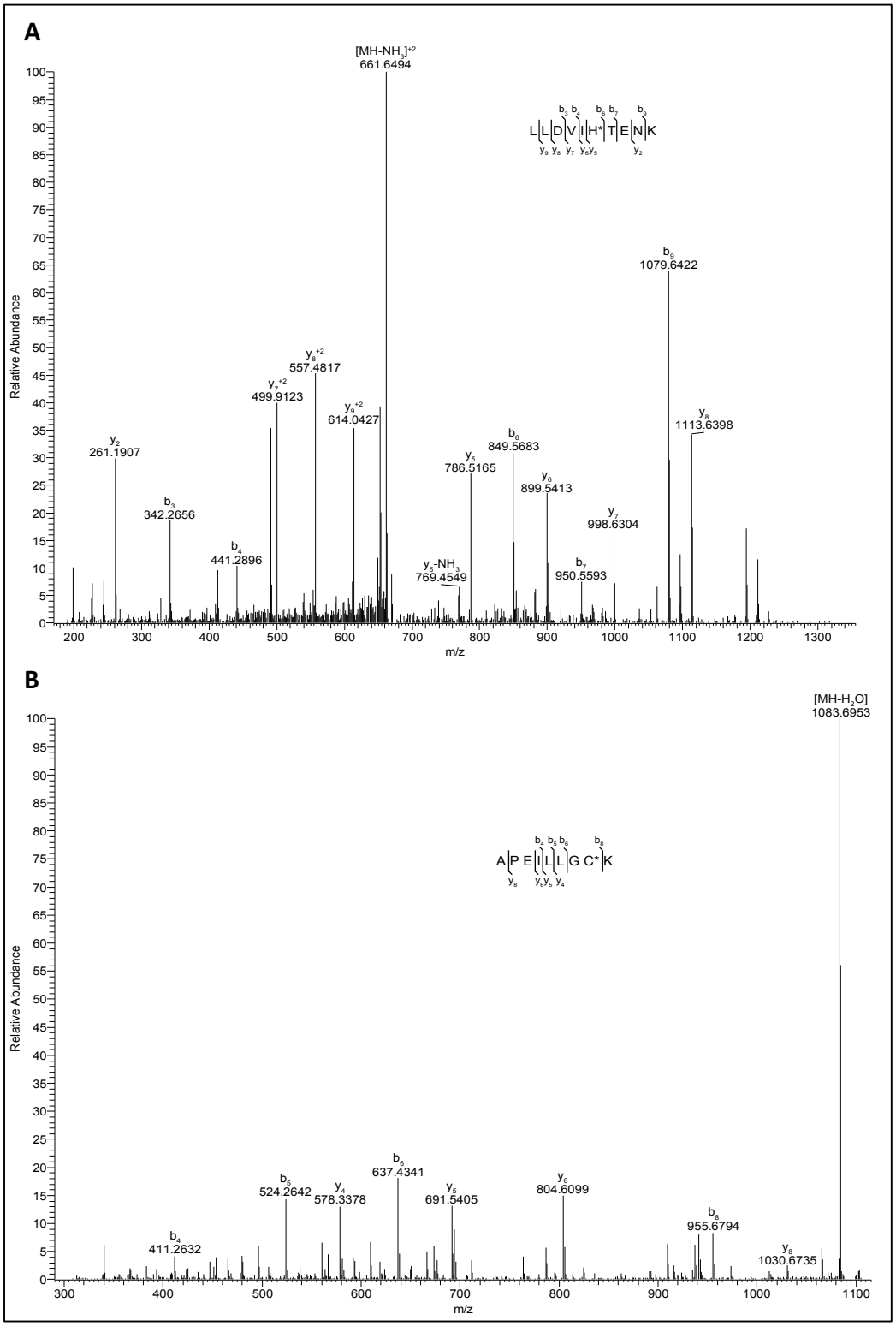

Figure 14. CDK2 is modified by HNE in cells. Tandem mass spectrometry was performed on CDK2-His from HNE-treated RKO cells. A) MS2 spectrum of LLDVIH*TENK. B) MS2 spectrum of APEILLGC*K. Sites of modification are represented by an asterisk (*). Reproduced with permission from *Camarillo et al.* (2016) Chem. Res. Toxicol. 29(3):323-32. Copyright 2016 American Chemical Society.

HNE-dependent modification of CDK2 temporally correlates with cell cycle arrest

Since CDK2 is modified at a number of sites in vitro, we wanted to further verify its modification in cells and assess if CDK2 adduction by HNE could be contributing to previously observed cell cycle dysregulation. To determine if CDK2 is modified by HNE within the relevant time frame to alter the cell cycle, we employed the 8,9-alkynyl analog of HNE, aHNE, and used click chemistry to evaluate the levels of modified CDK2 in cells. RKO cells synchronized in G1/G0 were treated with aHNE or DMSO for 1 h and released into 10% serum-containing medium to allow for cell cycle progression. Click chemistry, streptavidin pull-down, and UV-cleavage enabled selective isolation of adducted proteins. Western blot analysis of eluates showed persistent modification of CDK2 by aHNE up to 16 h (Figure 15). There was a decrease in adducted CDK2 over time, indicative of protein turnover or adduct reversal. These data show that CDK2 is modified rapidly in cells, and that the modification persists for a substantial time period, consistent with the hypothesis that the modification may lead to functional alterations affecting the role of CDK2 in cell cycle progression.

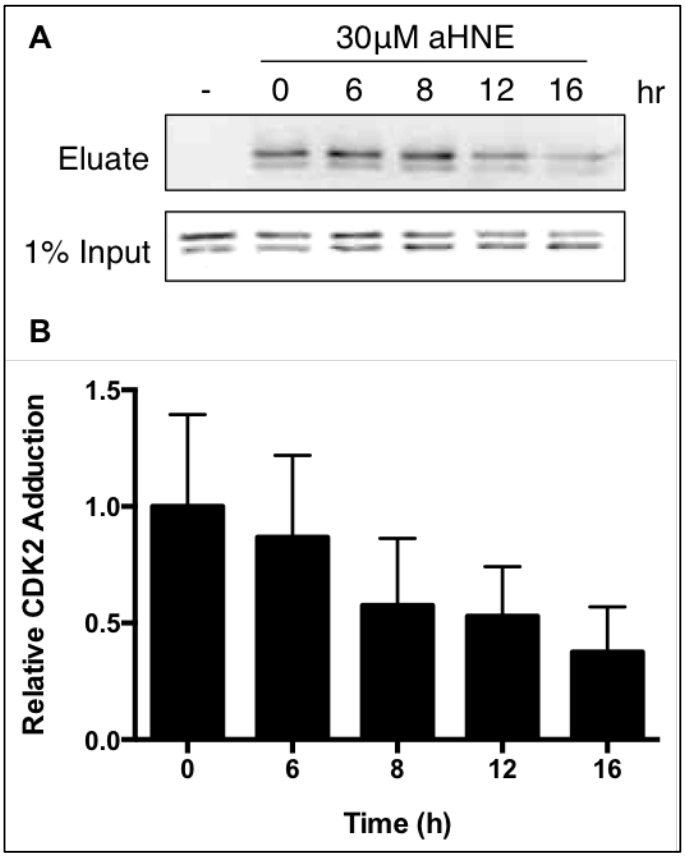

Figure 15. aHNE modifies CDK2 in RKO cells. RKO cells were serum starved for 24 h to synchronize them in G0/G1, then treated for 1 h with 30 μM aHNE or DMSO. Treatment medium was removed, and 10% serum-containing medium was added to allow the cells to enter into the cell cycle. Cells were collected at the indicated times and lysates subjected to click chemistry and streptavidin pull down. UV eluates and 1% input were subjected to SDS-PAGE and western blot. A) Western blot shows levels of aHNE-modified CDK2 decline over time after initial treatment, while levels of total CDK2 remain unchanged. B) Densitometry of adducted CDK2 normalized to the 0 h eluate. Reproduced with permission from *Camarillo et al.* (2016) Chem. Res. Toxicol. 29(3):323-32. Copyright 2016 American Chemical Society.[6]

HNE treatment decreases kinase activity in CDK2/Cyclin A complexes in vitro

CDK2 phosphorylates a number of proteins in late G1 to promote cell cycle progression.[136,137,124,138] Since HNE has previously been shown to inhibit the activity of another protein kinase, ERK1/2,[139] we sought to investigate the possible effects of HNE on CDK2 kinase activity. To assess the functional impact of HNE modification, we determined changes in CDK2 kinase activity of recombinant CDK2-cyclin complexes following HNE exposure. CDK2/Cyclin E or CDK2/Cyclin A complexes were modified in vitro with HNE and subjected to radioactive

kinase assays using histone H1 as a model substrate.[135] As shown in Figure 16A, there was a significant decrease in histone H1 phosphorylation in CDK2/Cyclin A complexes (Figure 16B) treated with 30 μM HNE, but not in CDK2/Cyclin E complexes, which exhibited a trend towards decreased activity that was not statistically significant (Figure 16C). These differences in the effects of HNE on CDK2 activity in the two complexes may be the result of structural differences in the way that each cyclin interacts with CDK2. Regardless of the mechanism, these data confirm that HNE modification can directly alter CDK2 activity.

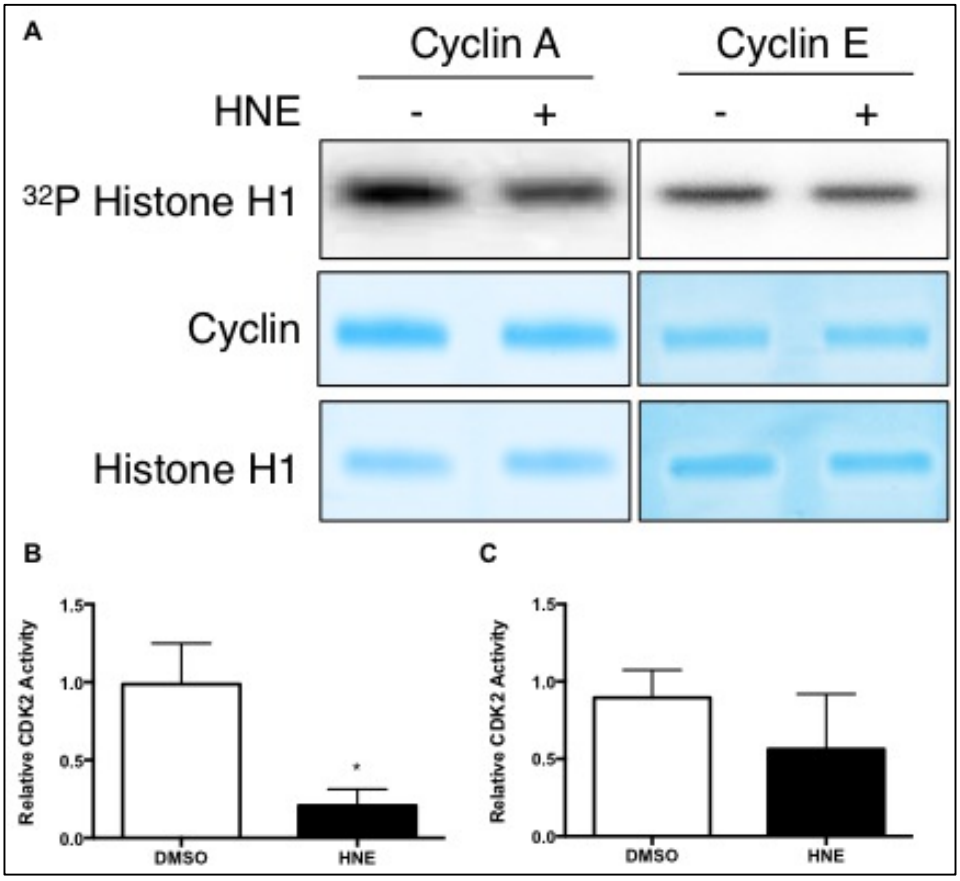

Figure 16. HNE treatment lowers CDK2 activity in vitro. Recombinant CDK2 protein with Cyclin A or Cyclin E was modified in vitro with 30 μM HNE. A) Kinase assays followed by autoradiography show an HNE-mediated decrease in CDK2 activity with Cyclin A but not Cyclin E. Quantification of CDK2 activity with B) Cyclin A and C) Cyclin E representing the mean ± S.D. (n=3), *, $p < 0.05$. Reproduced with permission from *Camarillo et al.* (2016) Chem. Res. Toxicol. 29(3):323-32. Copyright 2016 American Chemical Society.[6]

HNE treatment decreases CDK2 activity in cells

To further investigate the functional implications of HNE adduction of CDK2 in the cell, we performed in vitro kinase assays utilizing endogenous CDK2-cyclin immunoprecipitates. Cells were arrested in G1 with serum-starvation, treated with HNE for 1 h, then released into the cell cycle with the addition of medium containing 10% FBS. Cells were lysed and CDK2-cyclin complexes captured at various time points up to 12 h thereafter. As shown in Figure 17, phosphorylation of histone H1 was low in CDK2-cyclin immunoprecipitates isolated from cells harvested immediately following treatment with HNE (lanes 1 and 2). Kinase activity has substantially increased by 6 h, but there is little difference in H1 phosphorylation between the control and HNE-treated cell immunoprecipitates until 8 h following release. At 8 h (lanes 5 and 6), HNE-treated CDK2 immunoprecipitates display significantly lower levels of kinase activity (Figure 17B). These data suggest that HNE treatment lowers the activity of CDK2 in a time-dependent fashion, possibly contributing to the delay in cell cycle progression.

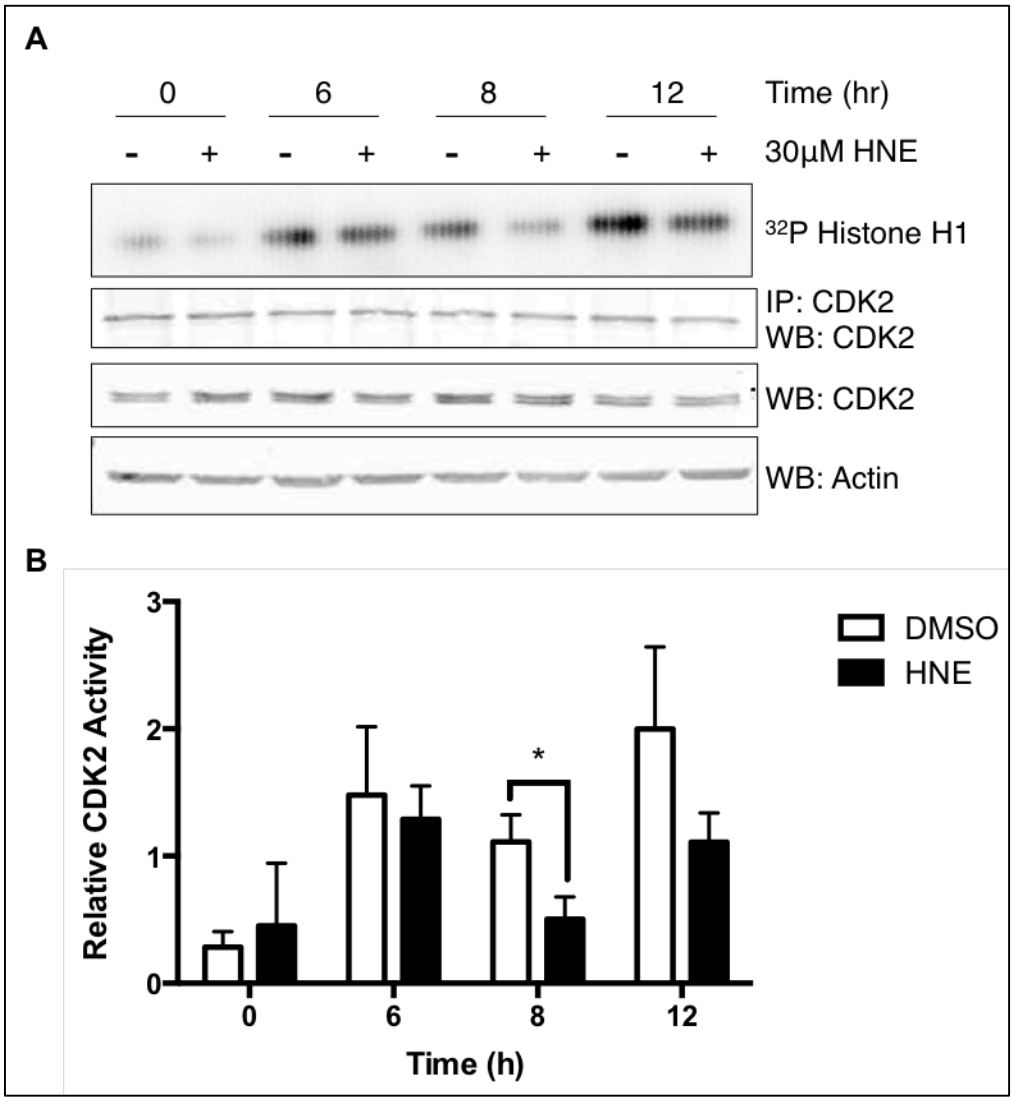

Figure 17. HNE treatment decreases CDK2 activity in cells. CDK2 was immunoprecipitated from RKO cells treated with HNE and subjected to kinase assays. A) CDK2 from cells treated with HNE shows a decrease in kinase activity at 8 h and 12 h. B) Quantification of CDK2 activity representing the mean ± S.D. (n=3). The difference in kinase activity was statistically significant at 8 h (*, $p < 0.05$) but not 12 h. Reproduced with permission from *Camarillo et al.* (2016) Chem. Res. Toxicol. 29(3):323-32. Copyright 2016 American Chemical Society.[6]

HNE delays entry into S-phase

Previous reports have shown that HNE inhibits cell growth via multiple mechanisms.[140,141,131] To further elucidate the mechanism of inhibition, RKO cells were synchronized in G1/G0 by serum withdrawal, treated with HNE, and then released from cell cycle arrest with serum-containing medium. As expected, cell cycle analysis showed a high percentage of cells arrested in G0/G1

following serum starvation (Figure 18). After 8 h in serum-containing medium, cells treated with DMSO displayed an increase in the percent of cells in S-phase, while the percentage HNE-treated cells in S-phase remained significantly lower. Although increasing in both sets of cultures by 12 h, the percentage of S-phase cells continued to be significantly lower in those exposed to HNE than in controls. However, these differences in the percent of cells in S-phase were abolished at 16 h, suggesting that HNE-treated cells have a delay in S-phase initiation.

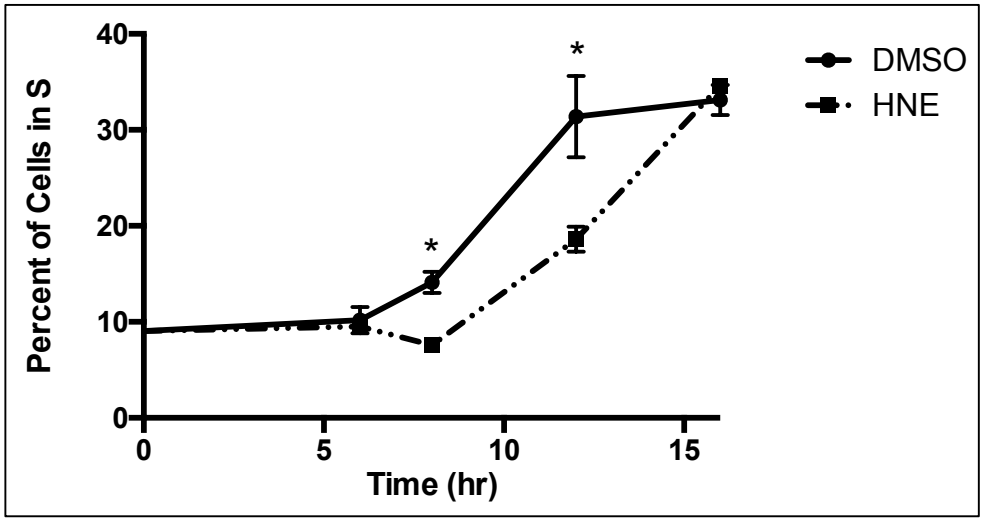

Figure 18. HNE delays entry into S-phase. RKO cells were serum-starved for 24 h to synchronize them in G0/G1, then treated for 1 h with 30 μM HNE or DMSO. Medium containing 10% serum was added to allow the cells to enter into the cell cycle. Cells were collected at the indicated times and cell cycle phase analyzed by flow cytometry. The data represent the mean ± S.D. (n=6; *, $p<0.05$ between HNE-treated and DMSO –treated, using one-way ANOVA with Bonferroni post-test). Reproduced with permission from *Camarillo et al.* (2016) Chem. Res. Toxicol. 29(3):323-32. Copyright 2016 American Chemical Society.[6]

HNE does not alter levels of total or phosphorylated cell cycle proteins

We tested the hypothesis that alterations in the levels or phosphorylation state of one or more of the proteins involved in the G1/S transition could account for the HNE-mediated delay in S-phase entry. Western blot analysis did not reveal any differences in levels of total CDK2 in the presence or absence of HNE at the observed times (Figure 19). Phosphorylation of CDK2 at Thr160, which is required to activate CDK2 in G1-phase,[142] also did not show any significant changes with

treatment, nor did phosphorylation of Thr821 on Rb, a CDK2 target. Additionally, levels of Cyclin E and Cyclin A, both of which are required for CDK2 activity, were unchanged with treatment.

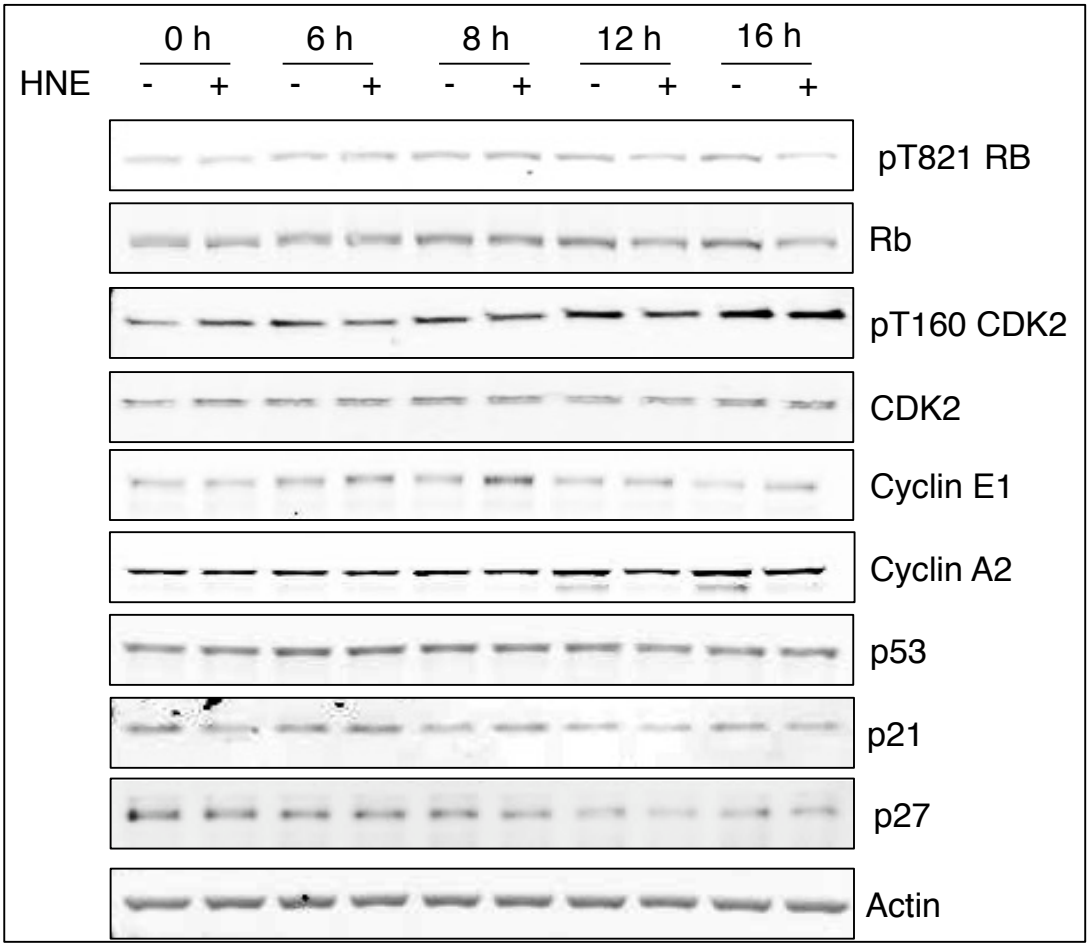

Figure 19. HNE does not alter levels of total or phosphorylated cell cycle proteins. RKO cells were serum-starved for 24 h to synchronize them in G0/G1 then treated for 1 h with 30 μM HNE or DMSO. Medium containing 10% serum was added to allow the cells to enter into the cell cycle. Cells were collected at the indicated times and analyzed for expression of G1/S-phase proteins. Reproduced with permission from *Camarillo et al.* (2016) Chem. Res. Toxicol. 29(3):323-32. Copyright 2016 American Chemical Society.[6]

We further investigated levels of G1 inhibitory proteins to rule out inhibition of CDK2 by these damage pathways. HNE is known to activate the p53 response pathway, upregulate p21, and induce apoptosis via caspase and PARP cleavage.[143] Levels of p53 did not increase over the observed times (Figure 19), consistent with previous reports showing that p53 is not upregulated

until 24 h following treatment.[131] We also determined the levels of p21, which is canonically regulated by p53, but can also be induced in a p53-independent manner.[144] Levels of p21 and p27, an additional G1 CDK inhibitor, remained unchanged in response to HNE, demonstrating that CDK2 is not being directly inhibited by this mechanism. Additionally, we did not observe PARP cleavage (data not shown), indicating that apoptosis was not being initiated during these observed times. Together, these data suggest that the observed delay into S-phase occurs independently of these S-phase inhibitory pathways.

Discussion

Here, we investigated the impact of HNE modification on CDK2 function and cell cycle progression. Since CDK2 has previously been identified as a target of aHNE,[84] we investigated the extent of CDK2 modification in RKO cells. Modified CDK2 was present up to 16 h following HNE exposure, though levels declined over time, consistent with turnover or reversal of adducts. Tandem mass spectrometry of HNE-treated recombinant CDK2 revealed a number of sites of modification (Table 1). The majority of adducts found were on surface-exposed His residues, likely due to their accessibility. A single Lys residue was also found to be modified, consistent with the lower reactivity of HNE toward Lys residues.[64] While CDK2 does contain Cys residues, the preferred targets of electrophile modification, all but a single Cys is disulfide bound. When sites of modification were determined in cells, Cys177 was shown as a target of HNE modification, in addition to His71, which had been identified in vitro. Previous work by Weerapana et al.[2] also demonstrated adduction of Cys177 by HNE, further supporting the validity of this modification. The data suggest that His71 and Cys177 represent the most readily accessible sites of modification in cells.

Of the seven modified residues, two appear to be in a location that could greatly impact CDK2 activity. Using published crystal structures of CDK2, we were able to model the HNE adducts on His71 (Figure 20A) and His161 (Figure 20B). His71 lies on the cyclin-binding interface. Crystal structures of CDK2 phosphorylated at Thr160 and in complex with Cyclin E or Cyclin A have revealed that His71 is capable of hydrogen bonding with both cyclins.[145,146] As the CDK2-cyclin interaction is required for CDK2 activation, it is possible that disruption of this interaction could ultimately inhibit kinase activity. Consistently, we observe a reduction in the kinase activity of HNE-treated recombinant CDK2/Cyclin A complexes. In contrast, activity assays using recombinant CDK2/Cyclin E complexes did not show significant differences with HNE treatment. We hypothesize that these differences in the effects of HNE on CDK2/cyclin complex kinase activity result from the structural differences between Cyclin E and Cyclin A and their required points of contact with CDK2. The Cyclin A/CDK2 interaction requires two additional contact points with Thr72 and Gln73, both of which are not required for Cyclin E.[146] These subtle differences in structure may account for the functional differences observed.

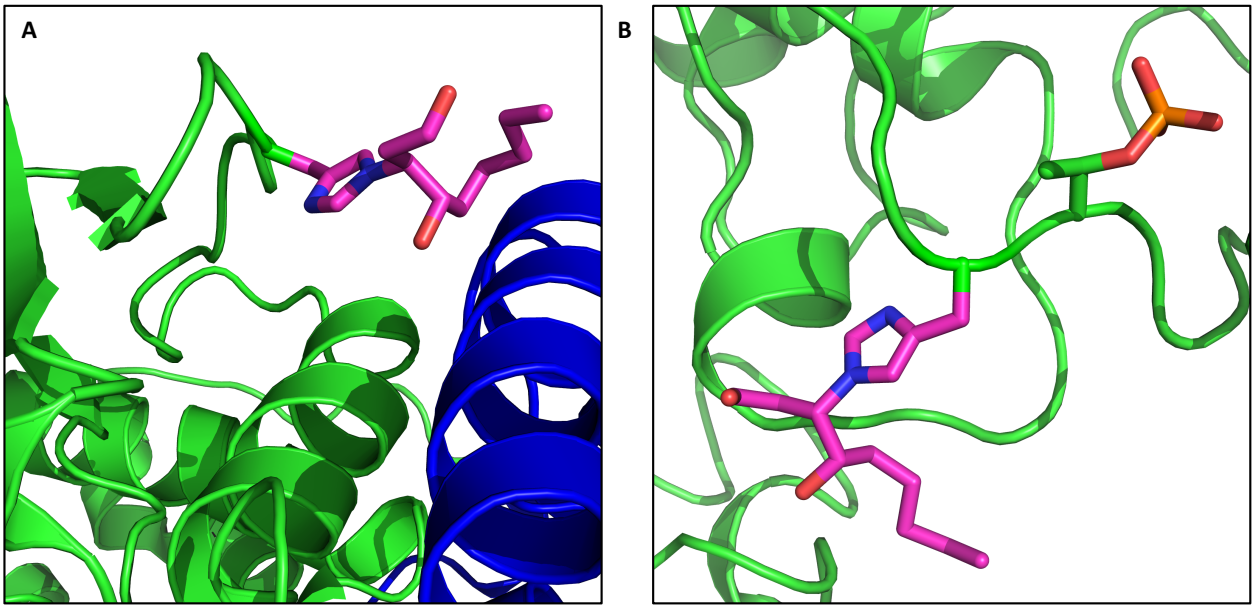

Figure 20. Modeling of HNE adducts on CDK2. HNE adducts (magenta) were modeled onto A) His71 of CDK2 in the CDK2 (green) with Cyclin E (blue) structure (1W98) and B) His161 in the phosphorylated Thr160 structure of CDK2 (4EOM). Reproduced with permission from *Camarillo et al.* (2016) Chem. Res. Toxicol. 29(3):323-32. Copyright 2016 American Chemical Society.[6]

This His161 HNE modification site is of significant interest due to its proximity to the activating phosphorylation site. Phosphorylation of Thr160 by CDK7/Cyclin H occurs in response to growth factor stimulation and results in a significant conformational change in the activation loop of CDK2.[147] Previous studies have shown that adduction of a similar His residue on the activation loop of ERK1/2 results in decreased activity.[139] Furthermore, Cyclin A is in contact with His161 in the active complex, and this interaction is not present in the complex with Cyclin E. These differences may contribute to the variances in HNE-mediated modification of kinase activity between CDK2/Cyclin A and CDK2/Cyclin E complexes in vitro. Notably, however, this site was not identified in intact cells, an observation that may correlate with the finding that HNE treatment had no effect on Thr160 phosphorylation of CDK2 in our model (Figure 19). Thus, it is not clear to what extent modification at this site may be important to the effects of HNE on cell cycle regulation in vivo.

Further evidence that HNE can negatively impact CDK2 signaling is shown in in vitro kinase assays. Activity assays using endogenous CDK2 from RKO cells show a decrease in histone H1 phosphorylation by immunoprecipitates from cells treated with HNE at 8 h. Due to temporal regulation of CDK2, activity of CDK2 is very low at 0 h, when the cells are arrested in G1, so no effect of HNE treatment is observed at that time. By 6 h, following addition of serum, substantial CDK2 activity could be measured, but no effect of HNE was observed. In contrast, at the 8 h time point a significant decrease in activity was observed between CDK2 immunoprecipitates recovered from control versus HNE-treated cells. Notably, the 8 h time point correlates when control, but not HNE-treated cells begin their progression into S phase. It is not clear why a reduction in CDK2 activity is not observed at 6 h after HNE treatment; however, our in vitro assays demonstrate that the effects of HNE differ depending on the CDK2/Cyclin complex formed. Thus, changes in post-translational modifications and/or binding partners during the CDK2 activation process may be responsible for these observed differences.

The most highly characterized substrate of CDK2 is Rb, phosphorylation of which inactivates its inhibitory effect on the E2F1 transcription factor. Thus, we expected to see that HNE treatment of RKO cells would result in a reduction of Rb phosphorylation at Thr821, a target site for CDK2. Although the data suggest a trend in reduced phosphorylation at 12 h and 16 h after serum addition, the differences were not statistically significant. It is possible that this lack of change in phosphorylation is the result of compensatory CDK4/6-dependent phosphorylation. While Thr821 is preferentially phosphorylated by CDK2,[148] CDK4 has been shown to phosphorylate this residue.[149] It is also possible that the immunoblot-based assay used lacked adequate sensitivity to observe a change.

Our data build upon previous work on the effects of HNE on the cell cycle.[128] Cell cycle analysis of G1/G0-synchronized RKO cells shows that HNE treatment delays entry into S-phase. Our data also show that this delay occurs in the absence of increases in the levels of p53, p21, and p27, suggesting that these inhibitory proteins do not play a primary role in initiating the failure to progress (Figure 19). We propose the following mechanism for CDK2 inhibition (Figure 21). Under normal conditions, CDK2 activation requires cyclin binding and phosphorylation of the activation loop. High levels of DNA damage promote activation of the p53 pathway, directly leading to the inhibition of CDK2 through the binding of p21. Our data suggest that covalent modification of CDK2 by HNE can immediately inhibit CDK2 activity. This mechanism of inactivation occurs via direct modification of CDK2 at multiple sites, thereby inhibiting kinase activity and delaying entry into S-phase. We hypothesize that CDK2 inactivation by adduction plays a role in the immediate cell cycle delay observed in response to HNE treatment, whereas p21, which is induced later, plays a longer-term role in the maintenance of genomic integrity during electrophile stress.

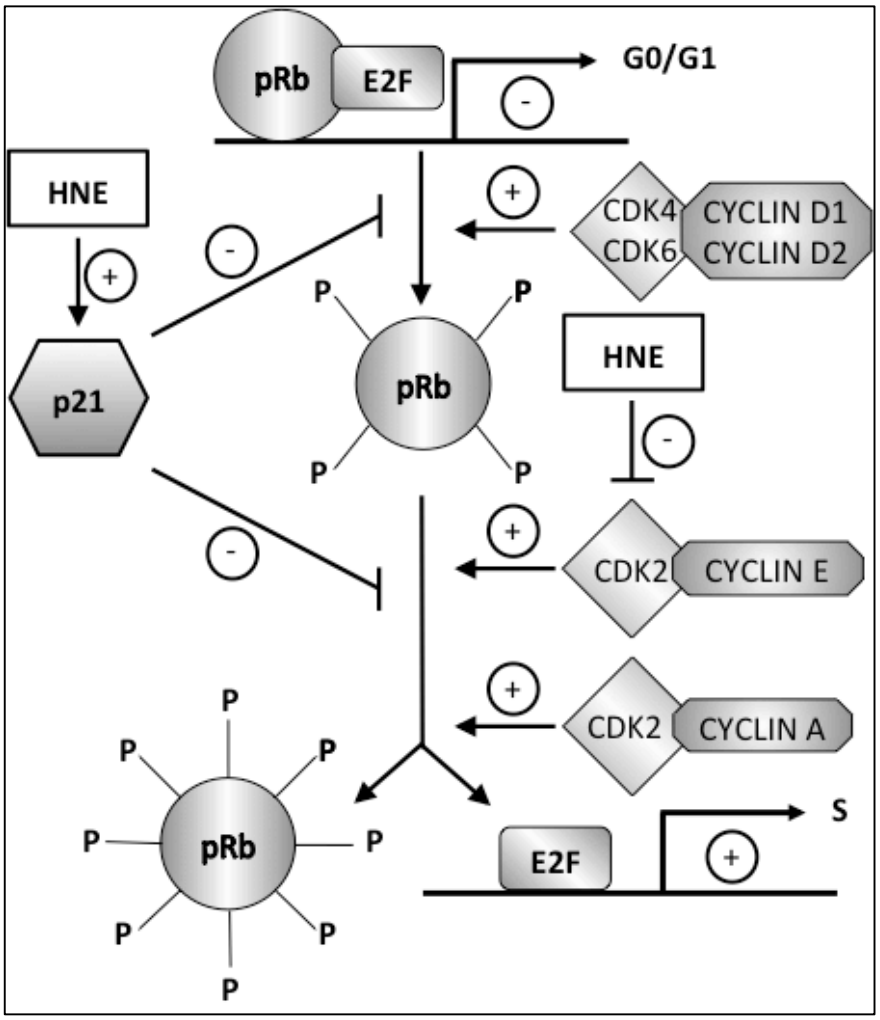

Figure 21. Proposed mechanism for the delay in S-phase entry. Under normal conditions, Rb remains bound to E2F until the G1 CDKs phosphorylate it, allowing for transcription of S-phase genes. Our model suggests that HNE covalently modifies CDK2, decreasing its activity toward Rb, and delaying S-phase entry. Reproduced with permission from *Camarillo et al.* (2016) Chem. Res. Toxicol. 29(3):323-32. Copyright 2016 American Chemical Society.[6]

CHAPTER III

SITE-SPECIFIC, INTRAMOLECULAR CROSS-LINKING OF PIN1 ACTIVE SITE RESIDUES BY THE LIPID ELECTROPHILE 4-OXO-2-NONENAL

Introduction

Polyunsaturated fatty acids in cellular membranes are major targets for oxidative damage induced by xenobiotics and inflammatory stimuli. The initial oxidation products are fatty acid hydroperoxides, which can be converted to a number of reactive lipid electrophiles. Some of these electrophiles are readily diffusible and can modify proteins and DNA, thereby propagating damage initiated by oxidation.[66,120] This may be an important contributor to diseases associated with environmental exposures or chronic inflammation such as Parkinson's disease, atherosclerosis, diabetes, and cancer.[121,119]

Lipid peroxidation generates a plethora of electrophilic products, varying in length and reactivity; two of considerable interest are 4-hydroxy-2-nonenal (HNE) and 4-oxo-2-nonenal (ONE) (Figure 22). HNE and ONE react rapidly with the side chains of Cys, His, and Lys residues in proteins via Michael addition. HNE and ONE can also form Schiff bases through reaction with Lys residues while ONE alone is capable of 4-ketoamide formation.[66,71] ONE is >150-fold more reactive than HNE and displays a broader range of reaction products due to differences in its stereoelectronic properties.[150,78] Comprehensive proteomic analyses indicate that HNE and ONE react with many proteins in cells (> 1,000), but they display significant differences in protein

targets and sites of reactivity;[86,84,5] few studies have investigated the precise mechanisms responsible for these differences.

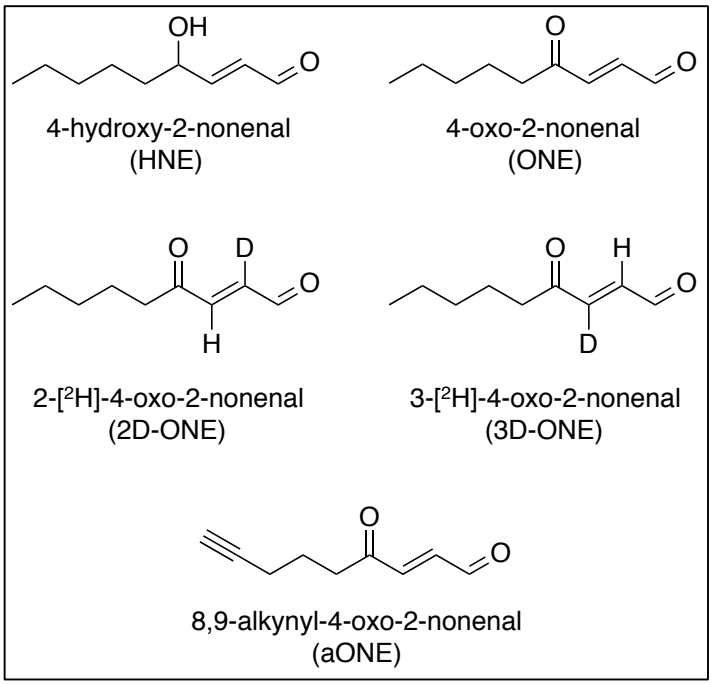

Figure 22. Structures of lipid electrophiles used in these studies. Reproduced with permission from *Aluise et al.* (2015) Chem. Res. Toxicol. 28(4):817-27. Copyright 2015 American Chemical Society.[1]

We recently reported that HNE reacts with the active site Cys of the peptidyl-prolyl isomerase, Pin1, to form a covalent Michael adduct *in vitro* and in cells exposed to HNE.[87] Pin1 is the only known isomerase to specifically target proline-directed epitopes preceded by a phosphorylated Ser/Thr residue. Pin1 isomerizes this bond from *cis* to *trans,* thereby facilitating dephosphorylation by isomer-specific phosphatases.[151] This unique activity of Pin1 results in the stabilization and/or transactivation of an impressive list of substrates, including p53,[152] β-catenin,[153] Raf,[154] Rb,[155] and tau,[151] among many others. Modification of Pin1 by HNE has been detected by immunochemical analysis of affected regions of brains from Alzheimer's disease patients, and the extent of modification appears to correlate to disease severity.[156,157]

Preliminary investigation of the reaction of ONE with Pin1 indicated that, like HNE, it targets the catalytic Cys. However, detailed analysis indicated that the product of ONE-mediated Pin1 modification is not a simple Michael addition product but rather a stable intramolecular cross-link that forms rapidly and in high yield. We report here the structure of the adduct, a potential mechanism of reactivity, and evidence for the modification of Pin1 by ONE in intact cells. Efficient production of this adduct in Pin1, and in other proteins with similar surface exposed, active site-localized Cys-Lys residues may contribute significantly to the cellular effects of ONE associated with oxidative stress.

Materials and Methods

Materials and Reagents. All reagents were purchased from Sigma Aldrich (St. Louis, MO) unless otherwise stated. ONE, 8,9-alkynyl-ONE (aONE), and UV-cleavable biotin azide were synthesized in the laboratory of Dr. Ned Porter at Vanderbilt University as previously described.[5] Cell culture medium was purchased from Invitrogen (Grand Island, NY). Fetal bovine serum (FBS) was purchased from Atlas Biologicals (Ft. Collins, CO). Purified Pin1 protein (GWB-523EFE) was purchased from Genway Biosciences (San Diego, CA). Anti-Pin1 antibodies were purchased from Cell Signaling (Danvers, MA), and secondary antibodies were purchased from Santa Cruz Biotechnologies (Santa Cruz, CA). All SDS-PAGE and western blot supplies were purchased from Bio-Rad (Hercules, CA) unless otherwise noted. Streptavidin Sepharose High Performance beads were purchased from GE Life Sciences (Pittsburg, PA).

Cell Culture and Treatments. The triple-negative human breast carcinoma MDA-MB-231 cell line was purchased from the American Type Culture Collection (ATCC). Cells were cultured in

RPMI1640 Medium (Gibco) with 10% FBS. Electrophiles dissolved in DMSO or vehicle control were added to cell culture medium to achieve the desired electrophile concentration while maintaining a DMSO concentration of less than 1%.

Synthesis of Deuterated ONE Analogues. Deuterated ONE analogues were synthesized according to the method of Blair[158] with some modification. 4-hydroxy-non-2-ynal diethylacetal was synthesized by the Grignard reaction of hexanal with propiolaldehyde diethylacetal magnesium bromide. The reduction of 4-hydroxy-non-2-ynal diethylacetal with lithium aluminum hydride and work-up with deuterium oxide saturated with deuterated ammonium chloride gave 2-[^{2}H]-4-hydroxy-non-2-enal-diethylacetal. Deprotection of 2-[^{2}H]-4-hydroxy-non-2-enal-diethylacetal in 1% citric acid gave 2-[^{2}H]-4-hydroxy-non-2-enal. Finally, Dess-Martin oxidation of 2-[^{2}H]-4-hydroxy-non-2-enal provided 2-[^{2}H]-4-oxo-non-2-enal (2D-ONE). For the synthesis of 3-[^{2}H]-4-oxo-non-2-enal (3D-ONE), 4-hydroxy-non-2-ynal diethylacetal was reduced with lithium aluminum deuteride, and the reaction was quenched by the addition of a saturated solution of ammonium chloride in water to give 3-[^{2}H]-4-hydroxy-non-2-enal-diethylacetal. Subsequent deprotection under acidic conditions followed by Dess-Martin oxidation resulted in the formation of 3D-ONE.

Click Chemistry. MDA-MB-231 cells were exposed to aONE for 1 h in serum-free medium. Following electrophile exposure, cells were washed with Dulbecco's-modified phosphate-buffered saline (DPBS, Gibco), collected by scraping, and centrifuged for 5 min at 1000 *x g*. Cell pellets were lysed in NETN buffer (50 mM HEPES, pH 7.5, 150 mM NaCl, 0.5% Igepal, and mammalian protease inhibitor cocktail (Sigma Aldrich, St. Louis, MO)). Pellets were sonicated by

ten 1s pulses with a Virsonic Cell Disruptor and cleared by centrifugation at 16,000 *x g* for 10 min. The bicinchoninic acid assay was used to determine protein concentration (Thermo Scientific, Waltham, MA). Click chemistry and photoelution were performed as previously described.[87]

SDS-PAGE and Western Blotting. Protein samples for SDS-PAGE were mixed 1:1 by volume with 2X Laemmli buffer containing 5% β-mercaptoethanol and boiled for 5 min. A 4-20% gradient Tris-HCl gel was used to separate proteins. Proteins in the gel were transferred onto a 0.45 μm nitrocellulose membrane and blocked with 5% nonfat dry milk in Tris-buffered saline containing 0.1% Tween-20 (TBST) for 1 h. Primary antibodies were incubated (1:1000 for anti-Pin1) with membranes overnight at 4°C. The following day, blots were washed with TBST three times and incubated with anti-rabbit secondary antibody (1:5000) for 1 h at room temperature (RT). Blots were washed three times with TBST and developed using luminol-based detection (Perkin-Elmer, Santa Clara, CA).

In-Solution Modification of Purified Pin1. Purified Pin1 was buffer-exchanged once with DPBS. Protein (2.5 μg, 6.9 μM) was diluted to 20 μL with DPBS and incubated with electrophile at 37°C as indicated. Reactions were terminated with the addition of $NaBH_4$ at a final concentration of 20 mM for 30 min at RT. Protein samples were dried *in vacuo* and reconstituted in 10 μL of 6 M guanidine hydrochloride for 30 min at RT. Samples were reduced with dithiothreitol (150 μM) for 30 min at 37°C, and alkylated by 750 μM iodoacetamide for 15 min at RT in the dark prior to being diluted to 200 μL with 20 mM NH_4HCO_3. Due to the potential of adducts on Lys residues to result in mis-cleavage by trypsin, samples were digested with 500 ng chymotrypsin (Promega, Madison, WI) for 24 h at 37°C. Chymotryptic digests were concentrated and desalted using

ZipTips, (EMD Millipore, Billerica, MA) and eluted from tips with 60% acetonitrile/0.1% trifluoroacetic acid. Samples were mixed 1:1 by volume with matrix (20 mg/ml α-cyano-hydroxycinnamic acid (CHCA) in 60% acetonitrile) and analyzed by MALDI-TOF MS.

Analysis of Pin1 Peptides via MALDI-TOF and MALDI-TOF/TOF MS. An Autoflex Speed TOF MS or an Ultraflextreme TOF/TOF MS (Bruker Daltonics), both equipped with a Nd:YAG (solid state) laser operating at 355 nm, were used to obtain spectra. All spectra were obtained in positive ion mode. Peptide-CHCA solutions (1 μL) were deposited on 384-spot MALDI target plates and air dried prior to analysis. Full mass spectra of peptides were obtained in reflectron mode on the Ultraflextreme, using a 500-4500 mass range. Spectra from treated and untreated samples were overlaid to identify peaks corresponding to masses appearing in spectra from ONE-treated Pin1 samples which did not appear in unmodified Pin1 samples. Selected peptide ions were dissociated using LIFT on the TOF/TOF. TOF/TOF fragmentation data were interrogated using FlexAnalysis software and analyzed against a theoretical Pin1 peptide digest using Protein Prospector.

Analysis of Pin1 Peptides via Orbitrap MS/MS. Purified Pin1 was buffer-exchanged once with DPBS. Protein (2 μg, 5.5 μM) was diluted to 20 μL with DPBS and incubated with 25 μM electrophile at 37^{o}C with agitation. Reactions were terminated with $NaBH_4$ at a final concentration of 20 mM for 30 min at RT. Samples were reduced with 150 μM DTT for 45 min, and available Cys residues were carbamidomethylated with 750 μM iodoacetamide for 45 min. Pin1 was digested with chymotrypsin (10 ng/μL) in 25 mM NH_4HCO_3 for three hours at 37°C. The samples were dried by vacuum centrifugation, and the peptides were reconstituted in 0.1% formic acid. Peptides were loaded onto a capillary reversed-phase analytical column (360 μm o.d. × 100 μm

i.d.) using an Eksigent NanoLC Ultra HPLC and autosampler. The analytical column was packed with 20 cm of C18 reversed-phase material (Jupiter, 3 μm beads, 300 Å, Phenomenex), directly into a laser-pulled emitter tip. Peptides were gradient-eluted at a flow rate of 500 nL/min, and the mobile phase solvents consisted of water containing 0.1% formic acid (solvent A) and acetonitrile containing 0.1% formic acid (solvent B). A 90 min gradient was performed, consisting of the following: 0–10 min, 2% B; 10–50 min, 2–45% B; 50–60 min, 45–90% B; 60–65 min, 95% B; 65–70 min 95–2% B; and 70–90 min, 2% B. Eluting peptides were mass analyzed on an LTQ Orbitrap Velos MS (Thermo Scientific), equipped with a nanoelectrospray ionization source. The instrument was operated using a data-dependent method with dynamic exclusion enabled. Full-scan (*m*/*z* 300–2000) spectra were acquired with the Orbitrap (resolution 60,000), and the top 16 most abundant ions in each MS scan were selected for fragmentation in the LTQ. An isolation width of 2 *m*/*z*, activation time of 10 ms, and 35% normalized collision energy were used to generate MS^2 spectra. Dynamic exclusion settings allowed for a repeat count of 2 within a repeat duration of 10 s, and the exclusion duration time was set to 15 s. For identification of Pin1 peptides, tandem mass spectra were searched with Sequest (Thermo Scientific) against a human subset database created from the UniprotKB protein database (www.uniprot.org). Variable modifications of +57.0214 on Cys (carbamidomethylation), +15.9949 on Met (oxidation), +141.1279 on Lys and Arg (corresponding to reduced Schiff base), +158.1306 on Cys, Lys, and His residues (corresponding to reduced ONE modification), +156.1150 on Lys (corresponding to the 4-ketoamide), and +118.0783 on Cys or Lys (corresponding to the pyrrole cross-link) were included for database searching. Search results were assembled using Scaffold 3.0 (Proteome Software). Spectra acquired of Pin1 peptides of interest were then inspected using Xcalibur 2.1 Qual Browser software (Thermo Scientific). The 4-ONE-cross-linked Pin1 peptide SDCSSAKARGDLGAF was

confirmed following manual examination of the corresponding MS^1 and MS^2 spectra. For analysis of sample sets including 2D and 3D 4-ONE treatments, Pin-1 was similarly digested with chymotrypsin and peptides were subsequently analyzed using a targeted LC-MS/MS method on the LTQ Orbitrap Velos. A 90 min gradient was performed, consisting of the following: 0–14 min, 2-5% B; 14–70 min, 5–40% B; 70–78 min, 40–92% B; 78-79 min, 92-2% B; 79–90 min, 2% B. For analysis of deuterium-containing cross-linked peptides, the LTQ Orbitrap Velos was operated using a combination method of data-dependent and targeted scan events. Targets were of specific m/*z* values corresponding to 4-ONE cross-linked peptide, SDCSSAKARGDLGAF, and m/z values included those that would correspond to non-deuterated as well as deuterated cross-link forms. For these targeted scan events, MS2 spectra were acquired using the Orbitrap as the mass analyzer such that data were collected at higher resolution. Specifically, mass resolution of 15,000 was employed and target AGC values were increased to $2e^5$ with a max ion time of 250ms. All high-resolution MS2 data were analyzed by manual interrogation of unprocessed spectra.

Results

Pin1 modification by ONE results in a Cys-Lys pyrrole-containing cross-link in the active site

To investigate the adduct chemistry of ONE-adducted Pin1, adducted peptides were examined for ions that were not present in an unmodified Pin1 digest; three new adduct ions were detected in the ONE-treated Pin1 sample. Our previous study identified the ion appearing at 1542 m/z to be the Cys113-containing peptide.[87] Although this peak was again present in the control Pin1 digest (Figure 23A), it was completely absent in the ONE-treated sample and was replaced by a peak at 1603 *m/z* (Figure 23B). The TOF/TOF spectrum of *m/z* 1603 (Figure 24B)was identified as the peptide containing Cys113, as evidenced by the most intense ions matching the theoretical peptide

spectrum, but with a mass shift of +61 *m/z* relative to the carbamidomethylated peptide (Figure 24A). This mass shift represents a total mass shift of +118 *m/z* relative to the unmodified, non-carbamidomethylated peptide. A previous study on the reaction of ONE with Histone H4 reported a +118 m/z mass shift corresponding to a His-Lys pyrrole-containing interpeptide cross-link.[79] Therefore, we interrogated the possibility of an active site cross-link resulting from ONE reaction with Pin1.

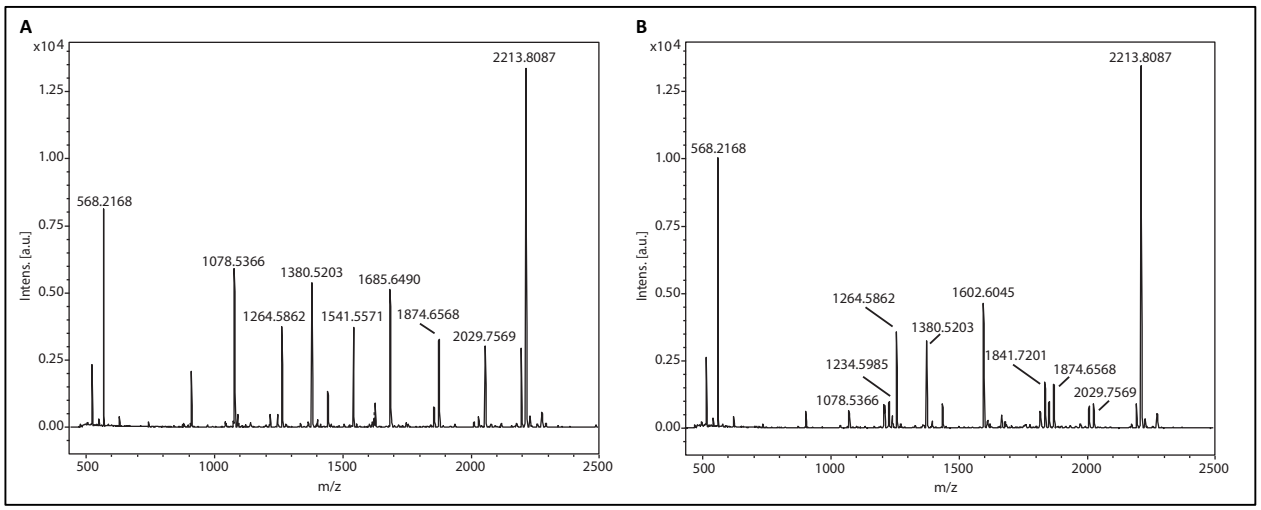

Figure 23. MALDI-TOF spectra of chymotryptic peptides generated from Pin1. Pin1 was treated with A) vehicle (DMSO) or B) 300 μM ONE, digested with chymotrypsin, and subjected to MALDI-TOF**.** Treatment with ONE results in complete or nearly complete disappearance of the 1078, 1542, and 1685 *m/z* peaks and the appearance of 1234, 1603, and 1841 *m/z* peaks. Reproduced with permission from *Aluise et al.* (2015) Chem. Res. Toxicol. 28(4):817-27. Copyright 2015 American Chemical Society.[1]

All of the most intense ions in the TOF/TOF fragmentation spectrum of 1603 *m/z* were identified as fragment masses of $SDC_{Cam}SSAKARGDLGAF$ N-terminal to Ala-118 with a variable mass shift of +61 *m/z* placed on either the Cys or Lys (Figure 24B). Reduction of ONE-modified Pin1 with $NaBH_4$, did not result in a mass shift, as evidenced by MALDI-TOF MS, suggesting the absence of a reducible carbonyl group (Figure 25B). By contrast, treatment of HNE-modified Pin1 with $NaBH_4$ resulted in a shift of +2 Da resulting from the reduction of the aldehyde group in the Cys113 Michael adduct to the corresponding alcohol (Figure 25A). The isotopic distribution of 1603 *m/z* in the ONE-Pin1 spectrum indicates a +1 charge state (data not shown), minimizing the possibility of a multiply charged interpeptide cross-link.

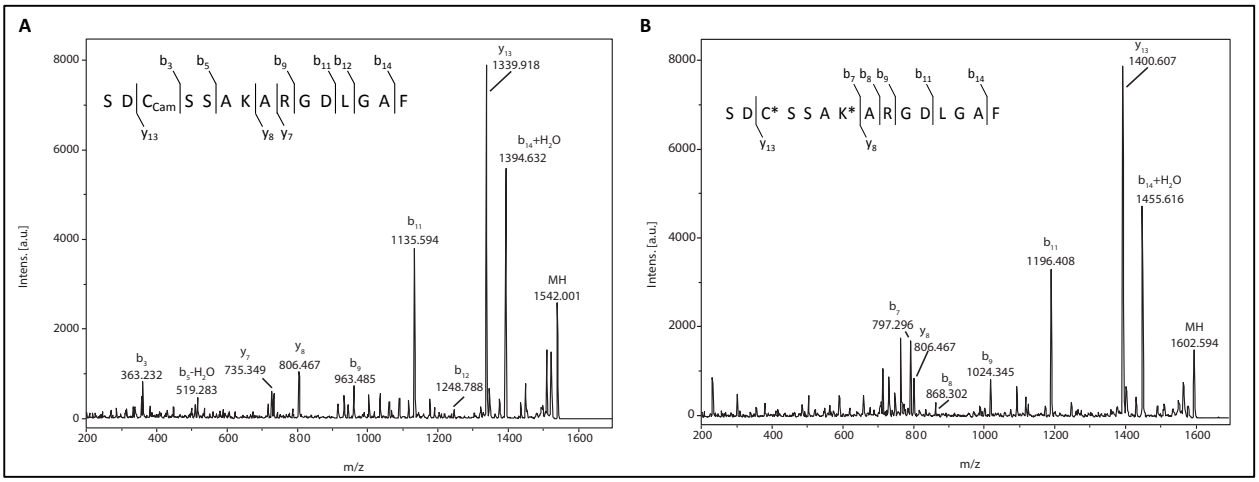

Figure 24. TOF/TOF spectra of the chymotryptic peptide containing the Pin1 active site. Pin1 active site Cys (SDCSSAKARGDLGAF) following A) carbamidomethylation (Cam) with a parent ion at 1542 *m/z* and B) ONE-treatment, resulting in a cross-link between Cys and Lys with a parent ion at 1603 *m/z*. In the cross-linked peptide fragmentation, the ions C-terminal to the Lys match the indicated peptide when an additional mass of +61 *m/z* relative to the carbamidomethylated peptide (57 Da + 61 Da = 118 Da) is considered on either the Cys or the Lys. Reproduced with permission from *Aluise et al.* (2015) Chem. Res. Toxicol. 28(4):817-27. Copyright 2015 American Chemical Society.[1]

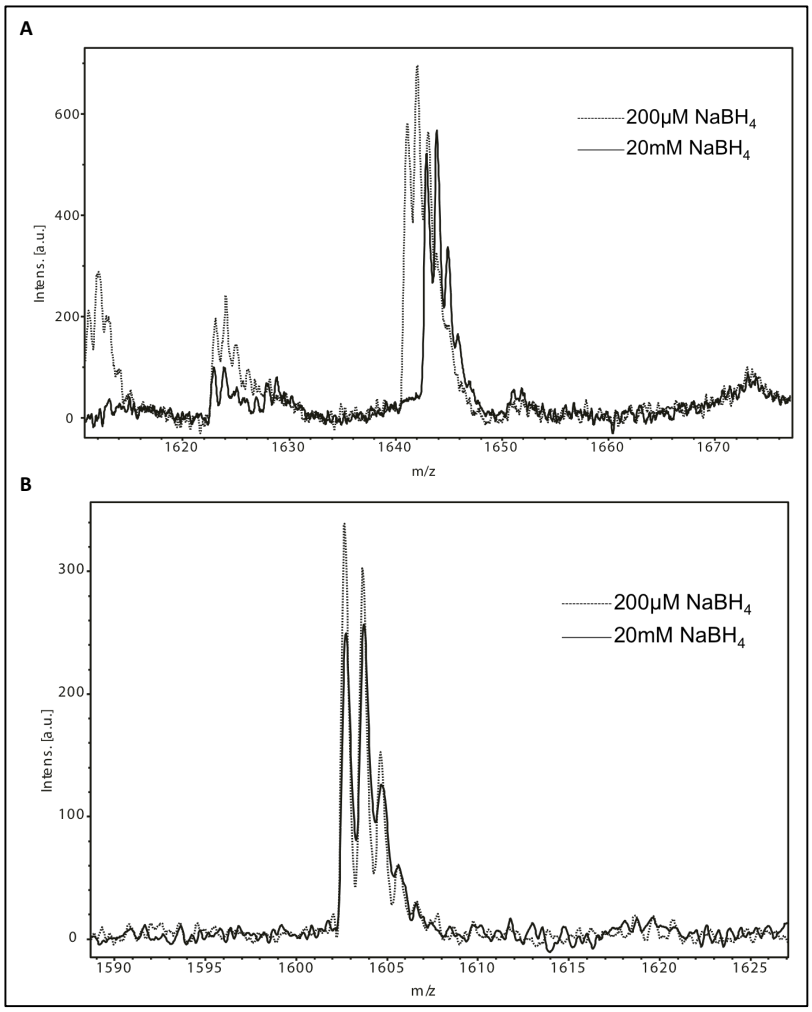

Figure 25. Analysis of the effects of $NaBH_4$ reduction on the Cys113-containing peptide. Pin1was treated with HNE or ONE, reduced with $NaBH_4$, and digested with chymotrypsin. Cys113-HNE and suspected Cys113-Lys117 pyrrole ONE adduct. A) Pin1 exposed to HNE and treated with (solid line) or without (dashed line) $NaBH_4$. B) Pin1 exposed to ONE with (solid line) or without (dashed line) $NaBH_4$. Reproduced with permission from *Aluise et al.* (2015) Chem. Res. Toxicol. 28(4):817-27. Copyright 2015 American Chemical Society.[1]

To determine the requirement of Cys113 for cross-link formation, Pin1 was pretreated with iodoacetamide to block Cys residues prior to ONE treatment. Under these conditions, the 1603 *m/z* peptide was eliminated; however, treatment with iodoacetamide after Pin1 modification by ONE did not interfere with the formation of the 1603 *m/z* peptide (Figure 26A). Similarly, to assess the requirement of Lys117, Pin1 was preteated with acetic anhydride, resulting in Lys acetylation, to block accessible Lys residues prior to ONE treatment. These conditions prevented the appearance

of the 1603 *m/z* ion whereas acetic anhydride treatment after ONE modification did not (Figure 26B). These data are supportive of an intrapeptide pyrrole-containing cross-link of +118 *m/z* resulting from the reaction of ONE with Cys113 and Lys117.

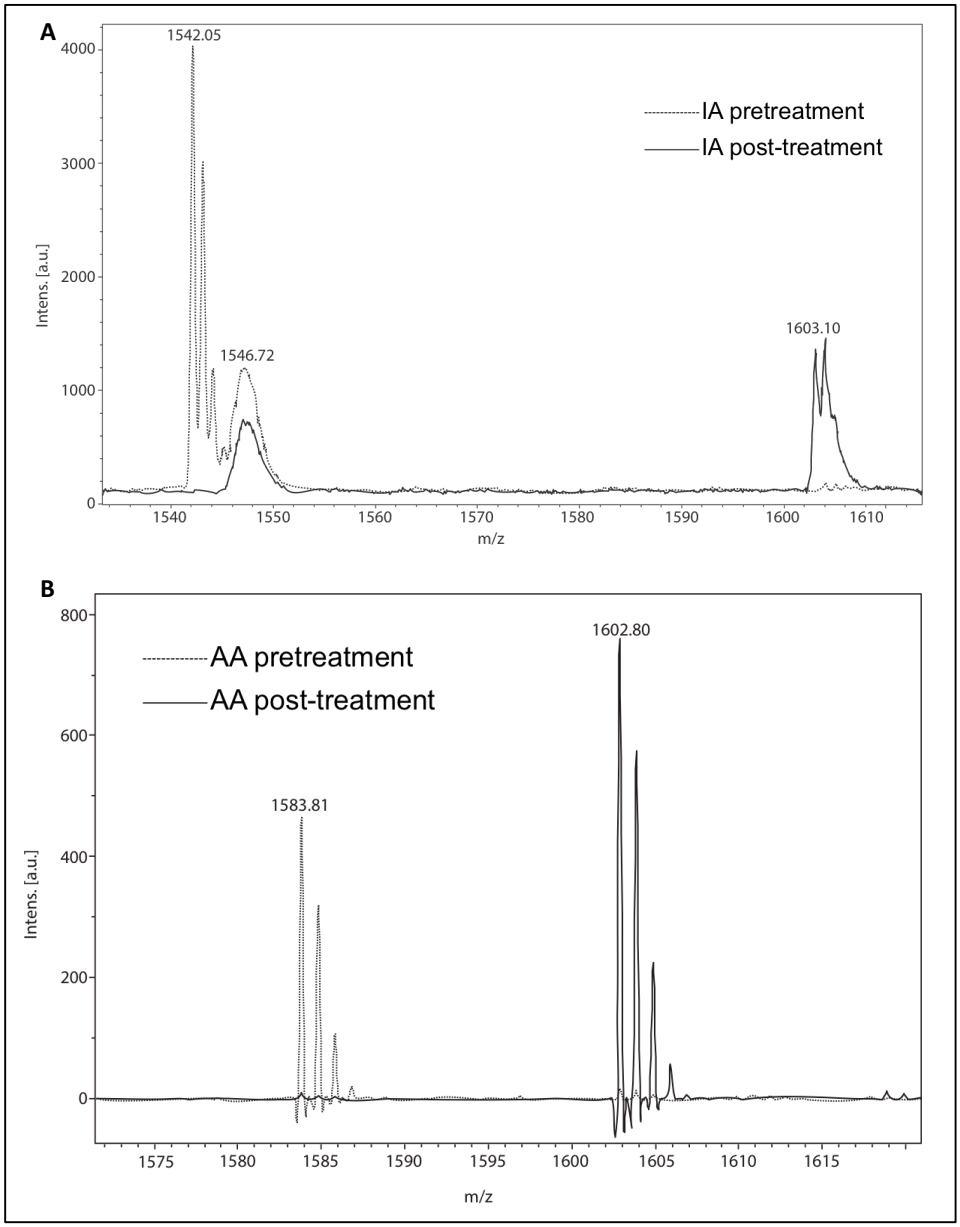

Figure 26. Effect of iodoacetamide and acetic anhydride on ONE-dependent Pin-1 adduction. A) Pin1 was treated with 750 μM iodoacetamide (IA) prior to (dashed line) or after (solid line) exposure to ONE. B) Pin1 was treated with 5mM acetic anhydride (AA) prior to (dashed line) or after (solid line) exposure to ONE. Pretreatment of Pin1 with either IA or AA prior to ONE prevents formation of the ONE adduct (1603 *m/z*), while treatment of Pin1 with either reagent after ONE exposure had no effect on adduct formation, suggesting a requirement for both Cys and Lys in adduct formation. Reproduced with permission from *Aluise et al.* (2015) Chem. Res. Toxicol. 28(4):817-27. Copyright 2015 American Chemical Society.[1]

The Cys-Lys pyrrole cross-link in the active site of Pin1 forms more rapidly than other observed ONE-modifications

Two additional peaks with *m/z* values corresponding to Pin1 peptides containing ONE-modifications were also identified (Figure 24B), although both were present in low abundance relative to the ion of the Cys113-Lys117 cross-link. Peptide masses of 1234 *m/z* and 1842 *m/z* in the spectrum of ONE-treated Pin1 corresponded to addition of +156 *m/z* to SRGQMQKPFEDSAF and ADEEKLPPGWEKRM, respectively. This mass shift is suggestive of reduced 4-ketoamide adducts derived from ONE modification of Lys residues.[71,72] Due to the relatively low ion intensities of these adducts formed upon Pin1 reaction with ONE, MALDI-TOF/TOF fragmentation resulted in rather low quality spectra; therefore to further verify the sites of these adducts using a more sensitive approach, we analyzed these peptides using LC-coupled tandem mass spectrometry (LC-MS/MS). LC-MS/MS analysis of Pin1 treated with ONE identified 3 total adducts: the suspected cross-link, and one each on Lys residues contained in the suspected peptides from the MALDI experiment (SRGQMQKPFEDSAF and ADEEKLPPGWEKRM). The fragmentation of 1234 *m/z* indicates a ketoamide at Lys132 (Figure 27A), which was previously identified as a site for Michael addition on Pin1 by HNE.[87] Because ADEEKLPPGWEKRM contains two Lys residues (Lys6 and Lys13), fragmentation of the ion was necessary to identify the specific amino acid site of modification. LC-MS/MS fragmentation spectra of peptides from Pin1 treated with ONE identified Lys13, not Lys6, as the site of adduction on this peptide (Figure 27B).

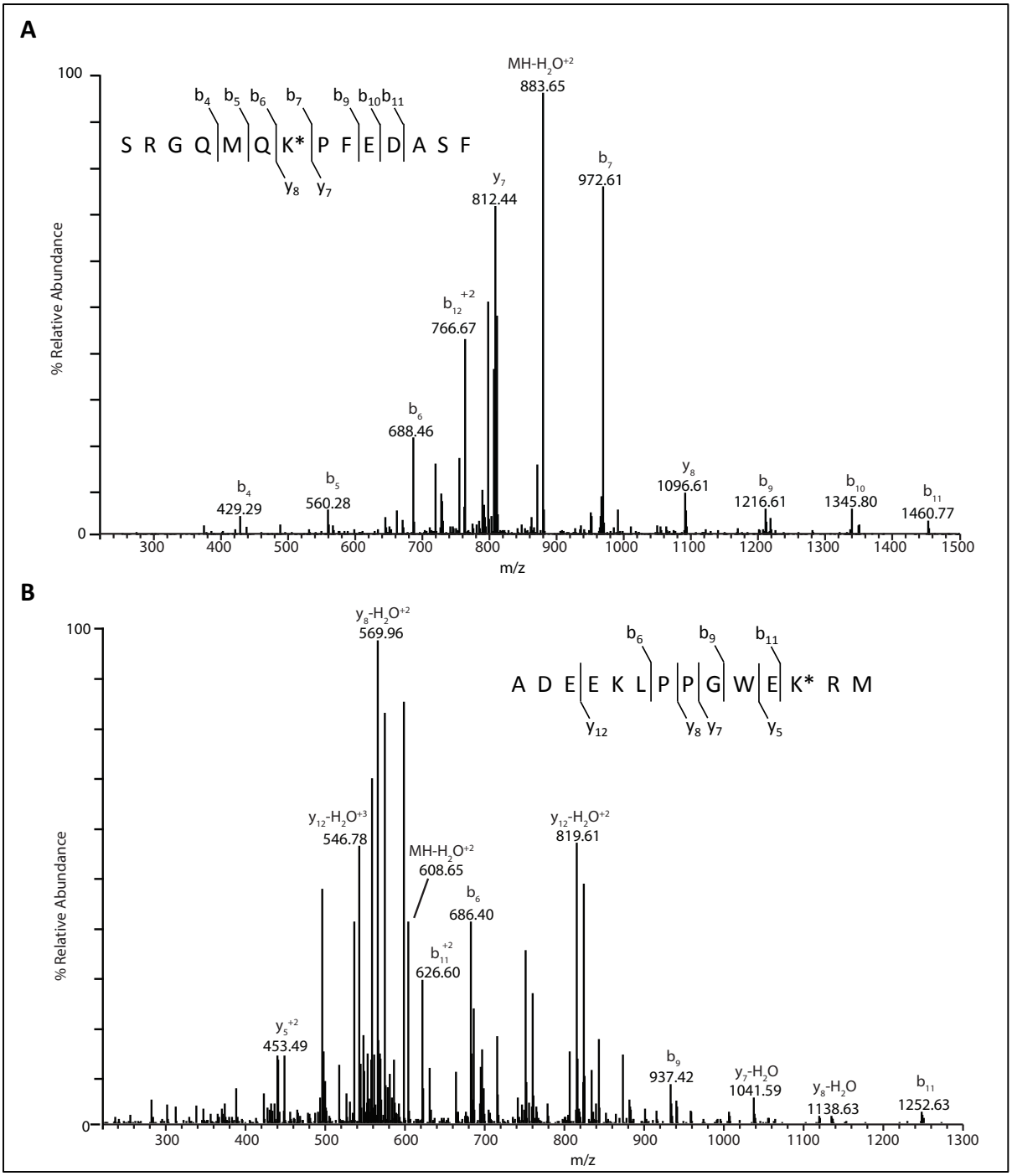

Figure 27. Tandem mass spectra of peptides with the 4-ketoamide adduct. Tandem mass spectra of A) *m/z* 1234 corresponding to SRGQMQKPFEDSAF and B) *m/z* 1842 corresponding to ADEEKLPPGWEKRM. Both spectra show a mass shift of +154 *m/z*, indicative of a 4-ketoamide adduct on Lys. Reproduced with permission from *Aluise et al.* (2015) Chem. Res. Toxicol. 28(4):817-27. Copyright 2015 American Chemical Society.[1]

Since more than one adduct was identified in ONE-treated Pin1, we examined their relative rates of formation using MALDI-TOF MS. After proteolysis, peaks corresponding to unmodified and modified Pin1 peptides are detectable simultaneously in the MALDI-TOF spectra, so the relative rates of modification of the individual sites can be deduced.[159] Pin1 was incubated with either a fixed concentration of ONE for varying times or with varying concentrations of ONE for a fixed time. As shown in Figure 28A, the Cys-Lys pyrrole cross-link is formed very rapidly and at the lowest concentration of ONE. In contrast, the formation of ketoamide adducts at Lys132 or Lys13 requires high ONE concentrations (Figure 28B) and long reaction times. Comparison of the modification of Cys113 by equivalent concentrations of ONE and HNE indicated high reactivity with ONE but no reaction with HNE (Figure 29).

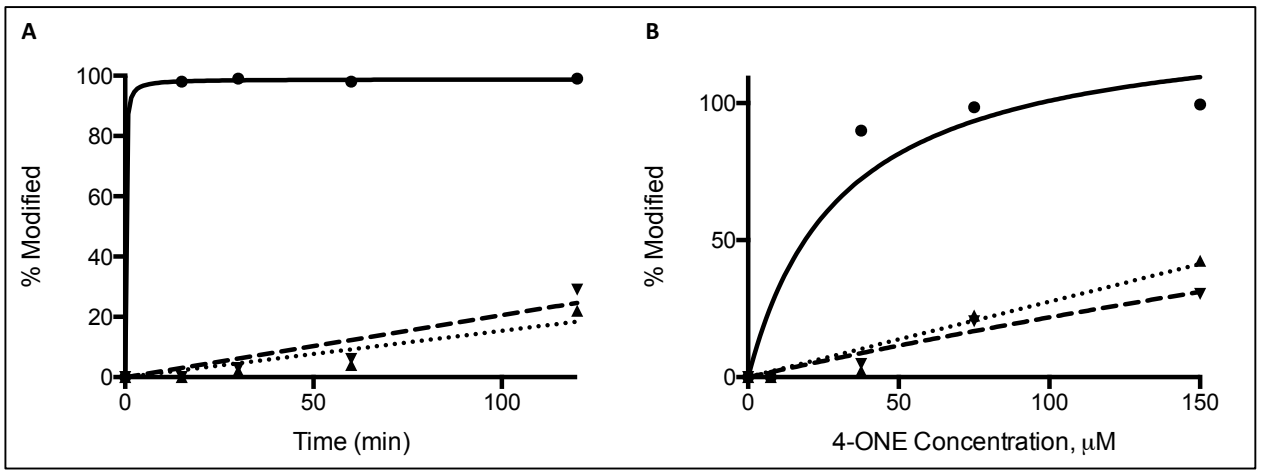

Figure 28. Relative reactivity of recovered Pin1 adducted peptides. Reactivity of Pin1 adducted peptides as a function of A) time of exposure to 200μM ONE and B) ONE concentration for 1 h. % Modified was calculated using the ion intensity of the formed adduct divided by the sum of the intensities of the adduct ion and the corresponding unadducted ion. The Cys113-Lys117 pyrrole adduct (solid line) outcompetes the other two adducts (Lys13 (dashed line), Lys132 (dotted line)) observed. Reproduced with permission from *Aluise et al.* (2015) Chem. Res. Toxicol. 28(4):817-27. Copyright 2015 American Chemical Society.[1]

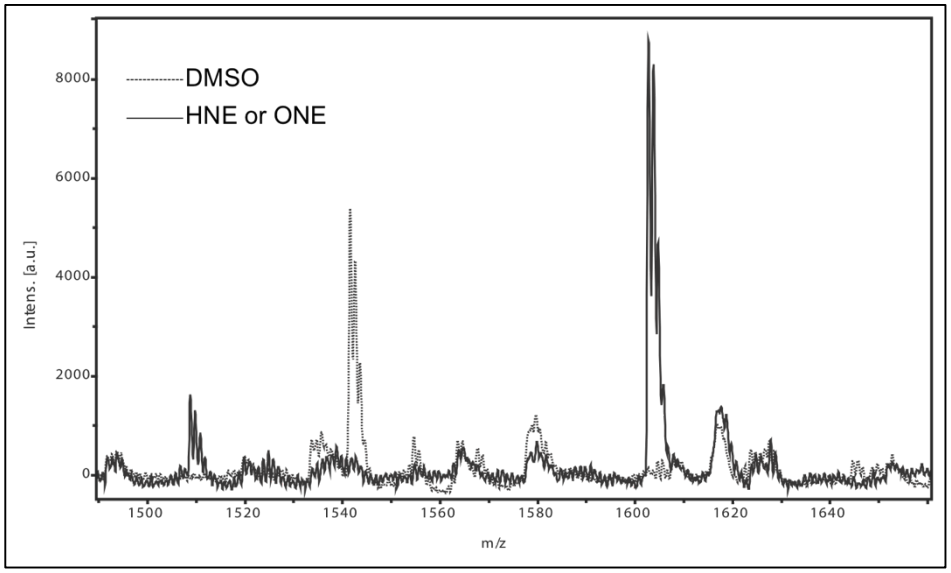

Figure 29. Competition of HNE versus ONE for the active site Cys (Cys113). Pin1 was incubated with DMSO (dashed line) or a 50:50 mixture of 150μM each HNE:ONE (solid line), digested with chymotrypsin, and analyzed by MADLI-TOF mass spectrometry for the presence of the Cys113-HNE Michael adduct (1643 *m/z*) and the Cys113-Lys117 ONE cross-link (1603 *m/z*). Reproduced with permission from *Aluise et al.* (2015) Chem. Res. Toxicol. 28(4):817-27. Copyright 2015 American Chemical Society.[1]

Reaction of Pin1 with Specifically Deuterated ONE

To determine the mechanism of cross-link formation and further elucidate the possible structure, deuterated ONE analogs were synthesized to contain a deuterium at C2 or at C3, designated 2D-ONE and 3D-ONE (Figure 22), respectively. Recombinant Pin1 was incubated with vehicle control, ONE, 2D-ONE, or 3D-ONE (25 μM) for 1 h, carbamidomethylated, and then digested with chymotrypsin. Under these conditions, the Cys113-containing peptide ($SDC_{Cam}SSAKARGDLGAF$), is observed as parent ion with a +2 charge at 771.35 *m/z* (Figure 30A). Treatment with ONE results in a mass shift of +61 (*m/z* 30.5), producing a parent ion at 801.88 *m/z* consistent with formation of the cross-link (Figure 30B). The 2D-ONE-treated sample has a major +2 parent ion at 802.38 *m/z*. This observed ion has a mass error of 1.2 ppm relative to the theoretical mass of the peptide containing a deuterium within the cross-link, thereby verifying the presence of deuterium at the C2 position in the cross-link. Additionally, fragmentation of

802.38 *m/z* showed a shift in the observed b-series ions corresponding to the presence of deuterium in fragment ions containing the cross-linked portion of the peptide (Figure 30C). Interestingly, the 801.88 *m/z* peak is still present in the isotopic distribution of SDCSSAKARGDLGAF with the 2D-ONE, indicative that some cross-linked peptides do not contain the deuterium. The spectrum for the 3D-ONE sample shows the dominant +2 parent ion at 801.88 *m/z*, 0.4 ppm relative to the theoretical mass of the non-deuterated cross-link. Fragmentation of this peptide shows a spectrum identical to that of the undeuterated ONE sample, further indicating that the deuterium is not present in the cross-link (Figure 30D). These data indicate that the first step in cross-link formation, Michael addition of Cys113, occurs through nucleophilic attack at C3 of ONE, resulting in the loss of the deuterium in that position (Figure 31).

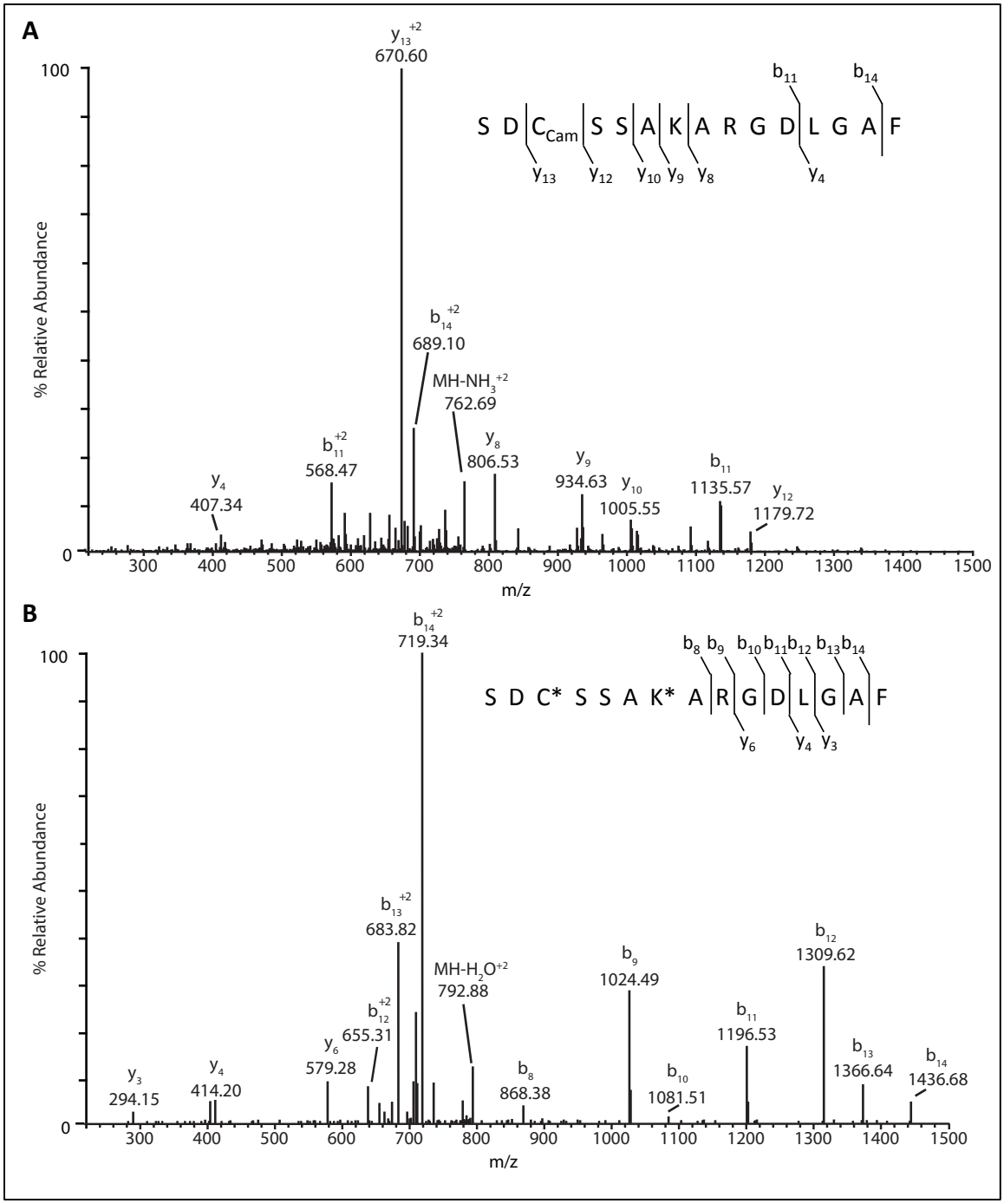
A
y13+2
670.60
100
% Relative Abundance
b11
b14
S D CCam S S A K A R G D L G A F
y13 y12 y10 y9 y8 y4
b14+2
689.10
MH-NH3+2
762.69
b11+2
568.47
y8
806.53
y9
934.63
y10
1005.55
b11
1135.57
y12
1179.72
y4
407.34
0
300 400 500 600 700 800 900 1000 1100 1200 1300 1400 1500
m/z
B
b14+2
719.34
100
% Relative Abundance
b8 b9 b10 b11 b12 b13 b14
S D C* S S A K* A R G D L G A F
y6 y4 y3
b13+2
683.82
MH-H2O+2
792.88
b12+2
655.31
y6
579.28
b9
1024.49
b12
1309.62
b11
1196.53
b13
1366.64
b14
1436.68
b8
868.38
b10
1081.51
y3
294.15
y4
414.20
0
300 400 500 600 700 800 900 1000 1100 1200 1300 1400 1500
m/z

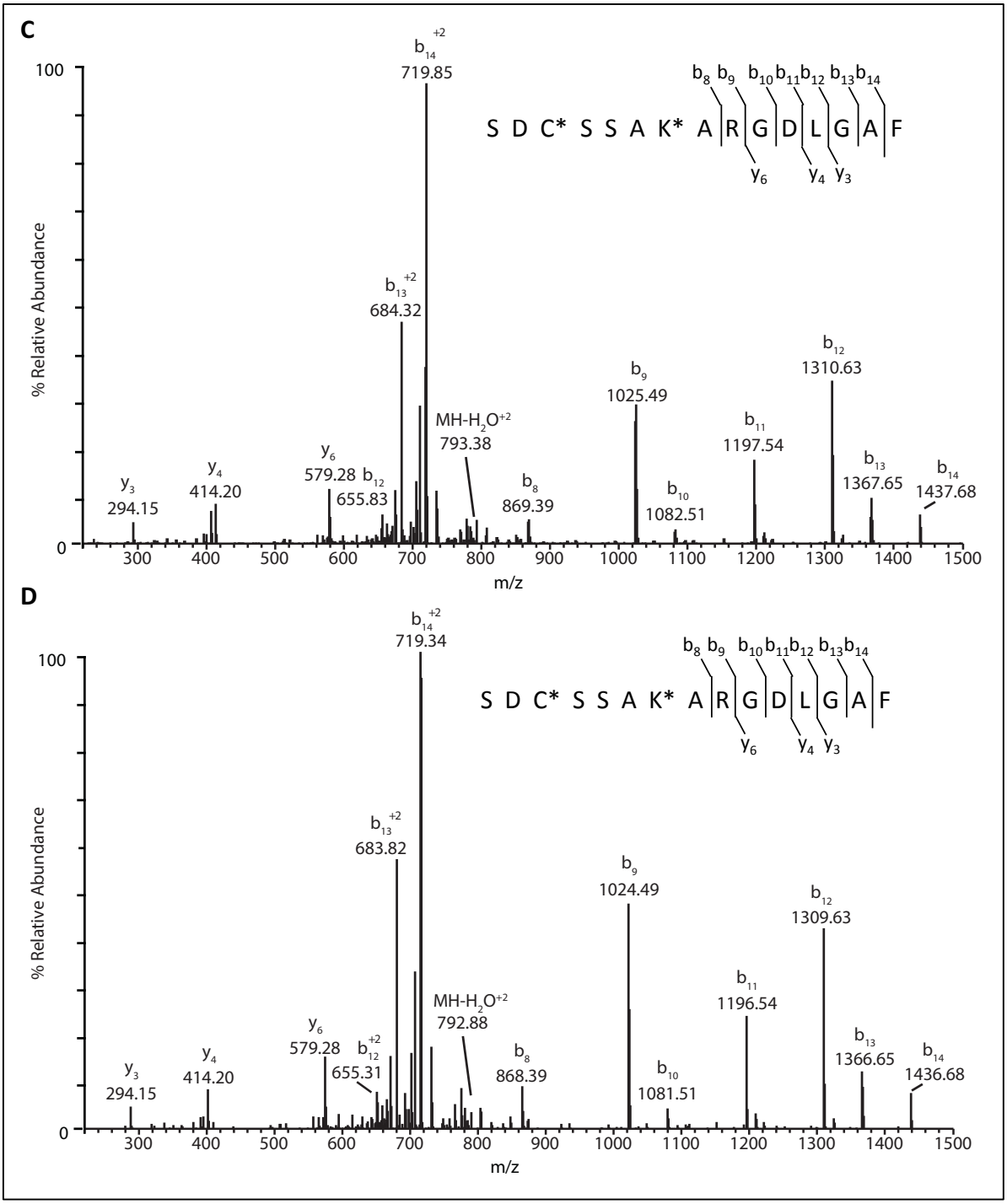

Figure 30. Tandem mass spectra of SDCSSAKARGDLGAF with deuterated ONE analogues. Tandem mass spectra of SDCSSAKARGDLGAF at A) *m/z* 771.35 for DMSO-treated, B) *m/z* 801.88 for ONE-treated, C) *m/z* 802.39 for 2D-ONE-treated, and D) *m/z* 801.88 for 3D-ONE-treated Pin1. Reproduced with permission from *Aluise et al.* (2015) Chem. Res. Toxicol. 28(4):817-27. Copyright 2015 American Chemical Society.[1]

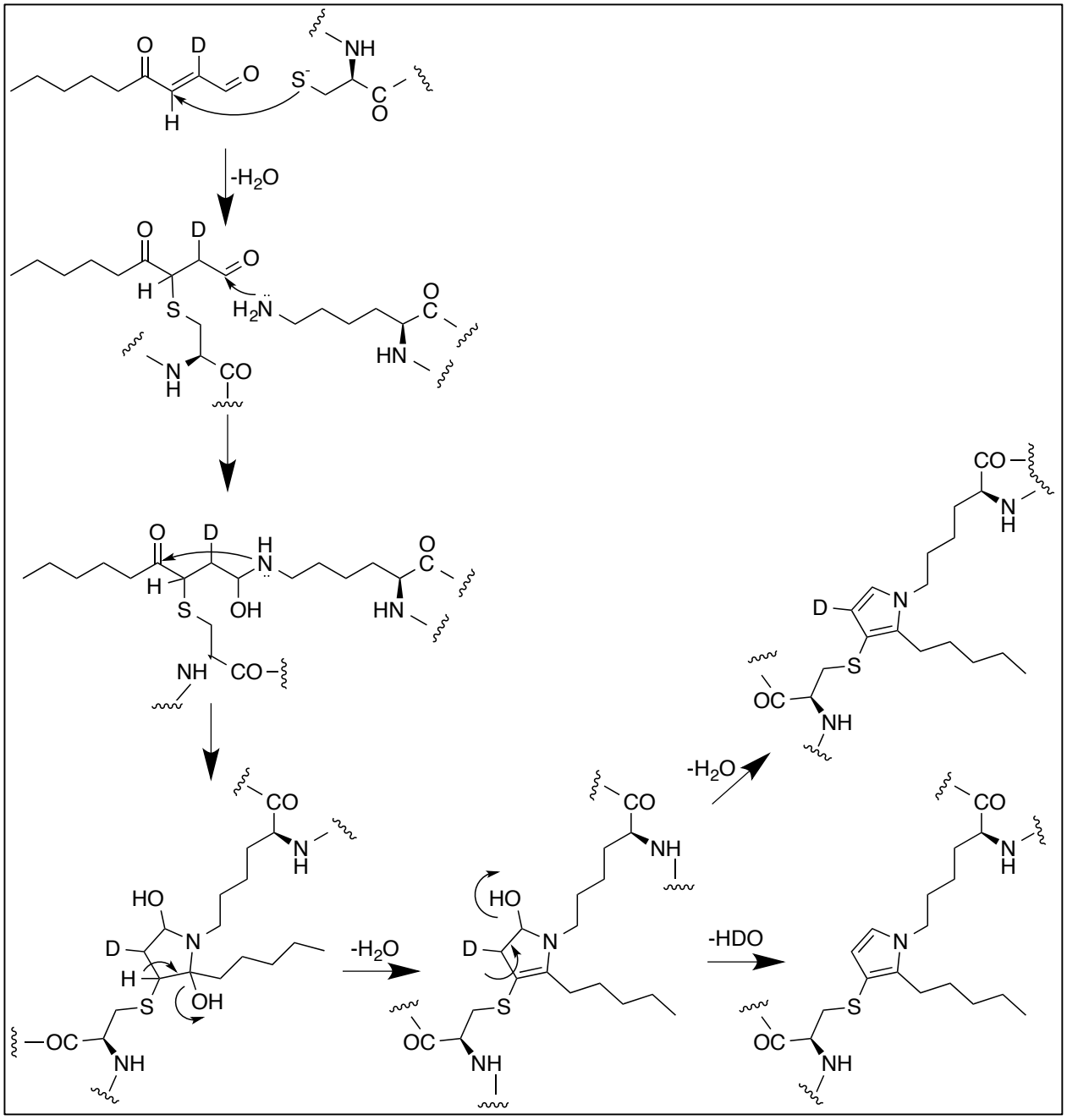

Figure 31. Proposed mechanism of cross-link formation. Cross-link formation is initiated by nucleophilic attack of the thiolate of Cys to C3 of ONE. The ε-amine of Lys then attacks C1 of ONE to form the carbinolamine, followed by an additional attack to C4 of ONE to form the pyrrolidine. Two dehydration reactions result in the formation of the pyrrole-containing cross-link. Reproduced with permission from *Aluise et al.* (2015) Chem. Res. Toxicol. 28(4):817-27. Copyright 2015 American Chemical Society.[1]

Pin1 is a target of ONE in MDA-MB-231 cells

To assess the susceptibility of Pin1 to modification by ONE in a cellular setting, MDA-MB-231 cells were treated with varying concentrations of aONE (Figure 22)for 1 h. Following click chemistry, streptavidin pull-down, and cleavage of the photocleavable biotin linker, Pin1 western blotting was conducted. As shown in Figure 32, Pin1 is susceptible to modification by aONE at 10 μM, which is within the pathological range of electrophiles.[66,160,161] Given the high efficiency of formation of the Cys-Lys cross-link *in vitro*, it is likely that this is the identity of the modification in the intact cells.

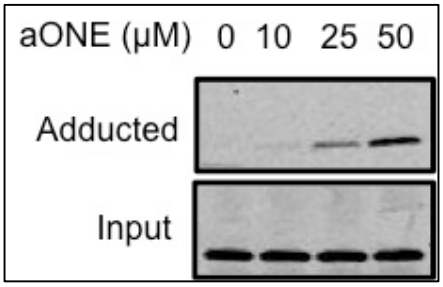

Figure 32. Western blot of adducted Pin1 from aONE-exposed MDA-MB-231 cells. Click chemistry was performed on total cells lysates with increasing concentrations on aONE. Following photo-elution of aONE-modified proteins, eluates (adducted) and total cell lysates (input) were separated by SDS-PAGE and subjected to western blot with anti-Pin1 antibody. Reproduced with permission from *Aluise et al.* (2015) Chem. Res. Toxicol. 28(4):817-27. Copyright 2015 American Chemical Society.[1]

Discussion

Many previous studies on the reactivity of lipid electrophiles with proteins have focused on HNE, as it has long been considered a major lipid hydroperoxide-derived electrophile. However, the discovery of ONE as another important electrophilic product of lipid peroxidation has generated interest in the relative reactivity of ONE with DNA and proteins, as compared to that of HNE. Relative to ONE, HNE-protein adducts are relatively straightforward to investigate, mainly because the principal reaction of HNE with proteins is the formation of Michael adducts to

Cys or His residues. In contrast, despite a difference in structure of only two hydrogen atoms, ONE-derived modifications to proteins can be profoundly more difficult to characterize, largely due to the rapid reactivity with Cys and Lys residues, the potential to cross-link between two residues, and the ability to generate adducts with multiple chemical structures depending on the microenvironment.[162,64,71,72] Therefore, the physiological spectrum of potential adducts arising from ONE is far more complicated than that of HNE.[64] Additionally, some ONE adducts, including the ketoamide and possibly the cross-link, are irreversible, making these adducts significantly more stable and inherently longer lived.[72] The more persistent effects of ONE modifications makes them a pivotal area of research.

Due to the fact that ONE generates various structural modifications, MS-based analysis of ONE-treated proteins likely provides the most information in elucidating site-specific protein adducts. Incubation of purified Pin1 with ONE revealed mass shifts of +156 *m/z* and +118 *m/z* relative to Pin1 chymotryptic peptides. Through multiple independent experiments, our data support the identity of an ONE adduct to Pin1 as a Cys-Lys pyrrole-containing cross-link in the active site of the protein (Figure 31). Blockage of either Cys113 or Lys117 by iodoacetamide and acetic anhydride, respectively, prevented the formation of the cross-link by ONE. Furthermore, reduction via $NaBH_4$ did not result in an additional mass shift. These data suggest that the resulting adduct does not contain a carbonyl functionality, further indicating the pyrrole adduct, which lacks a carbonyl. This adduct was formed at lower concentrations of ONE and shorter incubation times, than other ONE adducts, and its formation also completely outcompeted the formation of the Cys-HNE Michael adduct, indicating that this reaction proceeds with considerable efficiency relative to those of many other electrophile-protein modifications.

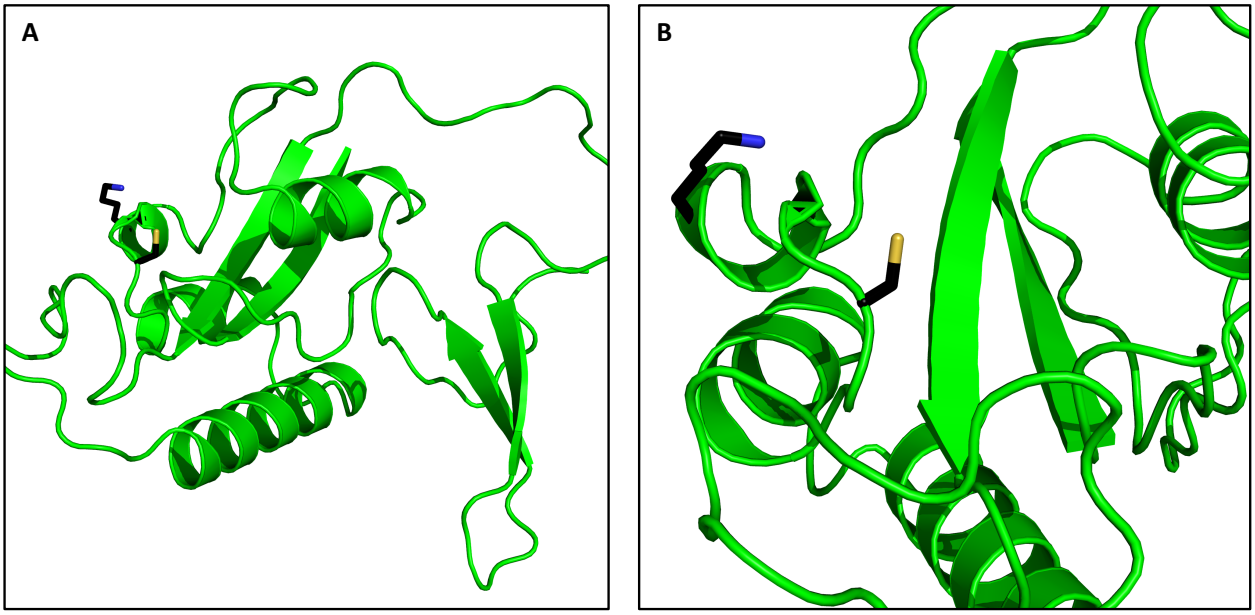

Figure 33. Pin1 crystal structure. A) Crystal structure of Pin1 highlighting Lys117 and Cys113 (black). B) Cys113 side chain orientation relative to Lys117. Reproduced with permission from *Aluise et al.* (2015) Chem. Res. Toxicol. 28(4):817-27. Copyright 2015 American Chemical Society.[1]

A Cys-Lys pyrrole-containing cross-link derived from ONE was detected by Zhu et al.[163] in the reaction of oxidized linoleic acid with β-lactoglobulin, but it represented a small fraction of the total ONE adduct burden; this contrasts with the present findings with Pin1, which indicate that the pyrrole-containing cross-link forms rapidly and in high yield. Examination of the crystal structure of Pin1 provides insights into the possible reasons for the high reactivity of Pin1 with regard to formation of this adduct (Figure 33). Cys113 sits in the active site of the enzyme and is separated from Lys117 by only 6.5 Å. Lys117 is located on the turn of a short alpha helix (5 amino acids) C-terminal to Cys113. The Lys117 side chain is directed toward Cys113, facilitating reaction of the amino group with the initial Michael adduct formed by reaction of ONE with the catalytic Cys (Figure 31). Since Cys113 participates as a nucleophile in peptidyl *cis-trans* isomerization, it has enhanced nucleophilicity compared to those of other nucleophilic sites in the protein, allowing it to trap ONE and position the carbonyl groups of the Michael adduct adjacent

to Lys117 for condensation. Oe et al.[79] have reported the formation of a His-Lys pyrrole-containing cross-link on reaction of ONE with Histone H4 between His75 and Lys77, and indicated that –HAK– amino acid sequences in proteins may represent a primary sequence target motif for formation of the pyrrole adduct resulting from ONE. This adduct could also likely be formed between a Cys/His residue distant from a Lys residue based on primary sequence, but spatially close based on the three dimensional structure of the protein. The Cys-Lys epitope modified by ONE in Pin1 is both spatially close and separated by only four amino acids, supporting the feasibility of the reaction for this specific protein. The studies with deuterated ONE analogs further support the mechanism of pyrrole cross-link formation predicted by Oe et al.[79] (Figure 31).

Treatment of cells with aONE followed by click chemistry conjugation to biotin revealed that Pin1 is modified by aONE as a function of concentration. The results support that aONE does not alter the total level of Pin1, but rather modifies the existing pool of protein. Interestingly, oxidative modification of Pin1 has been observed in the brains of Alzheimer's disease patients, and the modification leads to inhibition of Pin1 isomerase activity.[164] Pin1 inhibition has been suggested to underlie the formation of neurofibrillary tangles in AD brain, thereby catalyzing disease pathogenesis.[165] Isomer-specific antibodies of tau, a Pin1 substrate, display increased *cis*-tau labeling in AD brain compared to control brain, indicating a Pin1 inhibitory event.[166] Due to the rapid formation of the Cys-Lys pyrrole adduct in our *in vitro* experiments, we expect the same modification to occur in cells exposed to ONE. Furthermore, Miyashita et al.[167] demonstrated that adduction of a pyrrole onto Lys residues increases protein surface electronegativity, resulting in the formation of a damage-associated molecular pattern capable of triggering an autoimmune response.

Cis isomers of proline-containing peptide bonds occur with a frequency of 5-6%, and many

of these bonds are present at bend, coil, or turn conformations, which are surface exposed.[168,169] Phosphorylation of serine or threonine preceding a proline in peptide bonds renders this motif resistant to isomerization by conventional PPIases, except Pin1. Pin1 binds protein substrates through a conserved WW-binding domain, followed by isomerization of the peptide bond by the PPIase domain. Some protein substrates of Pin1 contain multiple pSer-Pro or pThr-Pro motifs, and the overall 3-dimensional structure and, therefore, protein activity, can be dictated by whether these bonds are in *cis* or *trans.*[170] Because modifications to Pin1 can adversely affect the network of proteins it controls, elucidation of potential oxidative adducts to this protein is of high importance, particularly considering that oxidative stress and Pin1 dysfunction coexist in some diseases.[171] The ONE adduct to Pin1 may be a particularly important contributor to cellular dysfunction associated with oxidative stress because it forms rapidly and in high yield, completely blocks the active site, and is irreversible. The biological implications of Pin1 cross-linking by ONE are currently being explored by our laboratory.

Additional Investigation into ONE Cross-links

Since ONE was able to form an intrapeptide cross-link on Pin1, we wished to investigate if other proteins were susceptible to ONE cross-linking. To address this question, we employed a computational approach in collaboration with Dr. Jarrod Smith in the Center for Structural Biology. We searched the Protein Data Bank (PDB) for crystal structures of 162 proteins that were shown to be highly reactive toward aONE based on the work of Codreanu et al.,[84] This search found 389 structures for 153 of the proteins. We then analyzed all these crystal structures for a Cys residue within 10 Å of a Lys residue, as the key structural criterion for ONE-dependent cross-link formation. The search revealed 30 unique proteins that fulfilled these criteria (Table 3).

Table 3. Possible proteins cross-linked by ONE.

Possible Proteins Cross-linked by ONE					
TXN	YWHAE	RUVBL2	CDC37	PABCP1	EIF4A1
PKM2	HSPA8	HSP90AB1	YWHAZ	CLTC	HSP86
HSPA9	HSPA2	SHMT2	TFRC	GARS	HNRNPM
PGK1	MYH9	HARS	PFN1	LDHA	HSPA1A
YWHAQ	ANXA2	MDH2	NME1	UBB	STIP1

Among the proteins identified was thioredoxin (TRX), which had previously been shown to be a target of HNE modification at the redox-sensitive Cys.[172] Using recombinant TRX1, we incubated the protein *in vitro* with ONE, digested with trypsin, and performed tandem mass spectrometry to assess sites of modification. While multiple Lys residues were adducted by ONE in the form of both Michael adducts and the 4-ketoamide, no modifications were observed on Cys. Additional attempts to reduce disulfides on recombinant TRX1 prior to ONE treatment did not yield observable cross-links at the active site.

The lack of ONE adducts on Cys was unexpected, especially due to the evidence that the redox-senstive Cys residues are adducted by HNE and because TRX1 is adducted by aONE based on the proteomic inventory published by Codreanu et al.[84] We hypothesize that the lack of Cys modifications was due to the incomplete reduction of disulfides or preferential reformation of disulfides prior to ONE exposure. Structurally, the two redox-active Cys residues are in close proximity, and mechanistically, disulfide bond formation is required as part of the redox cycle of TRX1. Therefore, in our *in vitro* setting, it is conceivable that disulfide bonds may reform immediately upon removal of reductant. In a cellular setting, ONE modification of the active-site Cys residues may occur, along with cross-link formation, but it is unlikely that we will be able to

observed the cross-link in cellular TRX1 due to inefficient protein purification. One additional residue, Cys72, is also in close proximity to a Lys and has the potential to form a cross-link. This Cys is not redox active, and no ONE adducts were found at this site.

CHAPTER IV

CLICK-SEQ: CLICK CHEMISTRY AND NEXT-GENERATION SEQUENCING FOR THE STUDY OF 4-OXO-2-NONENAL HISTONE MODIFICATIONS

Introduction

Oxidative stress plays a key role in a number of diseases, including cancer, atherosclerosis, neurodegenerative disease, and asthma.[121] Reactive oxygen species generated during periods of high oxidative stress readily react with cellular proteins, DNA, and polyunsaturated fatty acids in the membranes. Decomposition of these oxidized lipids results in the formation of reactive lipid aldehydes, such as 4-hydroxy-2-nonenal (HNE) and 4-oxo-2-nonenal (ONE), which can react with nucleophilic centers in the cell, particularly Cys, His, and Lys residues on proteins, to form covalent Michael modifications.[66,64] Additionally, ONE displays high reactivity with Lys residues, resulting in the formation of Schiff base adducts and the stable 4-ketoamide adduct.[71,72] These covalent adducts are capable of altering protein function and disrupting key cellular processes.

Recent advancements utilizing click chemistry have allowed for proteome-wide identification of electrophile targets. Alkyne analogues of HNE and ONE, aHNE and aONE, respectively, display similar reactivity to their native counterparts, but allow for selective isolation by click chemistry conjugation to a photo-cleavable azido-biotin and subsequent streptavidin capture and photo-elution.[84] While a large number of proteins were found to be targets of the aHNE and aONE, histones were highly enriched in the aONE-treated samples. Further reports by Galligan et al.[88] showed that Lys residues of histones were modified with the stable 4-ketoamide adduct (4-Kam-Lys) and that modification of nucleosomes by ONE disrupted nucleosome-DNA complexes. H3K27 was determined to contain this adduct in RAW264.7 macrophage cells under

inflammatory conditions, suggesting that these modifications occur under pathophysiological conditions.

Epigenetic studies mainly focus on Lys modifications, the most abundant post-translationally modified residue in histones. Acetylated Lys (AcLys) is a known transcriptional activator, likely due to charge neutralization and relaxation of DNA around histones.[173] Conversely trimethyl Lys (me_3Lys) contributes to a net positive change on Lys, resulting in chromatin compaction and gene silencing. These post-translational modifications (PTMs) occur at distinct residues on the various core histones, and different combinations of these PTMs control chromatin structure, DNA accessibility, and the binding of proteins associated with transcriptional regulation.

Canonical PTMs are tightly regulated by writer, reader and eraser proteins which add the modifications, detect them, and remove them. Adduction of Lys by ONE blocks these sites from subsequent addition of regulatory PTMs. It is currently unknown if reader proteins can bind to 4-Kam-Lys. Very recently, SIRT2 was discovered to be an eraser of the 4-ketoamide adduct, though removal of the adduct occurs at much lower rates than removal of an acetyl group at the same site.[174] The stability of the 4-Kam-Lys and its inefficient removal, paired with the disruption of canonical regulatory histone PTMs, makes this adduct of great interest in the study of chromatin structure and accessibility.

Here, we employ the RKO cell line to develop a method for isolating DNA associated with adducted chromatin proteins using click chemistry. Successful development of this method allowed us to apply this technique with DNA sequencing using the K562 cell line, which has been used extensively in the ENCODE project, to determine the regions of DNA which are enriched with these modifications. Furthermore, we perform absolute quantitation of 4-Kam-Lys in cells to show its abundance compared to canonical PTMs. We show that ONE relaxes chromatin and

increases accessibility, similar to acetylation, and that these histone adducts are long-lived, persisting up to 24 h following initial treatment. Together, our data show that these ONE-derived histone modifications may have a significant and sustainable impact on chromatin structure and gene regulation.

Materials and Methods

Materials and Reagents. All reagents were purchased from Sigma Aldrich (St. Louis, MO) unless otherwise stated. 4-Hydroxy-2-nonenal (HNE), 4-oxo-2-nonenal (ONE), alkynyl-HNE (aHNE), and alkynyl-ONE (aONE) were synthesized in the laboratory of Dr. Ned Porter at Vanderbilt University. Cell culture media was purchased from Invitrogen (Grand Island, NY). Fetal bovine serum was purchased from Atlas Biologicals (Ft. Collins, CO). Anti-H3 (1:10,000) was purchased from Abcam (Cambridge, MA) and IR-streptavidin was purchased from Li-Cor Biosceinces (Superior, NE). All SDS-PAGE and western blot supplies were purchased from Bio-Rad (Hercules, CA) unless otherwise noted. SimpleBlue SafeStain was purchased from Invitrogen (Grand Island, NY). Streptavidin Sepharose High Performance beads were purchased from GE Life Sciences (Pittsburg, PA). Dithiothreitol was purchased from Research Products International (Mt. Proscpect, IL).

Cell Culture and Treatments. The human myelogenous leukemia cell line, K562, was cultured in RPMI with 10% fetal bovine serum. The human colorectal cancer cell line, RKO, were culured in DMEM with glutamax with 10% FBS. Cells were incubated at 37°C with 5% CO_2. All cell treatments were performed with DMSO at a concentration < 0.1%.

Chromatin Extraction. Cells were collected by centrifugation at 1000rpm for 5 minutes, washed PBS, and stored at -80°C until lysis. Cells were lysed with hypotonic lysis buffer (10mM HEPES/KOH, pH 7.9, 1.5mM $MgCl_2$, 10mM KCl, 5mM sodium butyrate, and 0.5% Igepal), with protease and phosphatase inhibitors (Sigma-Aldrich, St. Louis, MO) on ice for 30 minutes and centrifuged at 4,000rpm for 15 minutes. Pelleted nuclei were washed once with hypotonic lysis buffer and chromatin was extracted overnight with end-over-end mixing in high salt buffer (20mM HEPES, pH 7.9, 25% glycerol, 420mM KCl, 1.5mM $MgCl_2$, 0.2mM EDTA, 5mM sodium butyrate). Precipitated chromatin was centrifuged at 4,000rpm for 10 min, washed with minimal salt buffer (20mM HEPES, pH 7.9, 1.5mM $MgCl_2$, 0.2mM EDTA, 5mM sodium butyrate) with protease and phosphatase inhibitors, and resuspended in minimal salt buffer. BCA assay was used to determine protein concentrations according to manufacturer's protocol (Thermo Fischer Scientific, Waltham, MA).

SDS-PAGE and Western Blots. Samples were denatured in 2X Laemmli buffer and heated at 95°C for 5 minutes. Proteins were resolved by SDS-PAGE and transferred onto nitrocellulose membranes. Membranes were blocked in Odyssey Blocking Buffer (Li-Cor Biosciences) for 1 h at room temperature and primary antibodies were applied overnight at 4°C in 1:1 Odyssey Blocking Buffer: TBST. Membranes were washed three times in TBST and infrared secondary antibodies (Li-Cor) were added at a 1:5000 dilution for 1 h at room temperature. Following three additional washes, blots were developed using the Odyssey Infrared Imaging System (Li-Cor).

Click-Seq. Chromatin (1 mg) was sonicated for 12 rounds of 30 1 s pulses at 35% duty cycle on a Virsonic Cell Disruptor to achieve DNA fragments averaging 200-500bp and incubated with

streptavidin sepharose beads for 2 h at 4°C to remove endogenously biotinylated proteins. Click chemistry was performed with 1 mM TCEP, 1 mM $CuSO_4$, 0.1 mM TBTA, and 0.1 mM N_3-biotin, final concentration, for 2 h at room temperature then dialyzed overnight against PBS to remove excess N_3-biotin. SDS was added to a final concentration of 0.1% and chromatin was incubated overnight with end-over-end mixing with streptavidin sepharose beads at 4 °C. Beads were washed three times with ChIP wash buffer I (20 mM Tris, pH 8.0, 150 mM NaCl, 2 mM EDTA, 1% Triton X-100, 0.1% SDS and 0.1% DOC) and ChIP wash buffer II (20 mM Tris, pH 8.0, 500 mM NaCl, 2 mM EDTA, 1% Triton X-100, 0.1% SDS and 0.1% DOC). DNA and unmodified proteins were eluted in 20 mM $NaHCO_3$ with 1% SDS at 65°C for 2 h with intermittent vortexing. Eluated supernatant was collected by centrifugation at 16,*000 x g* for 5 min and split in half for protein and DNA analysis. For DNA, remaining protein was digested with 20 μg proteinase K for 2 h at 55°C. DNA was purified by phenol/chloroform extraction and ethanol precipitation with 20 μg glycogen. DNA was submitted to HudsonAlpha (Huntsville, AL) for ChIP library generation and sequencing. Libraries were sequenced on the Illumina HiSeq 2500 with paired-end 50 bp reads at a sequencing depth of 25M reads/sample.

DNA Sequencing Analysis. Fastq files were downloaded from HudsonAlpha and concatenated according to form single files. Paired-end reads were aligned to the hg19 build using Bowtie2 and converted to BAM files, sorted, and indexed using Samtools1.2. Sorted BAM files were used as input for MACS2 using the broad option with default settings, which calls peaks by the tag distribution along the genome modeled by a Poisson distribution. Called peaks were investigated with Integrated Genome Viewer.

Partial MNase Digest. ONE was added for 3 h in serum-free medium and chromatin was extracted according to above. Following collection of precipitated chromatin, 500 µl of IP Dilution Buffer with 3 mM $CaCl_2$ was added. Micrococcal nuclease (MNase; 150 U) was added and samples were incubated at 37 °C for the indicated time. Reactions were quenched with the addition of 10 mM EDTA and 20 mM EGTA. DNA was extracted using phenol/chloroform extraction and precipitated with isopropanol. DNA was resolved on a 1.5% agarose gel.

Proteolytic Digest for Amino Acid Analysis. Chromatin (50 µg) was precipitated with ice-cold methanol for 20 min at -20 °C, collect by centrifugation at 14,000 *x g*, and resuspended in 153 µl 50 mM NH_4HCO_3. Digests were performed according to Galligan et al.[175] Briefly, isotopically-labelled internal standards (10 µl) were spiked into the protein sample. Sequencing-grade trypsin (Promega) was added (1:50 w/w in 10 µl) and incubated overnight at 37 °C with mixing. Trypsin was inactivated by heating at 95 °C for 10 min. Aminopeptidase (25 ul, 2U) was added and incubated overnight at 37 °C with mixing, followed by inactivation by heating at 95 °C for 10 min. Heptafluorobutyric acid (HFBA; 2 µl) was added as an ion paring agent at a final concentration of 50 mM. Undigested proteins were removed by centrifugation at 14,000 *x g* for 10 min and the supernatant was analyzed by LC-MS/MS.

Quantitation of Histone PTMs. Amino acid digests were injected onto a Shimadzu Nexera UPLC system and separated on a reverse-phase Phenomenex Luna C8 column (2.1 X 50 mm, 3.5 µm) (Phenomenex, Torrance, CA) with H_2O with 50 mM HFBA (buffer A) and ACN with 50 mM HFBA (buffer B) at a flow rate of 0.325 ml/min. The following gradient was used: 0.5 min (2.5%

B) → 5.5 min (50% B) → 6 min (80% B) → 9 min (80% B) → 9.5 min (50% B). The following transitions were monitored on a SCIEX 6500 QTrap mass spectrometer:

Table 4. Analytes and the corresponding transitions monitored by LC-MS/MS.

Q1 (m/z)	**Q3 (m/z)**	**Analyte**
147.1	84.1	Lys
155.1	90.1	$^{13}C_6{}^{15}N_2$ Lys
175.1	70.1	Arg
185.1	75.1	$^{13}C_6{}^{15}N_4$ Arg
189.2	84.1	acLys/me_3Lys
197.2	91.1	acLys-d_8
197.2	90.1	$^{13}C_6{}^{15}N_2$ me_3Lys
132.1	86.1	Leu
139.1	93.1	$^{13}C_6{}^{15}$N Leu
161.1	84.1	meLys
175.1	84.1	me_2Lys
203.1	70.1	S/ADMA
210.1	77.1	ADMA-d_7
301.2	84.1	4-Kam-Lys
309.1	90.1	4-Kam-$^{13}C_6{}^{15}N_2$ Lys

Results

Development of the Click-Seq method for the isolation of DNA associated with adducted chromatin-binding proteins

To assess if these adducts were associated with distinct regions in the genome, we developed a method derived from traditional chromatin immunoprecipitation (ChIP) protocols that utilized click chemistry and streptavidin capture in place of antibodies. This method, named chromatin click and sequencing (Click-Seq) to isolate and sequence the regions of DNA with which these adducts associate. The general scheme is depicted in Figure 34.

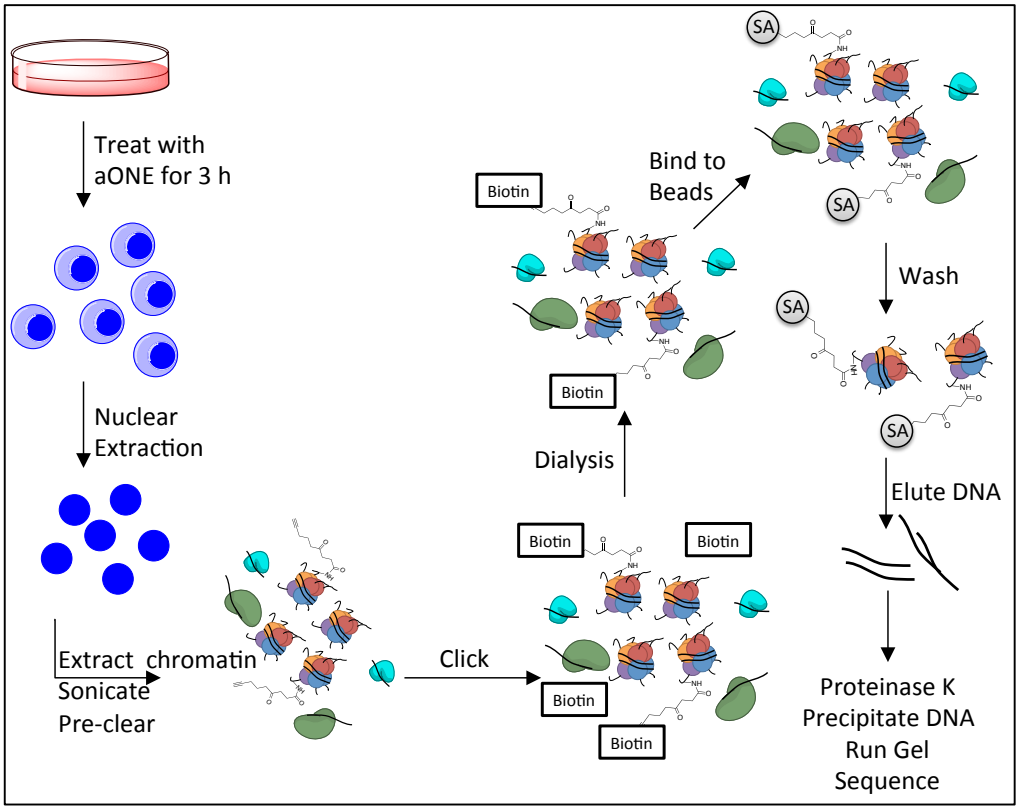

Figure 34. General scheme for Click-Seq. Schematic of cell treatment, chromatin isolation, click chemistry, and selective isolation and elution of DNA.

RKO cells, which we have used extensively in all of our alkyne electrophile studies, were treated with DMSO or 25 μM aONE prior to chromatin extraction. Enrichment of histones in the chromatin faction was assessed by Coomassie staining (Figure 35A). DNA was sheared by sonication to an average fragment size of < 500 bp (Figure 35B), which is necessary for Illumina DNA sequencing. Following click chemistry conjugation of biotin to adducted proteins (Figure 35C), biotinylated proteins were bound to streptavidin beads, washed, and eluted. The eluates were analyzed by agarose gel electrophoresis, which revealed the presence of DNA in the eluate from the aONE-treated, but not the control cells (Figure 35D).

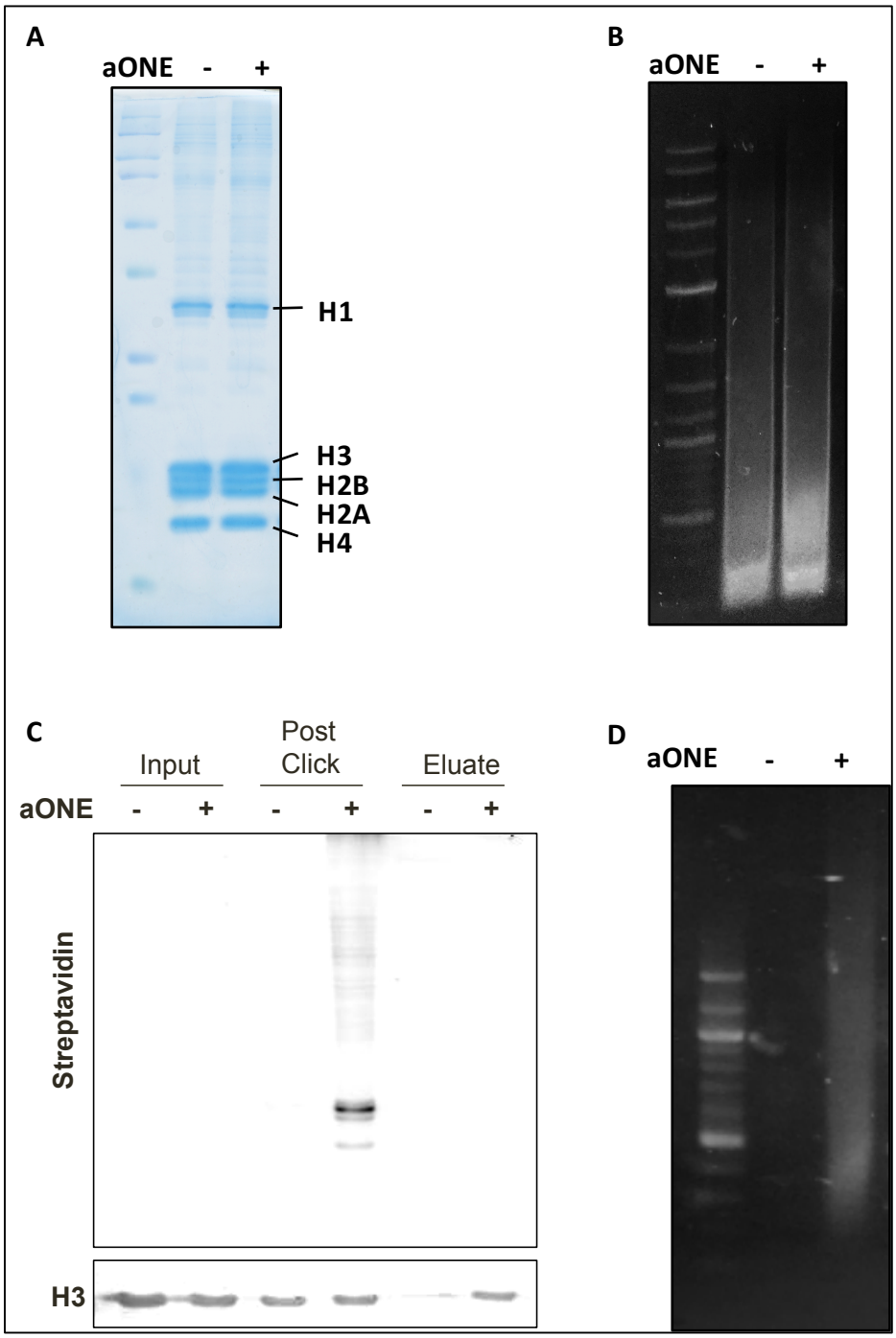

Figure 35. Click-Seq method validation. RKO cells were treated with 25 μM aONE or DMSO for 3 h and chromatin was extracted. Chromatin (1mg) was subjected to click chemistry and adducts conjugated to N_3-biotin, bound to beads, washed, and eluted according to the Click-Seq protocol described in Fig. A) Coomassie staining of input (0.5%) chromatin. B) Agarose gel electrophoresis of input DNA. C) Western blot analysis of input (0.5%), post-click (PC, 1%) protein, and eluate (20%). D) Agarose gel electrophoresis of eluted DNA.

Western blot analysis of eluted proteins showed that H3 was selectively present in the samples from aONE-treated cells (Figure 35C, lanes 5 and 6). We further examined the eluate for the presence of all four core histones using western blot. We observed that histones H2A, H2B, H3 and H4 were all enriched in the eluate, with little to no detectable histones in the control elution (Figure 36). This result shows that protein complexes are dissociated under these conditions, which is known to occur. However, there was no streptavidin in the eluted samples (data not shown), suggesting that the adducted histone proteins remain associated with the beads, while other unadducted histones within the nucleosome octamer are eluted.

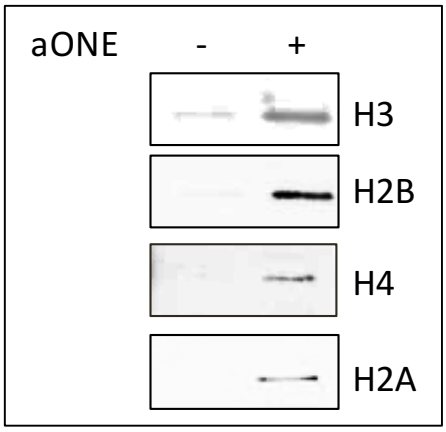

Figure 36. Click-Seq protein elution shows the four core histones. The Click-Seq protocol was performed on chromatin from cells treated with 25 μM aONE (+) or DMSO (-). Following the final elution, half of the eluted supernatant was precipitated with ice-cold methanol, centrifuged at 16,000 *x g* for 5 min, dried, and resuspended in 2X Laemmli sample buffer. Proteins were separated by SDS-PAGE, and western blot was performed using antibodies again all four core histones. All histones were present in the aONE eluate, but were at low or undetectable levels in the DMSO control.

Click-Seq shows distinct regions of enrichment in K562 cells from 25 μM aONE

To assess the potential impact that ONE-mediated adducts have on chromatin structure and gene regulation, we employed Click-Seq to isolate and sequence the regions of DNA with which these adducts associate. K562 cells were used for these experiments as they had been extensively studied in the Encyclopedia of DNA elements (ENCODE) project. The cells were treated with aONE, and

chromatin was extracted. DNA was sheared to an average fragment size of < 500 bp via sonication. Following click chemistry-mediated conjugation of biotin to adducted proteins, biotinylated proteins were bound to streptavidin beads, washed, and eluted. ChIP sequencing libraries were generated for the DNA input and elution samples and sequenced with paired-end reads.

Following ChIP library sequencing, paired-end sequences were aligned to the human genome, and regions of DNA enriched in the aONE-treated samples were examined. Thirteen enriched peaks were identified, mapping back to twelve genes and one region not associated with any RefSeq annotations (Table 5). One region of particular interest is within the *TXNIP* gene. TXNIP (thioredoxin interacting protein) interacts with thioredoxin at its active-site Cys residues. Overexpression of TXNIP results in decreased thioredoxin activity, decreased cell growth, and promotion of apoptosis.[176-178] Enrichment was observed at the final exon of the *TXNIP* gene. Due to the role of thioredoxin in mediating the response to oxidative stress,[179] this finding is especially intriguing, and more work is needed to determine if mRNA and protein levels of TXNIP are altered in response to ONE.

Table 5. Regions of enrichment from MACS2 in K562 cells

Chromosome	Start	End	Length	-log (p-value)	Fold Enrichment	Associated Gene
chr1	145441341	145442294	954	7.26984	4.41908	TXNIP
chr11	65266624	65268097	1474	21.33661	5.39616	MALAT1
chr12	15095284	15095540	257	8.81985	5.54723	ARHGDIB
chr12	92537470	92537968	499	6.72422	4.58353	BTG1
chr15	45009852	45010263	412	25.78767	6.54398	B2M
chr19	12902618	12904021	1404	8.37724	5.10707	JUNB
chr2	43449929	43450540	612	7.84529	5.03318	ZNF36L2
chr2	89156779	89157096	318	11.49731	5.9549	N/A
chr2	92305742	92306009	268	7.60495	2.57251	TMSB10
chr6	30461260	30461762	503	6.65824	3.79385	HLA-E
chr6	31321681	31322048	368	10.1766	4.81204	HLA-B
chr7	5566923	5568223	1301	13.06847	5.74017	ACTB
chrX	12994983	12995255	273	12.39963	6.52527	TMSB4X

ONE adducts on histones occur at levels comparable to those of canonical enzymatic modification

Since the 4-ketoamide modification was observed in a physiologically relevant model of inflammation,[88] we wanted to determine the levels of 4-Kam-Lys in chromatin. Recently, Galligan et al.[175] developed Quantitative Analysis of Arginine and Lysine Modifications (QuARK-Mod), a method to quantify levels of modified amino acids in chromatin and individual histones. Using QuARK-Mod, we digested chromatin from RKO cells treated with 25 μM ONE or DMSO in the

presence of an isotopically labeled 4-Kam-Lys internal standard. The resulting digest was analyzed by multiple reaction monitoring using the *m/z* 301.2→84.1 transition for the native 4-Kam-Lys and *m/z* 309.1→90.1 for the isotopically labeled standard. When normalized to Leu as a digestion control, levels of 4-Kam-Lys were ~0.72 pmol/nmol Leu in the treated samples, whereas the control did not have any detectable 4-Kam-Lys (Figure 37A). Levels of AcLys (Figure 37B) and me_3Lys (Figure 37C) were almost two order of magnitude higher than the 4-Kam-Lys, while the less abundant ADMA (Figure 37) was only one order of magnitude higher. No significant differences in the canonical histone PTMs were observed upon ONE treatment.

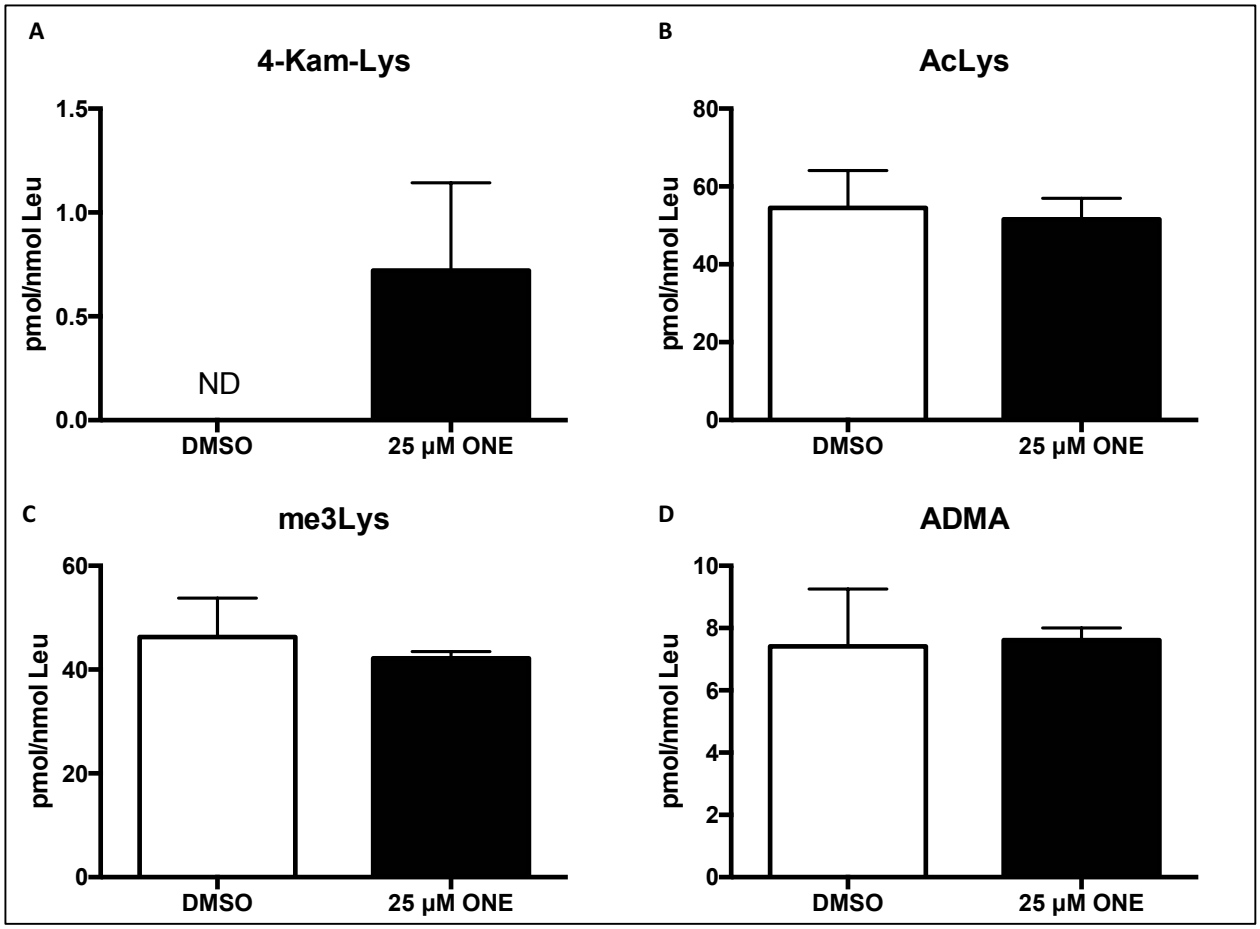

Figure 37. Level of chromatin PTMs with ONE. RKO cells were treated with DMSO or 25 μM ONE for 3 h. Extracted chromatin was digested to single amino acids using the QuARK-Mod approach and the levels of different PTMs were determined using isotopically labeled internal standards.

To determine if 4-Kam-Lys was produced in a dose-dependent fashion, we exposed RKO cells to increasing levels of ONE then performed amino acid analysis of chromatin isolated from the cells. Interestingly, levels of 4-Kam-Lys following 100 μM ONE treatment (Figure 38) were higher than those of AcLys or me_3Lys under basal conditions (Figure 37B and C). At 50 μM, the levels were comparable to those of ADMA (Figure 38). The 4-Kam-Lys was below the limit of detection at concentrations of ONE < 10 μM. These data show that the formation of this adduct on chromatin does not occur in a linear fashion, but rather increases rapidly between 50 μM and 100 μM.

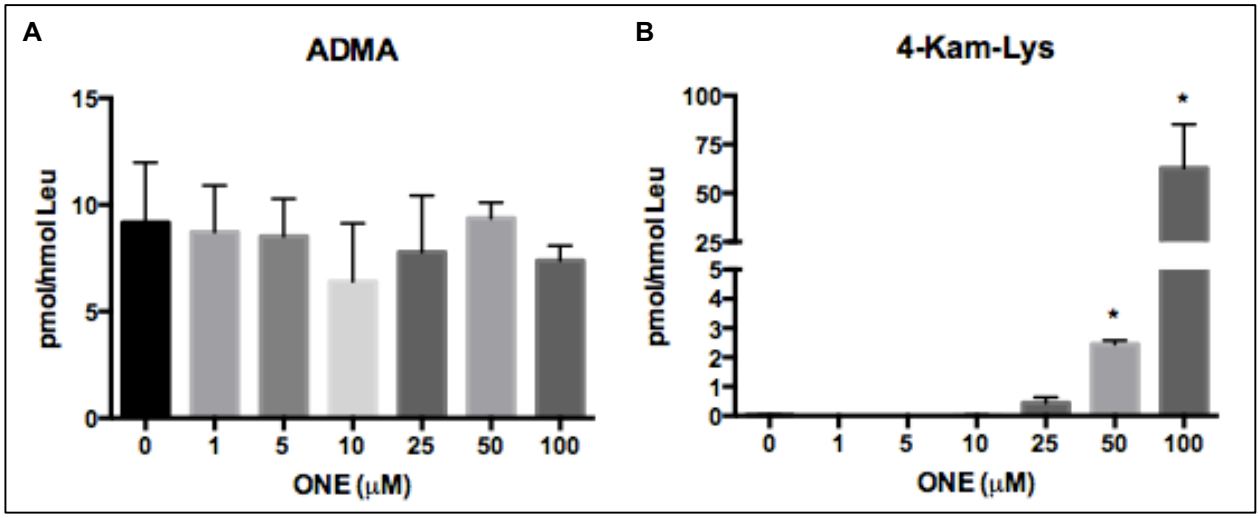

Figure 38. Dose-response relationship between ONE exposure and low abundance PTMs. RKO cells were treated with increasing concentrations of ONE for 3 h, and chromatin was extracted and subjected to QuARK-Mod. Levels of A) ADMA and B) 4-Kam-Lys were determined with isotopically labelled internal standards.

ONE increases chromatin accessibility in a dose-dependent manner

Previous reports have shown that the α,β-unsaturated carbonyl, acrolein, is capable of modifying histones in a manner similar to ONE.[180] The authors showed that acrolein can adduct both free and nucleosomal histones, and exposure of cells results in increased chromatin accessibility as

measured by partial micrococcal nuclease (MNase) digestion.[180] To assess chromatin accessibility in response to aONE, cells were treated with low (10 μM) or high (25 μM) aONE. Digestion with MNase and analysis of extracted DNA showed that treatment with aONE increased chromatin accessibility in a dose-dependent manner (Figure 39A-C). Specifically, treatment with 25 μM aONE caused a significant increase in the amount of mononucleosomes after 5 min digestion (Figure 39D), suggesting that aONE adduction results in chromatin relaxation.

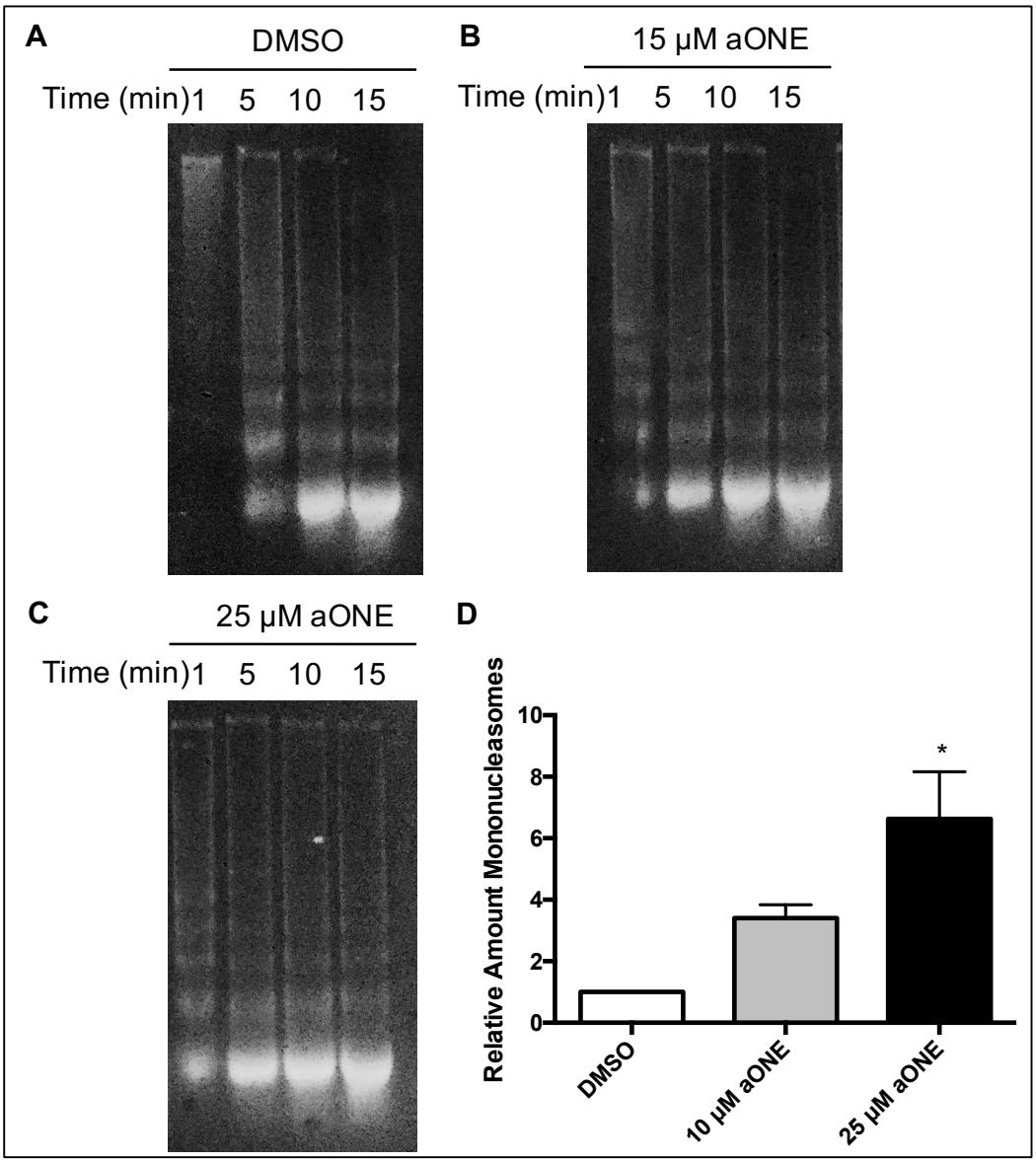

Figure 39. ONE increases chromatin accessibility. Chromatin from cells treated with A) DMSO, B) 10 μM ONE, or C) 25 μM ONE and digested with MNase for the indicated times. D) After 5min with MNase, DNA accessibility increases in a dose-dependent manner.

ONE adducts are long-lived histone modifications.

The turnover rate for histone PTMs varies depending on the modification and the residue. On histone H3 in HeLa cells, there are 12 acetylation sites that exhibit rapid turnover (1-2 h) and 7 sites that exhibit a turnover of > 30 h.[181] PTMs with longer turnovers may contribute to differential

gene expression on a broader time scale. Furthermore, histone adduction by ONE may inhibit PTMs at key epigenetic sites, thereby exacerbating dysregulation of gene expression.

Since the 4-Kam-Lys adduct is stable, we wanted to determine how long it remained on histones following an initial treatment. Using 25 μM aONE, we treated RKO cells in the absence of serum for 3 h. Then, we either collected the cells for chromatin extraction (0 h) or removed the medium and added fresh medium with or without serum for 24 h. Using click chemistry followed by SDS-PAGE and western blot with a streptavidin probe, we are able to observe the levels of adduction under these conditions. At the 0 h time point, there was a large amount of protein adduction following aONE treatment (Figure 40). After 24 h, the levels of adduction declined slightly in both the presence and absence of serum relative to the 0 h time point. Quantitation of these results revealed little difference in adduction between the treatments, though additional replicates may yield more definitive differences.

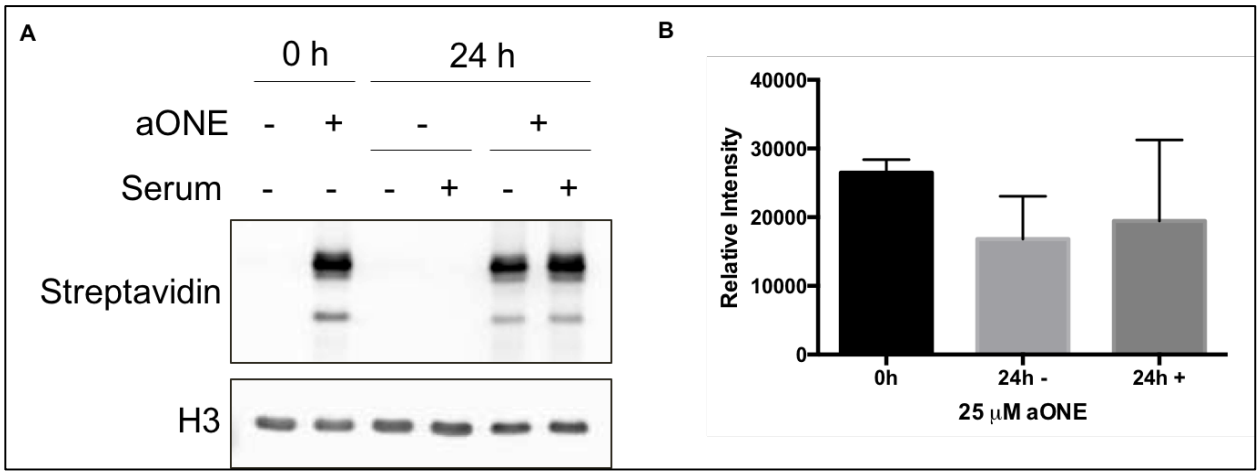

Figure 40. Histone adducts are long-lived. RKO cells were treated with DMSO or 25 μM aONE for 3 h in serum-free medium. Cells were either collected (0 h) or the medium was replaced with fresh medium with or without serum for 24 h. Chromatin was subjected to click chemistry, proteins separated by SDS-PAGE, and western blot with a streptavidin probe was used to measure amounts of adduction. Histone H3 was used as a loading control. Adduction decreased over time, but little differences were observed following 24 h between the with and without serum conditions.

Discussion

Here, we have developed a technique that enables the selective isolation of DNA associated with aONE-modified chromatin proteins. Click chemistry can be used to conjugate biotin to adducted proteins within chromatin. This provides a significant advantage over traditional ChIP approaches. First, only proteins that have the alkyne will be biotinylated, which provides greater selectively over that of antibodies, which may bind non-specifically to many motifs/proteins. Second, this approach is applicable to many different adduct structures, such as the 4-ketoamide of Lys and the Michael adduct on His, since it only requires the presence of the alkyne. Antibodies would not provide such broad structural recognition without exhibiting a large loss of specificity.

We applied this technique to the highly utilized K562 cell line to investigate chromatin alterations in response to aONE. The ENCODE consortium has performed hundreds of ChIP-Seq experiments, as well as a number of other DNA isolation and sequencing techniques, in this cell line, providing an ideal model for our studies. Very few regions of enrichment of adduct-associated DNA were found in the K562 cells using Click-Seq. All regions showing statistically significant enrichment, with the exception of one region on Chr2, were within an exonic region along a gene. Enrichment of some genes of interest, such as TXNIP, suggest that aONE may associate with some distinct regions. However, such few regions of enrichment suggest that aONE adducts occur broadly and nonspecifically on chromatin, thereby not contributing to enrichment in Click-Seq. Negative peaks were also not observed in these data, showing that there were no regions of de-enriched DNA that would correlate to areas that were inaccessible to adduction.

Recent work by Jin et al.[174] shows that SIRT2 enzymatically removes the ONE adduct from 4-Kam-Lys on histones, most notably on H3K27 and H3K23. The evidence that this ONE modification is enzymatically removable has large implications for its downstream effects on gene

expression. This also suggests that levels of the modification may be enzymatically regulated. Using the QuARK-Mod approach, we were able to determine that the 4-Kam-Lys is present at < 1 pmol/nmol Leu in chromatin following 25 μM ONE treatment. These levels are almost two orders of magnitude lower than those of AcLys and me_3Lys, the two most abundant histone modification, and within one order of magnitude from the lesser studied ADMA.

Investigation into the dose dependence of these adducts showed that 4-Kam-Lys levels surpassed basal levels of AcLys and me_3Lys at 50μM and 100μM ONE. It is important to note that the levels of histone adducts we report only take into account the 4-Kam-Lys, but not the Michael adduct on His which was previously shown to be present on histones.[88]While we are currently unable to quantify the levels of the ONE-His adduct, these adducts will contribute to higher levels of ONE adducts on histone and may make the levels comparable to lower abundance modifications such as ADMA.

The levels of 4-Kam-Lys did not increase in a linear manner, but rather increased rapidly at higher concentrations. This fits with observation by Codreanu et al.,[84] which noted that the histones were members of the Class I protein group, which were only adducted at high concentrations of aONE. It is possible that at low concentrations, ONE may be preferentially conjugated to GSH and remain in the cytosol, whereas at higher concentrations, more ONE can bypass the cell detoxification systems in the cytosol and make it into the nucleus. Once in the nucleus, ONE can adduct histones and contribute to the potentially deleterious effect.

We investigated whether or not ONE can alter chromatin structure and increase accessibility following histone adduction. Using a partial MNase digestion, we showed that ONE increases chromatin accessibility, facilitating more rapid MNase digestion of chromatin to mononucleosomes. This outcome was similar to what has previously been observed with acrolein,

the simplest α,β-unsaturated carbonyl compound. Acrolein increases chromatin accessibility to MNase digestion, enabling increased transcription of genes within regions of greater accessibility.[180] It is possible that ONE may have a similar effect on gene expression, which may not be observed using the Click-Seq method.

The longevity of these adducts may also contribute to dysregulation of chromatin structure and gene expression. The samples were not reduced with $NaBH_4$, showing that the adducts present at 24 h were stable long-term. Since the doubling time of these cells is ~24 h, we would anticipate about a 50% reduction in histone modification in the serum-containing samples, though this was not observed. It is possible that newly synthesized histones may be targets of free aONE that has undergone a retro-Michael reaction or reversal of the Schiff base from other proteins in the cell, prior to reacting with the histone to form a more stable 4-ketoamide adduct. It is likely, though, that very low levels of free aONE would be produced by this reaction.

While the Click-Seq method was developed for the study of aONE, it can also be applied to any biological studies that employ click chemistry. Much work has gone into the generating aminoacyltranferases which can accommodate non-natural amino acids, many of which have been used as click chemistry tools.[182] The non-natural amino acids can then be incorporated into proteins at specific sites. Click-Seq can be used to study transcription factors that have been coded to include a non-natural alkyne-containing amino acid, providing more selective isolation without larger tags (e.g. FLAG, hexahistidine, etc.). Furthermore, it can be used to solely interrogate protein-protein binding, similar to co-immunoprecipitations. This method may provide a useful, reliable, and consistent approach to broad areas of biological investigation.

CHAPTER V

CONCLUSIONS AND FUTURE DIRECTIONS

Conclusions

As discussed in Chapter I, inflammation is a beneficial process that combats infection, limits injury, and promotes healing. A large number of proinflammatory and chemically reactive species are produced during the inflammatory response. These species are primarily targeted against invading pathogens, but they can also have deleterious effects on host cells. Reactive oxygen (ROS) and reactive nitrogen species (RNS) can react with proteins, DNA, and lipids in host cells.

Of particular interest to our laboratory is the reaction of ROS/RNS with membrane lipids. Strong oxidants can abstract H-atoms from polyunsaturated fatty acids (PUFAs), forming lipid radicals that can react with molecular oxygen to generate lipid peroxyl radicals. The entire lipid peroxidation process can produce a collection of oxidized products, depending on the original PUFA. Additionally, these oxidized lipids can decompose to generate reactive α,β-unsaturated lipid aldehydes that can react with DNA and proteins, most notably at Cys, His, and Lys residues. The resultant electrophilic protein adducts are capable of altering protein function and activity.

4-Hydroxy-2-nonenal (HNE) is one of the most widely studied lipid electrophiles, and 4-oxo-2-nonenal (ONE), the 4-keto cousin of HNE, is gaining increasing attention due to its higher reactivity. Both these electrophiles can covalently modify Cys, His, and Lys, but the structures of the resulting adducts differ greatly. HNE preferentially forms Michael adducts with all three residues, forming products that can undergo retro-Michael reaction at varying degrees unless

stabilized by reduction with $NaBH_4$. ONE can also form Michael adducts at Cys, His, and Lys, although the predominant modification at Lys has been shown to be the 4-ketoamide adduct, a chemically stable modification that can be long-lived in the cell. Cross-linking is also more prevalent with ONE than with HNE; however identification and quantification of these cross-links remains technically challenging.

The application of click chemistry to the study of HNE and ONE has been instrumental in the discovery of their various targets. Alkyne analogues of HNE (aHNE) and ONE (aONE) were used in conjunction with click chemistry to generate protein inventories of the targets isolated from cells exposed to a range of electrophile concentrations. More than 1000 proteins were identified by this method, facilitating subsequent interrogation of individual protein targets for sites of modification, types of adducts, and functional implications of adduction.

An HNE target of particular interest was cyclin-dependent kinase 2 (CDK2), a main cell cycle regulator. Bioinformatic analysis of gene expression changes in response to HNE exposure and the inventory of HNE target proteins showed that the genes modulated by CDK2 were significantly down-regulated in response to HNE treatment and that CDK2 was itself a target of adduction.[132] Alterations in CDK2 activity in cells as a result of adduction could be expected to affect cell growth, given the role of CDK2 in regulating the G1/S-phase transition. Thus, we sought to determine the sites of adduction on CDK2, the type(s) of adduct(s), and the consequences of modification on CDK2 activity and overall cell growth (Chapter II).

In studies using purified protein, we identified a number of sites of modification on CDK2, mainly on His residues, in the form of Michael adducts. Investigation of the crystal structure of CDK2 revealed two modified residues, His71 and His161, that may greatly impact CDK2 activity. His71 of CDK2 hydrogen bonds with Cyclin A, a potentially critical interaction as an association

between CKD2 and Cyclin A is required for CDK2 activity. His 161 immediately follows Thr160, a site of phosphorylation that activates CDK2. Adduction of both of these residues by CDK2 could inhibit CDK2 activity, resulting in the gene expression changes that were previously observed.

In vitro assessment revealed a loss of CDK2/CyclinA kinase activity in response to HNE treatment. This observation was recapitulated in RKO cells, confirming that CDK2 activity is significantly decreased in response to HNE. Furthermore, in cells synchronized in G1/G0, HNE treatment resulted in a delay in cell cycle progression from G1 to S-phase, thereby supporting the hypothesis that HNE-dependent inhibition of CDK2 kinase activity is physiologically relevant.

We then moved our focus to targets of ONE adduction. Peptidyl-prolyl *cis/trans* isomerase (PIN1) was identified as a target of both HNE and ONE, based on the proteomic adduct inventory. Previous work had focused on the effects of HNE on PIN1 by identifying the active site Cys as the main site of adduction.[87] With ONE, the active site Cys was similarly modified, but the mass shift associated with the adduct was not the anticipated +158 *m/z* corresponding to a Michael adduct (Chapter III). Further investigation showed that the adduct was insensitive to reduction with $NaBH_4$, suggesting that it did not retain the aldehyde or ketone groups.

Selective covalent blockade allowed us to decipher which residue(s) were associated with Pin1-ONE adduct. Blocking Cys resulted in the disappearance of the adducted peptides, as did blocking Lys. This information led to the hypothesis that this modification was an ONE crosslink between Cys and Lys. We were able to identify a novel cross-link between the active site Cys (Cys113) and Lys117 by mass spectrometry. Modification of Cys113 would abolish catalytic activity and inactivate PIN1. Using deuterated analogues of ONE, we were able to propose a mechanism for cross-link formation. While this is only the second publication on an ONE cross-

link between two residues on a protein, our computational work suggested that a number of additional proteins may be susceptible to formation of a similar cross-link.

As shown in previous work,[88] histones are preferential targets for ONE adduction, and their high Lys content makes them highly susceptible to 4-ketoamide formation. Gene expression is extensively regulated by post-translation modifications (PTMs) of histones, mainly on Lys residues. Chromatin immunoprecipitation and sequencing (ChIP-Seq) is traditionally used to assess the regions of the genome with which a particular histone PTM associates. This technique requires antibodies that are highly specific for the PTM as well as the histone of interest. This method presents obvious issues for the investigation of ONE adducts on histones, necessitating multiple antibodies for distinct adduct type (e.g., Michael adduct, 4-ketoamide, etc.). We aimed to develop an approach that allows us to bypass the use of antibodies by employing click chemistry.

Combining ChIP-Seq and click chemistry allowed us to develop the chromatin click precipitation and sequencing (Click-Seq) technique. This method enabled selective isolation of DNA associated with adducted chromatin proteins by conjugating N_3-biotin to aONE-modified chromatin proteins and capturing them with streptavidin. Isolated DNA was then sequenced by Illumina sequencing and analyzed according to established ChIP-Seq pipelines.

While Click-Seq allowed us to determine DNA sequences that were selectively associated with ONE-dependent modifications, we also wanted to assess the magnitude of the ONE adduct burden in cells. Our laboratory has recently developed Quantitative Analysis of Arginine and Lysine Modifications (QuARK-Mod) to measure the levels of PTMs on Lys and Arg. Using this approach, we were able to determine that 4-Kam-Lys levels were approximately two orders of magnitude lower than those of the canonical AcLys and me_3Lys PTMs following treatment with 25 μM ONE. Using a dose-response curve with increasing concentrations of ONE, we did not

observe a linear increase in the formation of 4-Kam-Lys. Surprisingly, at higher concentrations of ONE, levels of 4-Kam-Lys surpassed levels of AcLys and me_3Lys. The levels of Lys modifications declined at the higher ONE concentrations, though the levels of ADMA were unaltered, showing that the alterations in histone modifications was Lys specific. These observations open up a new area of investigation into the regulation and cross-talk of histone modifications.

Future Directions

Cross-linking of proteins by ONE

Our collaboration with Dr. Jarrod Smith has suggested a number of proteins that may be cross-linked by ONE. We attempted to detect a cross-link within thioredoxin (TRX), but those efforts did not reveal any Cys modifications. On the other hand, there were multiple Lys residues that were adducted. All of these adducts were the 4-ketoamide modification. Since TRX is known to be adducted by HNE at the active site Cys residues (Cys32/Cys35),[172,2] it is conceivable that ONE may also be able to modify these residues. We believe that the complete absence of any Cys adducts may be due to extensive disulfide bond formation in the protein. While it is also possible that very low concentrations of ONE may contribute to extensive cross-linking, the high percentage of sequence coverage in the treated samples suggests that this is likely not occurring.

Moving forward, we can investigate additional proteins that were identified by our computational approach. We have exhaustively characterized another protein on the list, PKM2, using LC-MS/MS to identify sites of adduction.[183] This glycolytic enzyme is modified by both HNE and ONE at Cys and His residues in the form of Michael adducts. No cross-links were observed by mass spectrometry, despite the overwhelming evidence by SDS-PAGE and Coomassie staining that recombinant PKM2 monomers were cross-linked following *in vitro*

modification with ONE. Inter-protein cross-linking of individual PKM2 monomers would be difficult to detect by LC-MS/MS. We were only able to identify the PIN1 cross-link because it joined Cys and Lys residues on the same peptide, resulting in a relatively small mass shift. To further investigate possible PKM2 cross-links, a MALDI-MS approach, which would be a complementary approach to LC-MS/MS, could be utilized to search for interpeptide cross links.

There still remain 28 proteins on the potential cross-link list that can be investigated. For all of these, available crystal structures and knowledge of a protein's enzymatic activity can be useful in selecting the most ideal proteins for these studies. The computation approach that we used searched for proteins that have Cys/His/Lys within 10 Å, though proteins containing a catalytic Cys, similar to Pin1, may simplify identification of cross-links. Using the previously published reactive Cys inventory,[2] we can determine which of the remaining 28 proteins have reactive Cys residues. From there, we can interrogate the crystal structures to determine which of these contain nearby Lys residues. We can employ this activity- and structure-based selection to allow for the best protein for mass spectrometric identification of intraprotein cross-links.

Measuring gene expression changes from ONE

Gene expression alterations have been studied extensively by both microarray and RNA-Seq following HNE treatment in RKO cells.[132,94] A number of genes associated with antioxidant (*HMOX1, GCLM, TXNRD1*) and stress responses (*ZFAND2A*, *GADD45B*, *DNAJB4, BAG3*) are induced in response to 30 μM HNE treatment for 6 h. There were also genes that were identified which had no connection to canonical cell stress responses, such as upregulation of the ADM gene, which encodes a preprohormone that plays a role in the vasculature and has antimicrobial activity.

It is possible that alterations in histone modifications as a result of adduction by HNE contributed to some dysregulation of gene expression.

It is possible that similar alterations in gene expression will be present with ONE. While we lack gene expression data for ONE, we expect that antioxidant and stress responses will be activated due to the presence of the electrophile. Dysregulation of gene expression may occur due to ONE adduction of histones, thereby altering expression of genes which would not typically be expressed in response to electrophiles. To accomplish this, RNA-Seq can be used to measure changes in gene expression under basal conditions and in response to ONE treatment. This will provide data that can be correlated with the Click-Seq data, allowing for a more comprehensive picture of the impact of ONE-dependent adduction of histones.

Click-Seq for long-term alterations in chromatin structure

Our data presented in Chapter IV show that ONE-derived histone adducts are stable for at least 24 h under normal cell growth conditions. The apparent longevity of aONE-histone adducts may contribute to a long-lived effect on differential gene expression. Adduction of Lys residues that are known sites of epigenetic regulation, such as H3K27, would block this residue from other PTMs, thereby altering the histone code and deregulating gene expression. The disruption of canonical epigenetic regulation may contribute to dysregulation of gene expression immediately following ONE exposure, but may also persist throughout the lifetime of the adducted histone.

We propose to utilize the Click-Seq method to interrogate the regions where these adducts are present 24 h post-treatment. Cells can be treated with aONE for three hours and then removed for 24 h in medium with and without serum. Click-Seq can then be used to assess regions of enrichment and we can then compare the results to the Click-Seq results obtained immediately

following ONE treatment. The results may also provide additional insight into how canonical histone modifications are altered by ONE adduction. Chromatin immunoprecipitation and sequencing (ChIP-Seq) can be performed with antibodies targeting known histone marks, such as H3K27Ac, which are also known to be adducted. This approach would allow us to determine if ONE can alter enrichment patterns of canonical histone modifications, thereby disrupting chromatin regulation.

Click-seq method to identify binding partners of adducted chromatin proteins

The Click-Seq method has provided a means to interrogate the DNA that is associated with adducted chromatin proteins, however, it also has the potential for investigation into proteins that associate with the adducted proteins. As shown in the Click-Seq method development in Chapter IV, the western blot loading control for the input and post-click samples, histone H3, was present in the streptavidin affinity eluate of aONE- but not DMSO-treated cells. Using western blot with antibodies for the four core histones, we were further able to determine that all of the four core histones are present in the aONE eluate and the levels are much lower or nonexistent in the DMSO control.

With these data, we hypothesize that the Click-Seq method will facilitate the isolation of proteins that associate with aONE-modified chromatin. In a preliminary proteomic identification of the eluted proteins, all the core histones were observed as well as many other chromatin-associated proteins. SIRT2, which has been shown to enzymatically remove the 4-ketoamide adduct from Lys,[174] was not identified by this method. Additional proteomic experiments can be designed to better investigate the proteins eluted in this assay and determine specific versus nonspecific hits. A dose-response including a range of aONE concentrations, similar to the

experimental design in Codreanu et al.,[84] would provide more confident identification of potential binding partners which associate with 4-Kam-Lys and other aONE adducts.

REFERENCES

(1) Aluise, C. D., Camarillo, J. M., Shimozu, Y., Galligan, J. J., Rose, K. L., Tallman, K. A. and Marnett, L. J. (2015) Site-specific, intramolecular cross-linking of Pin1 active site residues by the lipid electrophile 4-oxo-2-nonenal. *Chem Res Toxicol. 28*, 817-827.

(2) Weerapana, E., Wang, C., Simon, G. M., Richter, F., Khare, S., Dillon, M. B., Bachovchin, D. A., Mowen, K., Baker, D. and Cravatt, B. F. (2010) Quantitative reactivity profiling predicts functional cysteines in proteomes. *Nature. 468*, 790-795.

(3) Taghizadeh, K., McFaline, J. L., Pang, B., Sullivan, M., Dong, M., Plummer, E. and Dedon, P. C. (2008) Quantification of DNA damage products resulting from deamination, oxidation and reaction with products of lipid peroxidation by liquid chromatography isotope dilution tandem mass spectrometry. *Nat Protoc. 3*, 1287-1298.

(4) McCann, S. and Roulston, C. (2013) NADPH Oxidase as a Therapeutic Target for Neuroprotection against Ischaemic Stroke: Future Perspectives. *Brain Sciences. 3*, 561.

(5) Vila, A., Tallman, K. A., Jacobs, A. T., Liebler, D. C., Porter, N. A. and Marnett, L. J. (2008) Identification of protein targets of 4-hydroxynonenal using click chemistry for ex vivo biotinylation of azido and alkynyl derivatives. *Chem Res Toxicol. 21*, 432-444.

(6) Camarillo, J. M., Rose, K. L., Galligan, J. J., Xu, S. and Marnett, L. J. (2016) Covalent Modification of CDK2 by 4-Hydroxynonenal as a Mechanism of Inhibition of Cell Cycle Progression. *Chem Res Toxicol. 29*, 323-332.

(7) Ryan, G. B. and Majno, G. (1977) Acute inflammation. A review. *The American Journal of Pathology. 86*, 183-276.

(8) Celsus, A. C. *De Medicina.* translated by G. W. Spencer; London, 1935

(9) Chandrasoma, P., Taylor, C. R. and Wells, K. E. (1995) Concise Pathology. *Plastic and Reconstructive Surgery. 96*, 1227.

(10) Ferrero-Miliani, L., Nielsen, O. H., Andersen, P. S. and Girardin, S. E. (2007) Chronic inflammation: importance of NOD2 and NALP3 in interleukin-1beta generation. *Clinical and experimental immunology. 147*, 227-235.

(11) Smith, J. A. (1994) Neutrophils, host defense, and inflammation: a double-edged sword. *Journal of leukocyte biology. 56*, 672-686.

(12) Balkwill, F. and Mantovani, A. (2001) Inflammation and cancer: back to Virchow? *The Lancet. 357*, 539-545.

(13) Coussens, L. M. and Werb, Z. (2002) Inflammation and cancer. *Nature. 420*, 860-867.

(14) Hollstein, M., Sidransky, D., Vogelstein, B. and Harris, C. C. (1991) p53 mutations in human cancers. *Science. 253*, 49-53.

(15) Li, J., Yen, C., Liaw, D., Podsypanina, K., Bose, S., Wang, S. I., Puc, J., Miliaresis, C., Rodgers, L., McCombie, R., Bigner, S. H., Giovanella, B. C., Ittmann, M., Tycko, B., Hibshoosh, H., Wigler, M. H. and Parsons, R. (1997) PTEN, a Putative Protein Tyrosine Phosphatase Gene Mutated in Human Brain, Breast, and Prostate Cancer. *Science. 275*, 1943-1947.

(16) Bos, J. L., Fearon, E. R., Hamilton, S. R., Verlaan-de Vries, M., van Boom, J. H., van der Eb, A. J. and Vogelstein, B. (1987) Prevalence of ras gene mutations in human colorectal cancers. *Nature. 327*, 293-297.

(17) Schwab, M. and Amler, L. C. (1990) Amplification of cellular oncogenes: a predictor of clinical outcome in human cancer. *Genes, chromosomes & cancer. 1*, 181-193.

(18) McGeer, P. L. and McGeer, E. G. (2007) NSAIDs and Alzheimer disease: Epidemiological, animal model and clinical studies. *Neurobiology of aging. 28*, 639-647.
(19) Chen, H., Jacobs, E., Schwarzschild, M. A., McCullough, M. L., Calle, E. E., Thun, M. J. and Ascherio, A. (2005) Nonsteroidal antiinflammatory drug use and the risk for Parkinson's disease. *Annals of Neurology. 58*, 963-967.
(20) Weggen, S., Rogers, M. and Eriksen, J. (2007) NSAIDs: small molecules for prevention of Alzheimer's disease or precursors for future drug development? *Trends in Pharmacological Sciences. 28*, 536-543.
(21) Schulte, T., Schöls, L., Müller, T., Woitalla, D., Berger, K. and Krüger, R. (2002) Polymorphisms in the interleukin-1 alpha and beta genes and the risk for Parkinson's disease. *Neuroscience Letters. 326*, 70-72.
(22) Nicoll, J. A., Mrak, R. E., Graham, D. I., Stewart, J., Wilcock, G., MacGowan, S., Esiri, M. M., Murray, L. S., Dewar, D., Love, S., Moss, T. and Griffin, W. S. (2000) Association of interleukin-1 gene polymorphisms with Alzheimer's disease. *Ann Neurol. 47*, 365-368.
(23) Wu, D. C., Jackson-Lewis, V., Vila, M., Tieu, K., Teismann, P., Vadseth, C., Choi, D. K., Ischiropoulos, H. and Przedborski, S. (2002) Blockade of microglial activation is neuroprotective in the 1-methyl-4-phenyl-1,2,3,6-tetrahydropyridine mouse model of Parkinson disease. *The Journal of neuroscience : the official journal of the Society for Neuroscience. 22*, 1763-1771.
(24) Gao, H.-M., Liu, B., Zhang, W. and Hong, J.-S. (2003) Novel anti-inflammatory therapy for Parkinson's disease. *Trends in Pharmacological Sciences. 24*, 395-401.
(25) Liu, B., Du, L. and Hong, J. S. (2000) Naloxone protects rat dopaminergic neurons against inflammatory damage through inhibition of microglia activation and superoxide generation. *The Journal of pharmacology and experimental therapeutics. 293*, 607-617.
(26) Zhang, W., Wang, T., Qin, L., Gao, H. M., Wilson, B., Ali, S. F., Zhang, W., Hong, J. S. and Liu, B. (2004) Neuroprotective effect of dextromethorphan in the MPTP Parkinson's disease model: role of NADPH oxidase. *Faseb j. 18*, 589-591.
(27) Jonasson, L., Holm, J., Skalli, O., Bondjers, G. and Hansson, G. K. (1986) Regional accumulations of T cells, macrophages, and smooth muscle cells in the human atherosclerotic plaque. *Arteriosclerosis (Dallas, Tex.). 6*, 131-138.
(28) Hansson, G. K. and Libby, P. (2006) The immune response in atherosclerosis: a double-edged sword. *Nat Rev Immunol. 6*, 508-519.
(29) Marx, N., Kehrle, B., Kohlhammer, K., Grüb, M., Koenig, W., Hombach, V., Libby, P. and Plutzky, J. (2002) PPAR Activators as Antiinflammatory Mediators in Human T Lymphocytes. *Implications for Atherosclerosis and Transplantation-Associated Arteriosclerosis. 90*, 703-710.
(30) Garcia, R. C. and Segal, A. W. (1984) Changes in the subcellular distribution of the cytochrome b-245 on stimulation of human neutrophils. *Biochemical Journal. 219*, 233-242.
(31) Borregaard, N., Heiple, J. M., Simons, E. R. and Clark, R. A. (1983) Subcellular localization of the b-cytochrome component of the human neutrophil microbicidal oxidase: translocation during activation. *The Journal of cell biology. 97*, 52-61.
(32) Groemping, Y., Lapouge, K., Smerdon, S. J. and Rittinger, K. Molecular Basis of Phosphorylation-Induced Activation of the NADPH Oxidase. *Cell. 113*, 343-355.
(33) Sumimoto, H., Hata, K., Mizuki, K., Ito, T., Kage, Y., Sakaki, Y., Fukumaki, Y., Nakamura, M. and Takeshige, K. (1996) Assembly and Activation of the Phagocyte

NADPH Oxidase: SPECIFIC INTERACTION OF THE N-TERMINAL Src HOMOLOGY 3 DOMAIN OF p47phox WITH p22phox IS REQUIRED FOR ACTIVATION OF THE NADPH OXIDASE. *Journal of Biological Chemistry. 271*, 22152-22158.

(34) Han, C.-H., Freeman, J. L. R., Lee, T., Motalebi, S. A. and Lambeth, J. D. (1998) Regulation of the Neutrophil Respiratory Burst Oxidase: IDENTIFICATION OF AN ACTIVATION DOMAIN IN p67 phox. *Journal of Biological Chemistry. 273*, 16663-16668.

(35) Koga, H., Terasawa, H., Nunoi, H., Takeshige, K., Inagaki, F. and Sumimoto, H. (1999) Tetratricopeptide Repeat (TPR) Motifs of p67 phox Participate in Interaction with the Small GTPase Rac and Activation of the Phagocyte NADPH Oxidase. *Journal of Biological Chemistry. 274*, 25051-25060.

(36) Bedard, K. and Krause, K.-H. (2007) The NOX Family of ROS-Generating NADPH Oxidases: Physiology and Pathophysiology. *Physiological Reviews. 87*, 245-313.

(37) Loschen, G., Azzi, A., Richter, C. and Flohe, L. (1974) Superoxide radicals as precursors of mitochondrial hydrogen peroxide. *FEBS Lett. 42*, 68-72.

(38) Lipinski, B. (2011) Hydroxyl Radical and Its Scavengers in Health and Disease. *Oxidative Medicine and Cellular Longevity. 2011*,

(39) Walling, C. (1975) Fenton's reagent revisited. *Accounts of Chemical Research. 8*, 125-131.

(40) Korhonen, R., Lahti, A., Kankaanranta, H. and Moilanen, E. (2005) Nitric oxide production and signaling in inflammation. *Current drug targets. Inflammation and allergy. 4*, 471-479.

(41) Huie, R. E. and Padmaja, S. (1993) The reaction of no with superoxide. *Free radical research communications. 18*, 195-199.

(42) Turrens, J. F. (2003) Mitochondrial formation of reactive oxygen species. *The Journal of Physiology. 552*, 335-344.

(43) Chance, B., Sies, H. and Boveris, A. (1979) Hydroperoxide metabolism in mammalian organs. *Physiol Rev. 59*, 527-605.

(44) Cadenas, E. and Davies, K. J. (2000) Mitochondrial free radical generation, oxidative stress, and aging. *Free radical biology & medicine. 29*, 222-230.

(45) Muller, F. (2000) The nature and mechanism of superoxide production by the electron transport chain: Its relevance to aging. *Journal of the American Aging Association. 23*, 227-253.

(46) Pacher, P., Beckman, J. S. and Liaudet, L. (2007) Nitric oxide and peroxynitrite in health and disease. *Physiol Rev. 87*, 315-424.

(47) Yin, H., Xu, L. and Porter, N. A. (2011) Free radical lipid peroxidation: mechanisms and analysis. *Chemical reviews. 111*, 5944-5972.

(48) Schopfer, F. J., Cipollina, C. and Freeman, B. A. (2011) Formation and signaling actions of electrophilic lipids. *Chemical reviews. 111*, 5997-6021.

(49) Howard, J. A. and Ingold, K. U. (1967) Absolute rate constants for hydrocarbon autoxidation. VI. Alkyl aromatic and olefinic hydrocarbons. *Canadian Journal of Chemistry. 45*, 793-802.

(50) Xu, L., Davis, T. A. and Porter, N. A. (2009) Rate constants for peroxidation of polyunsaturated fatty acids and sterols in solution and in liposomes. *J Am Chem Soc. 131*, 13037-13044.

(51) Bergstrom, S. (1945) Autoxidation of linoleic acid. *Nature. 156*, 717.

(52) Brash, A. R. (2000) Autoxidation of methyl linoleate: Identification of the bis-allylic 11-hydroperoxide. *Lipids. 35*, 947-952.
(53) Schauenstein, E. (1967) Autoxidation of polyunsaturated esters in water: chemical structure and biological activity of the products. *Journal of lipid research. 8*, 417-428.
(54) Esterbauer, H. and Schauenstein, E. (1966) Über die Autoxydation von Linolsäure-methylester in Wasser, 2. Mitteilung: Isolierung und Identifizierung von 4-Hydroperoxy-nonen-2,3-al-1 und 8-Hydroperoxy-caprylsäure-methylester. *Fette, Seifen, Anstrichmittel. 68*, 7-14.
(55) Benedetti, A., Comporti, M. and Esterbauer, H. (1980) Identification of 4-hydroxynonenal as a cytotoxic product originating from the peroxidation of liver microsomal lipids. *Biochimica et Biophysica Acta (BBA) - Lipids and Lipid Metabolism. 620*, 281-296.
(56) Schneider, C., Tallman, K. A., Porter, N. A. and Brash, A. R. (2001) Two distinct pathways of formation of 4-hydroxynonenal. Mechanisms of nonenzymatic transformation of the 9- and 13-hydroperoxides of linoleic acid to 4-hydroxyalkenals. *The Journal of biological chemistry. 276*, 20831-20838.
(57) Spickett, C. M. (2013) The lipid peroxidation product 4-hydroxy-2-nonenal: Advances in chemistry and analysis. *Redox biology. 1*, 145-152.
(58) Pryor, W. A. and Porter, N. A. (1990) Suggested mechanisms for the production of 4-hydroxy-2-nonenal from the autoxidation of polyunsaturated fatty acids. *Free radical biology & medicine. 8*, 541-543.
(59) Loidl-Stahlhofen, A., Hannemann, K. and Spiteller, G. (1994) Generation of α-hydroxyaldehydic compounds in the course of lipid peroxidation. *Biochimica et Biophysica Acta (BBA) - Lipids and Lipid Metabolism. 1213*, 140-148.
(60) Schneider, C., Porter, N. A. and Brash, A. R. (2008) Routes to 4-hydroxynonenal: fundamental issues in the mechanisms of lipid peroxidation. *The Journal of biological chemistry. 283*, 15539-15543.
(61) Lee, S. H., Oe, T. and Blair, I. A. (2001) Vitamin C-induced decomposition of lipid hydroperoxides to endogenous genotoxins. *Science. 292*, 2083-2086.
(62) Lee, S. H. and Blair, I. A. (2000) Characterization of 4-oxo-2-nonenal as a novel product of lipid peroxidation. *Chem Res Toxicol. 13*, 698-702.
(63) Uchida, K. (2003) 4-Hydroxy-2-nonenal: a product and mediator of oxidative stress. *Progress in lipid research. 42*, 318-343.
(64) Sayre, L. M., Lin, D., Yuan, Q., Zhu, X. and Tang, X. (2006) Protein adducts generated from products of lipid oxidation: focus on HNE and one. *Drug Metab Rev. 38*, 651-675.
(65) Nadkarni, D. V. and Sayre, L. M. (1995) Structural definition of early lysine and histidine adduction chemistry of 4-hydroxynonenal. *Chem Res Toxicol. 8*, 284-291.
(66) Esterbauer, H., Schaur, R. J. and Zollner, H. (1991) Chemistry and biochemistry of 4-hydroxynonenal, malonaldehyde and related aldehydes. *Free radical biology & medicine. 11*, 81-128.
(67) Sayre, L. M., Arora, P. K., Iyer, R. S. and Salomon, R. G. (1993) Pyrrole formation from 4-hydroxynonenal and primary amines. *Chem Res Toxicol. 6*, 19-22.
(68) Shibata, T., Shimozu, Y., Wakita, C., Shibata, N., Kobayashi, M., Machida, S., Kato, R., Itabe, H., Zhu, X., Sayre, L. M. and Uchida, K. (2011) Lipid peroxidation modification of protein generates Nepsilon-(4-oxononanoyl)lysine as a pro-inflammatory ligand. *The Journal of biological chemistry. 286*, 19943-19957.

(69) Salomon, R. G., Kaur, K., Podrez, E., Hoff, H. F., Krushinsky, A. V. and Sayre, L. M. (2000) HNE-Derived 2-Pentylpyrroles Are Generated during Oxidation of LDL, Are More Prevalent in Blood Plasma from Patients with Renal Disease or Atherosclerosis, and Are Present in Atherosclerotic Plaques. *Chemical Research in Toxicology. 13*, 557-564.
(70) Sayre, L. M., Zelasko, D. A., Harris, P. L., Perry, G., Salomon, R. G. and Smith, M. A. (1997) 4-Hydroxynonenal-derived advanced lipid peroxidation end products are increased in Alzheimer's disease. *Journal of neurochemistry. 68*, 2092-2097.
(71) Zhu, X. and Sayre, L. M. (2007) Long-lived 4-oxo-2-enal-derived apparent lysine michael adducts are actually the isomeric 4-ketoamides. *Chem Res Toxicol. 20*, 165-170.
(72) Zhu, X. and Sayre, L. M. (2007) Mass spectrometric evidence for long-lived protein adducts of 4-oxo-2-nonenal. *Redox Rep. 12*, 45-49.
(73) Zhang, W.-H., Liu, J., Xu, G., Yuan, Q. and Sayre, L. M. (2003) Model Studies on Protein Side Chain Modification by 4-Oxo-2-nonenal. *Chemical Research in Toxicology. 16*, 512-523.
(74) Xu, G. and Sayre, L. M. (1998) Structural characterization of a 4-hydroxy-2-alkenal-derived fluorophore that contributes to lipoperoxidation-dependent protein cross-linking in aging and degenerative disease. *Chem Res Toxicol. 11*, 247-251.
(75) Xu, G. and Sayre, L. M. (1999) Structural elucidation of a 2:2 4-ketoaldehyde-amine adduct as a model for lysine-directed cross-linking of proteins by 4-ketoaldehydes. *Chem Res Toxicol. 12*, 862-868.
(76) Xu, G., Liu, Y., Kansal, M. M. and Sayre, L. M. (1999) Rapid cross-linking of proteins by 4-ketoaldehydes and 4-hydroxy-2-alkenals does not arise from the lysine-derived monoalkylpyrroles. *Chem Res Toxicol. 12*, 855-861.
(77) Xu, G., Liu, Y. and Sayre, L. M. (2000) Polyclonal antibodies to a fluorescent 4-hydroxy-2-nonenal (HNE)-derived lysine-lysine cross-link: characterization and application to HNE-treated protein and in vitro oxidized low-density lipoprotein. *Chem Res Toxicol. 13*, 406-413.
(78) Doorn, J. A. and Petersen, D. R. (2002) Covalent modification of amino acid nucleophiles by the lipid peroxidation products 4-hydroxy-2-nonenal and 4-oxo-2-nonenal. *Chem Res Toxicol. 15*, 1445-1450.
(79) Oe, T., Arora, J. S., Lee, S. H. and Blair, I. A. (2003) A novel lipid hydroperoxide-derived cyclic covalent modification to histone H4. *The Journal of biological chemistry. 278*, 42098-42105.
(80) Rouach, H., Fataccioli, V., Gentil, M., French, S. W., Morimoto, M. and Nordmann, R. (1997) Effect of chronic ethanol feeding on lipid peroxidation and protein oxidation in relation to liver pathology. *Hepatology. 25*, 351-355.
(81) Proceedings of the Chemical Society. October 1961. *Proceedings of the Chemical Society.* 357-396.
(82) Kolb, H. C., Finn, M. G. and Sharpless, K. B. (2001) Click Chemistry: Diverse Chemical Function from a Few Good Reactions. *Angew Chem Int Ed Engl. 40*, 2004-2021.
(83) Chan, T. R., Hilgraf, R., Sharpless, K. B. and Fokin, V. V. (2004) Polytriazoles as copper(I)-stabilizing ligands in catalysis. *Organic letters. 6*, 2853-2855.
(84) Codreanu, S. G., Ullery, J. C., Zhu, J., Tallman, K. A., Beavers, W. N., Porter, N. A., Marnett, L. J., Zhang, B. and Liebler, D. C. (2014) Alkylation damage by lipid electrophiles targets functional protein systems. *Mol Cell Proteomics. 13*, 849-859.

(85) Tallman, K. A., Vila, A., Porter, N. A. and Marnett, L. J. (2009) Measuring electrophile stress. *Curr Protoc Toxicol. Chapter 17*, Unit17.11.
(86) Codreanu, S. G., Zhang, B., Sobecki, S. M., Billheimer, D. D. and Liebler, D. C. (2009) Global analysis of protein damage by the lipid electrophile 4-hydroxy-2-nonenal. *Mol Cell Proteomics. 8*, 670-680.
(87) Aluise, C. D., Rose, K., Boiani, M., Reyzer, M. L., Manna, J. D., Tallman, K., Porter, N. A. and Marnett, L. J. (2013) Peptidyl-prolyl cis/trans-isomerase A1 (Pin1) is a target for modification by lipid electrophiles. *Chem Res Toxicol. 26*, 270-279.
(88) Galligan, J. J., Rose, K. L., Beavers, W. N., Hill, S., Tallman, K. A., Tansey, W. P. and Marnett, L. J. (2014) Stable Histone Adduction by 4-Oxo-2-nonenal: A Potential Link between Oxidative Stress and Epigenetics. *Journal of the American Chemical Society. 136*, 11864-11866.
(89) Oberley, L. W. and Buettner, G. R. (1979) Role of Superoxide Dismutase in Cancer: A Review. *Cancer Research. 39*, 1141-1149.
(90) Thannickal, V. J. and Fanburg, B. L. (2000) Reactive oxygen species in cell signaling. *Am J Physiol Lung Cell Mol Physiol. 279*, L1005-1028.
(91) MatÉs, J. M., Pérez-Gómez, C. and De Castro, I. N. (1999) Antioxidant enzymes and human diseases. *Clinical biochemistry. 32*, 595-603.
(92) Meister, A. and Anderson, M. E. (1983) Glutathione. *Annual review of biochemistry. 52*, 711-760.
(93) West, J. D. and Marnett, L. J. (2005) Alterations in gene expression induced by the lipid peroxidation product, 4-hydroxy-2-nonenal. *Chem Res Toxicol. 18*, 1642-1653.
(94) Liu, Q., Ullery, J., Zhu, J., Liebler, D. C., Marnett, L. J. and Zhang, B. (2013) RNA-seq data analysis at the gene and CDS levels provides a comprehensive view of transcriptome responses induced by 4-hydroxynonenal. *Mol Biosyst. 9*, 3036-3046.
(95) Wattenberg, L. W. (1978) Inhibitors of chemical carcinogenesis. *Advances in cancer research. 26*, 197-226.
(96) Rushmore, T. H., Morton, M. R. and Pickett, C. B. (1991) The antioxidant responsive element. Activation by oxidative stress and identification of the DNA consensus sequence required for functional activity. *The Journal of biological chemistry. 266*, 11632-11639.
(97) Kobayashi, A., Kang, M. I., Okawa, H., Ohtsuji, M., Zenke, Y., Chiba, T., Igarashi, K. and Yamamoto, M. (2004) Oxidative stress sensor Keap1 functions as an adaptor for Cul3-based E3 ligase to regulate proteasomal degradation of Nrf2. *Mol Cell Biol. 24*, 7130-7139.
(98) McMahon, M., Itoh, K., Yamamoto, M. and Hayes, J. D. (2003) Keap1-dependent proteasomal degradation of transcription factor Nrf2 contributes to the negative regulation of antioxidant response element-driven gene expression. *The Journal of biological chemistry. 278*, 21592-21600.
(99) Zhang, D. D. and Hannink, M. (2003) Distinct Cysteine Residues in Keap1 Are Required for Keap1-Dependent Ubiquitination of Nrf2 and for Stabilization of Nrf2 by Chemopreventive Agents and Oxidative Stress. *Molecular and Cellular Biology. 23*, 8137-8151.
(100) Rachakonda, G., Xiong, Y., Sekhar, K. R., Stamer, S. L., Liebler, D. C. and Freeman, M. L. (2008) Covalent modification at Cys151 dissociates the electrophile sensor Keap1 from the ubiquitin ligase CUL3. *Chem Res Toxicol. 21*, 705-710.
(101) Itoh, K., Chiba, T., Takahashi, S., Ishii, T., Igarashi, K., Katoh, Y., Oyake, T., Hayashi, N., Satoh, K., Hatayama, I., Yamamoto, M. and Nabeshima, Y.-i. (1997) An Nrf2/Small Maf

Heterodimer Mediates the Induction of Phase II Detoxifying Enzyme Genes through Antioxidant Response Elements. *Biochemical and Biophysical Research Communications. 236*, 313-322.

(102) Alam, J., Stewart, D., Touchard, C., Boinapally, S., Choi, A. M. and Cook, J. L. (1999) Nrf2, a Cap'n'Collar transcription factor, regulates induction of the heme oxygenase-1 gene. *The Journal of biological chemistry. 274*, 26071-26078.

(103) Friling, R. S., Bensimon, A., Tichauer, Y. and Daniel, V. (1990) Xenobiotic-inducible expression of murine glutathione S-transferase Ya subunit gene is controlled by an electrophile-responsive element. *Proceedings of the National Academy of Sciences of the United States of America. 87*, 6258-6262.

(104) Moinova, H. R. and Mulcahy, R. T. (1999) Up-Regulation of the Human γ-Glutamylcysteine Synthetase Regulatory Subunit Gene Involves Binding of Nrf-2 to an Electrophile Responsive Element. *Biochemical and Biophysical Research Communications. 261*, 661-668.

(105) Thimmulappa, R. K., Mai, K. H., Srisuma, S., Kensler, T. W., Yamamoto, M. and Biswal, S. (2002) Identification of Nrf2-regulated genes induced by the chemopreventive agent sulforaphane by oligonucleotide microarray. *Cancer Res. 62*, 5196-5203.

(106) Benjamin, I. J. and McMillan, D. R. (1998) Stress (heat shock) proteins: molecular chaperones in cardiovascular biology and disease. *Circulation research. 83*, 117-132.

(107) Zou, J., Guo, Y., Guettouche, T., Smith, D. F. and Voellmy, R. (1998) Repression of heat shock transcription factor HSF1 activation by HSP90 (HSP90 complex) that forms a stress-sensitive complex with HSF1. *Cell. 94*, 471-480.

(108) Abravaya, K., Myers, M. P., Murphy, S. P. and Morimoto, R. I. (1992) The human heat shock protein hsp70 interacts with HSF, the transcription factor that regulates heat shock gene expression. *Genes Dev. 6*, 1153-1164.

(109) Jacobs, A. T. and Marnett, L. J. (2010) Systems analysis of protein modification and cellular responses induced by electrophile stress. *Acc Chem Res. 43*, 673-683.

(110) Carbone, D. L., Doorn, J. A., Kiebler, Z., Ickes, B. R. and Petersen, D. R. (2005) Modification of heat shock protein 90 by 4-hydroxynonenal in a rat model of chronic alcoholic liver disease. *The Journal of pharmacology and experimental therapeutics. 315*, 8-15.

(111) Carbone, D. L., Doorn, J. A., Kiebler, Z., Sampey, B. P. and Petersen, D. R. (2004) Inhibition of Hsp72-mediated protein refolding by 4-hydroxy-2-nonenal. *Chem Res Toxicol. 17*, 1459-1467.

(112) Jacobs, A. T. and Marnett, L. J. (2007) Heat shock factor 1 attenuates 4-Hydroxynonenal-mediated apoptosis: critical role for heat shock protein 70 induction and stabilization of Bcl-XL. *The Journal of biological chemistry. 282*, 33412-33420.

(113) Jacobs, A. T. and Marnett, L. J. (2009) HSF1-mediated BAG3 expression attenuates apoptosis in 4-hydroxynonenal-treated colon cancer cells via stabilization of anti-apoptotic Bcl-2 proteins. *The Journal of biological chemistry. 284*, 9176-9183.

(114) Ji, C., Kozak, K. R. and Marnett, L. J. (2001) IkappaB kinase, a molecular target for inhibition by 4-hydroxy-2-nonenal. *The Journal of biological chemistry. 276*, 18223-18228.

(115) Rossi, A., Kapahi, P., Natoli, G., Takahashi, T., Chen, Y., Karin, M. and Santoro, M. G. (2000) Anti-inflammatory cyclopentenone prostaglandins are direct inhibitors of IkappaB kinase. *Nature. 403*, 103-108.

(116) Straus, D. S., Pascual, G., Li, M., Welch, J. S., Ricote, M., Hsiang, C. H., Sengchanthalangsy, L. L., Ghosh, G. and Glass, C. K. (2000) 15-deoxy-delta 12,14-prostaglandin J2 inhibits multiple steps in the NF-kappa B signaling pathway. *Proc Natl Acad Sci U S A. 97*, 4844-4849.
(117) Yoritaka, A., Hattori, N., Uchida, K., Tanaka, M., Stadtman, E. R. and Mizuno, Y. (1996) Immunohistochemical detection of 4-hydroxynonenal protein adducts in Parkinson disease. *Proc Natl Acad Sci U S A. 93*, 2696-2701.
(118) Dalle-Donne, I., Giustarini, D., Colombo, R., Rossi, R. and Milzani, A. (2003) Protein carbonylation in human diseases. *Trends Mol Med. 9*, 169-176.
(119) Hussain, S. P., Hofseth, L. J. and Harris, C. C. (2003) Radical causes of cancer. *Nat Rev Cancer. 3*, 276-285.
(120) Marnett, L. J., Riggins, J. N. and West, J. D. (2003) Endogenous generation of reactive oxidants and electrophiles and their reactions with DNA and protein. *J Clin Invest. 111*, 583-593.
(121) Ullery, J. C. and Marnett, L. J. (2012) Protein modification by oxidized phospholipids and hydrolytically released lipid electrophiles: Investigating cellular responses. *Biochim Biophys Acta. 1818*, 2424-2435.
(122) Ekholm, S. V. and Reed, S. I. (2000) Regulation of G(1) cyclin-dependent kinases in the mammalian cell cycle. *Curr Opin Cell Biol. 12*, 676-684.
(123) Lees, E., Faha, B., Dulic, V., Reed, S. I. and Harlow, E. (1992) Cyclin E/cdk2 and cyclin A/cdk2 kinases associate with p107 and E2F in a temporally distinct manner. *Genes Dev. 6*, 1874-1885.
(124) Harbour, J. W., Luo, R. X., Dei Santi, A., Postigo, A. A. and Dean, D. C. (1999) Cdk phosphorylation triggers sequential intramolecular interactions that progressively block Rb functions as cells move through G1. *Cell. 98*, 859-869.
(125) Giacinti, C. and Giordano, A. (2006) RB and cell cycle progression. *Oncogene. 25*, 5220-5227.
(126) Harper, J. W., Adami, G. R., Wei, N., Keyomarsi, K. and Elledge, S. J. (1993) The p21 Cdk-interacting protein Cip1 is a potent inhibitor of G1 cyclin-dependent kinases. *Cell. 75*, 805-816.
(127) Wang, Y., Fisher, J. C., Mathew, R., Ou, L., Otieno, S., Sublet, J., Xiao, L., Chen, J., Roussel, M. F. and Kriwacki, R. W. (2011) Intrinsic disorder mediates the diverse regulatory functions of the Cdk inhibitor p21. *Nat Chem Biol. 7*, 214-221.
(128) Barrera, G., Pizzimenti, S. and Dianzani, M. U. (2004) 4-hydroxynonenal and regulation of cell cycle: effects on the pRb/E2F pathway. *Free radical biology & medicine. 37*, 597-606.
(129) Wonisch, W., Kohlwein, S. D., Schaur, J., Tatzber, F., Guttenberger, H., Zarkovic, N., Winkler, R. and Esterbauer, H. (1998) Treatment of the budding yeast Saccharomyces cerevisiae with the lipid peroxidation product 4-HNE provokes a temporary cell cycle arrest in G1 phase. *Free radical biology & medicine. 25*, 682-687.
(130) Barrera, G., Pizzimenti, S., Muraca, R., Barbiero, G., Bonelli, G., Baccino, F. M., Fazio, V. M. and Dianzani, M. U. (1996) Effect of 4-Hydroxynonenal on cell cycle progression and expression of differentiation-associated antigens in HL-60 cells. *Free radical biology & medicine. 20*, 455-462.
(131) Laurora, S., Tamagno, E., Briatore, F., Bardini, P., Pizzimenti, S., Toaldo, C., Reffo, P., Costelli, P., Dianzani, M. U., Danni, O. and Barrera, G. (2005) 4-Hydroxynonenal

modulation of p53 family gene expression in the SK-N-BE neuroblastoma cell line. *Free radical biology & medicine. 38*, 215-225.
(132) Zhang, B., Shi, Z., Duncan, D. T., Prodduturi, N., Marnett, L. J. and Liebler, D. C. (2011) Relating protein adduction to gene expression changes: a systems approach. *Mol Biosyst. 7*, 2118-2127.
(133) McGrath, C. E., Tallman, K. A., Porter, N. A. and Marnett, L. J. (2011) Structure-activity analysis of diffusible lipid electrophiles associated with phospholipid peroxidation: 4-hydroxynonenal and 4-oxononenal analogues. *Chem Res Toxicol. 24*, 357-370.
(134) van den Heuvel, S. and Harlow, E. (1993) Distinct roles for cyclin-dependent kinases in cell cycle control. *Science. 262*, 2050-2054.
(135) Schonthal, A. H. (2004) Measuring cyclin-dependent kinase activity. *Methods Mol Biol. 281*, 105-124.
(136) Xu, M., Sheppard, K. A., Peng, C. Y., Yee, A. S. and Piwnica-Worms, H. (1994) Cyclin A/CDK2 binds directly to E2F-1 and inhibits the DNA-binding activity of E2F-1/DP-1 by phosphorylation. *Mol Cell Biol. 14*, 8420-8431.
(137) Sheaff, R. J., Groudine, M., Gordon, M., Roberts, J. M. and Clurman, B. E. (1997) Cyclin E-CDK2 is a regulator of p27Kip1. *Genes Dev. 11*, 1464-1478.
(138) Akiyama, T., Ohuchi, T., Sumida, S., Matsumoto, K. and Toyoshima, K. (1992) Phosphorylation of the retinoblastoma protein by cdk2. *Proceedings of the National Academy of Sciences of the United States of America. 89*, 7900-7904.
(139) Sampey, B. P., Carbone, D. L., Doorn, J. A., Drechsel, D. A. and Petersen, D. R. (2007) 4-Hydroxy-2-nonenal adduction of extracellular signal-regulated kinase (Erk) and the inhibition of hepatocyte Erk-Est-like protein-1-activating protein-1 signal transduction. *Mol Pharmacol. 71*, 871-883.
(140) Barrera, G., Pizzimenti, S., Laurora, S., Moroni, E., Giglioni, B. and Dianzani, M. U. (2002) 4-Hydroxynonenal affects pRb/E2F pathway in HL-60 human leukemic cells. *Biochem Biophys Res Commun. 295*, 267-275.
(141) Sharma, A., Sharma, R., Chaudhary, P., Vatsyayan, R., Pearce, V., Jeyabal, P. V., Zimniak, P., Awasthi, S. and Awasthi, Y. C. (2008) 4-Hydroxynonenal induces p53-mediated apoptosis in retinal pigment epithelial cells. *Arch Biochem Biophys. 480*, 85-94.
(142) Gu, Y., Rosenblatt, J. and Morgan, D. O. (1992) Cell cycle regulation of CDK2 activity by phosphorylation of Thr160 and Tyr15. *The EMBO journal. 11*, 3995-4005.
(143) Ji, C., Amarnath, V., Pietenpol, J. A. and Marnett, L. J. (2001) 4-hydroxynonenal induces apoptosis via caspase-3 activation and cytochrome c release. *Chem Res Toxicol. 14*, 1090-1096.
(144) Macleod, K. F., Sherry, N., Hannon, G., Beach, D., Tokino, T., Kinzler, K., Vogelstein, B. and Jacks, T. (1995) p53-dependent and independent expression of p21 during cell growth, differentiation, and DNA damage. *Genes Dev. 9*, 935-944.
(145) Russo, A. A., Jeffrey, P. D. and Pavletich, N. P. (1996) Structural basis of cyclin-dependent kinase activation by phosphorylation. *Nature structural biology. 3*, 696-700.
(146) Honda, R., Lowe, E. D., Dubinina, E., Skamnaki, V., Cook, A., Brown, N. R. and Johnson, L. N. (2005) The structure of cyclin E1/CDK2: implications for CDK2 activation and CDK2-independent roles. *The EMBO journal. 24*, 452-463.
(147) Fisher, R. P. and Morgan, D. O. (1994) A novel cyclin associates with MO15/CDK7 to form the CDK-activating kinase. *Cell. 78*, 713-724.

(148) Chi, Y., Welcker, M., Hizli, A. A., Posakony, J. J., Aebersold, R. and Clurman, B. E. (2008) Identification of CDK2 substrates in human cell lysates. *Genome Biol. 9*, R149.
(149) Grafstrom, R. H., Pan, W. and Hoess, R. H. (1999) Defining the substrate specificity of cdk4 kinase–cyclin D1 complex. *Carcinogenesis. 20*, 193-198.
(150) Doorn, J. A. and Petersen, D. R. (2003) Covalent adduction of nucleophilic amino acids by 4-hydroxynonenal and 4-oxononenal. *Chem Biol Interact. 143-144*, 93-100.
(151) Zhou, X. Z., Kops, O., Werner, A., Lu, P. J., Shen, M., Stoller, G., Kullertz, G., Stark, M., Fischer, G. and Lu, K. P. (2000) Pin1-dependent prolyl isomerization regulates dephosphorylation of Cdc25C and tau proteins. *Mol Cell. 6*, 873-883.
(152) Zheng, H., You, H., Zhou, X. Z., Murray, S. A., Uchida, T., Wulf, G., Gu, L., Tang, X., Lu, K. P. and Xiao, Z. X. (2002) The prolyl isomerase Pin1 is a regulator of p53 in genotoxic response. *Nature. 419*, 849-853.
(153) Ryo, A., Nakamura, M., Wulf, G., Liou, Y. C. and Lu, K. P. (2001) Pin1 regulates turnover and subcellular localization of beta-catenin by inhibiting its interaction with APC. *Nat Cell Biol. 3*, 793-801.
(154) Dougherty, M. K., Muller, J., Ritt, D. A., Zhou, M., Zhou, X. Z., Copeland, T. D., Conrads, T. P., Veenstra, T. D., Lu, K. P. and Morrison, D. K. (2005) Regulation of Raf-1 by direct feedback phosphorylation. *Mol Cell. 17*, 215-224.
(155) Rizzolio, F., Lucchetti, C., Caligiuri, I., Marchesi, I., Caputo, M., Klein-Szanto, A. J., Bagella, L., Castronovo, M. and Giordano, A. (2012) Retinoblastoma tumor-suppressor protein phosphorylation and inactivation depend on direct interaction with Pin1. *Cell Death Differ. 19*, 1152-1161.
(156) Smith, M. A., Richey, P. L., Taneda, S., Kutty, R. K., Sayre, L. M., Monnier, V. M. and Perry, G. (1994) Advanced Maillard reaction end products, free radicals, and protein oxidation in Alzheimer's disease. *Ann N Y Acad Sci. 738*, 447-454.
(157) Butterfield, D. A., Poon, H. F., St Clair, D., Keller, J. N., Pierce, W. M., Klein, J. B. and Markesbery, W. R. (2006) Redox proteomics identification of oxidatively modified hippocampal proteins in mild cognitive impairment: insights into the development of Alzheimer's disease. *Neurobiology of disease. 22*, 223-232.
(158) Arora, J. S., Oe, T. and Blair, I. A. (2011) Synthesis of deuterium-labeled analogs of the lipid hydroperoxide-derived bifunctional electrophile 4-oxo-2(E)-nonenal. *Journal of Labelled Compounds and Radiopharmaceuticals. 54*, 247-251.
(159) Kislinger, T., Humeny, A., Peich, C. C., Becker, C. M. and Pischetsrieder, M. (2005) Analysis of protein glycation products by MALDI-TOF/MS. *Ann N Y Acad Sci. 1043*, 249-259.
(160) Long, E. K., Olson, D. M. and Bernlohr, D. A. (2013) High-fat diet induces changes in adipose tissue trans-4-oxo-2-nonenal and trans-4-hydroxy-2-nonenal levels in a depot-specific manner. *Free radical biology & medicine. 63*, 390-398.
(161) Selley, M. L. (1997) Determination of the lipid peroxidation product (E)-4-hydroxy-2-nonenal in clinical samples by gas chromatography--negative-ion chemical ionisation mass spectrometry of the O-pentafluorobenzyl oxime. *Journal of chromatography. B, Biomedical sciences and applications. 691*, 263-268.
(162) Rindgen, D., Nakajima, M., Wehrli, S., Xu, K. and Blair, I. A. (1999) Covalent modifications to 2'-deoxyguanosine by 4-oxo-2-nonenal, a novel product of lipid peroxidation. *Chem Res Toxicol. 12*, 1195-1204.

(163) Zhu, X., Tang, X., Anderson, V. E. and Sayre, L. M. (2009) Mass spectrometric characterization of protein modification by the products of nonenzymatic oxidation of linoleic acid. *Chem Res Toxicol. 22*, 1386-1397.
(164) Sultana, R., Boyd-Kimball, D., Poon, H. F., Cai, J., Pierce, W. M., Klein, J. B., Markesbery, W. R., Zhou, X. Z., Lu, K. P. and Butterfield, D. A. (2006) Oxidative modification and down-regulation of Pin1 in Alzheimer's disease hippocampus: A redox proteomics analysis. *Neurobiology of aging. 27*, 918-925.
(165) Liou, Y. C., Sun, A., Ryo, A., Zhou, X. Z., Yu, Z. X., Huang, H. K., Uchida, T., Bronson, R., Bing, G., Li, X., Hunter, T. and Lu, K. P. (2003) Role of the prolyl isomerase Pin1 in protecting against age-dependent neurodegeneration. *Nature. 424*, 556-561.
(166) Nakamura, K., Greenwood, A., Binder, L., Bigio, E. H., Denial, S., Nicholson, L., Zhou, X. Z. and Lu, K. P. (2012) Proline isomer-specific antibodies reveal the early pathogenic tau conformation in Alzheimer's disease. *Cell. 149*, 232-244.
(167) Miyashita, H., Chikazawa, M., Otaki, N., Hioki, Y., Shimozu, Y., Nakashima, F., Shibata, T., Hagihara, Y., Maruyama, S., Matsumi, N. and Uchida, K. (2014) Lysine pyrrolation is a naturally-occurring covalent modification involved in the production of DNA mimic proteins. *Sci. Rep. 4*,
(168) Stewart, D. E., Sarkar, A. and Wampler, J. E. (1990) Occurrence and role of cis peptide bonds in protein structures. *Journal of molecular biology. 214*, 253-260.
(169) Pal, D. and Chakrabarti, P. (1999) Cis peptide bonds in proteins: residues involved, their conformations, interactions and locations. *Journal of molecular biology. 294*, 271-288.
(170) Yaffe, M. B., Schutkowski, M., Shen, M., Zhou, X. Z., Stukenberg, P. T., Rahfeld, J. U., Xu, J., Kuang, J., Kirschner, M. W., Fischer, G., Cantley, L. C. and Lu, K. P. (1997) Sequence-specific and phosphorylation-dependent proline isomerization: a potential mitotic regulatory mechanism. *Science. 278*, 1957-1960.
(171) Butterfield, D. A., Perluigi, M. and Sultana, R. (2006) Oxidative stress in Alzheimer's disease brain: new insights from redox proteomics. *European journal of pharmacology. 545*, 39-50.
(172) Fang, J. and Holmgren, A. (2006) Inhibition of thioredoxin and thioredoxin reductase by 4-hydroxy-2-nonenal in vitro and in vivo. *J Am Chem Soc. 128*, 1879-1885.
(173) Struhl, K. (1998) Histone acetylation and transcriptional regulatory mechanisms. *Genes & Development. 12*, 599-606.
(174) Jin, J., He, B., Zhang, X., Lin, H. and Wang, Y. (2016) SIRT2 Reverses 4-Oxononanoyl Lysine Modification on Histones. *Journal of the American Chemical Society.*
(175) Galligan, J. J., Kingsley, P. J., Wauchope, O. R., Mitchener, M. M., Camarillo, J. M., Wepy, J. A., Harris, P. S., Fritz, K. S. and Marnett, L. J. (2016) Quantitative Analysis of Arginine and Lysine Modifications (QuARK-Mod) from Complex Biological Samples.
(176) Yamanaka, H., Maehira, F., Oshiro, M., Asato, T., Yanagawa, Y., Takei, H. and Nakashima, Y. (2000) A Possible Interaction of Thioredoxin with VDUP1 in HeLa Cells Detected in a Yeast Two-Hybrid System. *Biochemical and Biophysical Research Communications. 271*, 796-800.
(177) Junn, E., Han, S. H., Im, J. Y., Yang, Y., Cho, E. W., Um, H. D., Kim, D. K., Lee, K. W., Han, P. L., Rhee, S. G. and Choi, I. (2000) Vitamin D3 Up-Regulated Protein 1 Mediates Oxidative Stress Via Suppressing the Thioredoxin Function. *The Journal of Immunology. 164*, 6287-6295.

(178) Nishiyama, A., Matsui, M., Iwata, S., Hirota, K., Masutani, H., Nakamura, H., Takagi, Y., Sono, H., Gon, Y. and Yodoi, J. (1999) Identification of thioredoxin-binding protein-2/vitamin D(3) up-regulated protein 1 as a negative regulator of thioredoxin function and expression. *The Journal of biological chemistry. 274*, 21645-21650.
(179) Lu, J. and Holmgren, A. (2014) The thioredoxin antioxidant system. *Free radical biology & medicine. 66*, 75-87.
(180) Chen, D., Fang, L., Li, H., Tang, M.-s. and Jin, C. (2013) Cigarette Smoke Component Acrolein Modulates Chromatin Assembly by Inhibiting Histone Acetylation. *Journal of Biological Chemistry. 288*, 21678-21687.
(181) Zheng, Y., Thomas, P. M. and Kelleher, N. L. (2013) Measurement of acetylation turnover at distinct lysines in human histones identifies long-lived acetylation sites. *Nature communications. 4*, 2203.
(182) Liu, W., Brock, A., Chen, S. and Schultz, P. G. (2007) Genetic incorporation of unnatural amino acids into proteins in mammalian cells. *Nature methods. 4*, 239-244.
(183) Camarillo, J. M., Ullery, J. C., Rose, K. L. and Marnett, L. J. (2016) Electrophilic modification of PKM2 by 4-hydroxynonenal and 4-oxononenal results in protein cross-linking and kinase inhibition. *Chem Res Toxicol.*